

The following publication Shi, X., Esan, O. C., Huo, X., Ma, Y., Pan, Z., An, L., & Zhao, T. S. (2021). Polymer electrolyte membranes for vanadium redox flow batteries: fundamentals and applications. *Progress in Energy and Combustion Science*, 85, 100926 is available at <https://doi.org/10.1016/j.pecs.2021.100926>.

## Table of Contents

Abstract .....	3
1. Introduction.....	4
2. The focus of the article.....	7
3. Functional requirements .....	8
4. Performance indicators.....	9
<b>4.1 Membrane level.....</b>	<b>9</b>
<b>4.1.1 Ionic conductivity .....</b>	<b>9</b>
<b>4.1.2 Water/Electrolyte uptake.....</b>	<b>10</b>
<b>4.1.3 Ion exchange capacity (IEC) .....</b>	<b>11</b>
<b>4.1.4 Vanadium-ion permeability/diffusivity .....</b>	<b>12</b>
<b>4.1.5 Chemical stability.....</b>	<b>14</b>
<b>4.1.6 Thermal stability .....</b>	<b>15</b>
<b>4.1.7 Mechanical property .....</b>	<b>16</b>
<b>4.2 Cell level .....</b>	<b>17</b>
<b>4.2.1 Polarization curve .....</b>	<b>17</b>
<b>4.2.2 Charge-discharge performance.....</b>	<b>18</b>
<b>4.2.3 Coulombic, Voltage, and Energy efficiencies .....</b>	<b>18</b>
<b>4.2.4 Cycle stability .....</b>	<b>19</b>
<b>4.2.5 Rate performance.....</b>	<b>20</b>
<b>4.2.6 Self-discharge .....</b>	<b>20</b>
5. Membrane classifications and preparations .....	21
<b>5.1 Cation-exchange membranes.....</b>	<b>21</b>
<b>5.1.1 Pure Nafion membranes .....</b>	<b>21</b>
<b>5.1.2 Modified Nafion membranes.....</b>	<b>22</b>
<b>5.1.2.1 Combining with other polymers.....</b>	<b>22</b>
<b>5.1.2.2 Combining with organic/inorganic materials .....</b>	<b>25</b>
<b>5.1.3 Other polymeric cation-exchange membranes.....</b>	<b>27</b>
<b>5.1.3.1 Sulfonated poly(ether ether ketone) (SPEEK)-based.....</b>	<b>28</b>
<b>5.1.3.2 Sulfonated polyimide (SPI)-based .....</b>	<b>30</b>
<b>5.1.3.3 Sulfonated poly (fluorenyl ether ketone) (SPFEK)-based .....</b>	<b>31</b>
<b>5.1.3.4 Polytetrafluoroethylene (PTFE)-based .....</b>	<b>32</b>
<b>5.1.3.5 Poly(ether sulfone) (PES)-based.....</b>	<b>33</b>
<b>5.1.3.6 Poly(vinylidene fluoride) (PVDF)-based .....</b>	<b>33</b>

5.1.3.7 Sulfonated poly(phthalazinone ether ketone) (SPPEK)-based .....	35
5.1.3.8 Other polymers-based .....	36
5.2 Anion-exchange membranes .....	37
5.2.1 Polysulfone (PSF)-based .....	38
5.2.2 Poly(aryl ether ketone) (PAEK)-based .....	39
5.2.3 Other polymers-based .....	39
5.3 Amphoteric-ion exchange membranes .....	41
5.3.1 Poly(vinylidene fluoride) (PVDF)-based .....	42
5.3.2 Other polymers-based .....	43
5.4 Porous membranes .....	44
5.4.1 Polybenzimidazole (PBI)-based .....	44
5.4.2 Poly(ether sulfone) (PES)-based .....	46
5.4.3 Polyacrylonitrile (PAN)-based .....	48
5.4.4 Porous glass-based .....	49
5.4.5 Other polymers-based .....	50
5.5 Summary .....	51
6. Transport mechanisms .....	56
6.1 Proton transport .....	56
6.2 Vanadium-ion transport .....	57
6.3 Water transport .....	59
7. Performance-enhancing strategies for membranes .....	61
7.1. Adjusting sulfonation degree .....	62
7.2. Blending/compositing with other polymers .....	63
7.3. Tuning pore structural parameters .....	65
7.4. Tuning geometric parameters and designs .....	66
7.5. Adding inorganic materials .....	67
8. Cost and commercialization .....	68
8.1 Cost .....	68
8.2 Commercialization .....	69
8.2.1 Membrane level .....	69
8.2.2 Battery level .....	71
9. Remaining challenges and perspectives .....	74
References .....	76

# **Polymer Electrolyte Membranes for Vanadium Redox Flow Batteries: Fundamentals and Applications**

Xingyi Shi<sup>1#</sup>, Oladapo Christopher Esan<sup>1#</sup>, Xiaoyu Huo<sup>1</sup>, Yining Ma<sup>1</sup>, Zhefei Pan<sup>1</sup>, Liang An<sup>1\*</sup>, T.S. Zhao<sup>2\*</sup>

<sup>1</sup> Department of Mechanical Engineering, The Hong Kong Polytechnic University, Hung Hom, Kowloon, Hong Kong SAR, China

<sup>2</sup> Department of Mechanical and Aerospace Engineering, The Hong Kong University of Science and Technology, Clear Water Bay, Kowloon, Hong Kong SAR, China

<sup>#</sup>Equal contribution.

\*Corresponding authors.

Email: [liang.an@polyu.edu.hk](mailto:liang.an@polyu.edu.hk) (L. An)

Email: [metzhao@ust.hk](mailto:metzhao@ust.hk) (T.S. Zhao)

## **Abstract**

Electrochemical energy storage systems are considered as one of the most viable solutions to realize large-scale utilization of renewable energy. Among the various electrochemical energy storage systems, flow batteries have increasingly attracted global attention due to their flexible structural design, high efficiencies, long operating life cycle, and independently tunable power and energy storage capacity. Although promising, a number of challenges including the high cost of flow battery materials hinder the broad market penetration of flow battery technology. Polymer electrolyte membrane, as a key component in flow batteries providing pathways for charge carriers transport and preventing electrolytes crossover, takes over 25 % of the entire cost of the battery system. Apparently, the membrane not only plays pivotal roles in the operation characteristics of a flow battery, but also largely influences the financial cost of the battery system. To provide insights and better understanding of membranes towards enhancing their performance and cost-effectiveness, we therefore present recent advances and research outcomes on the development of polymer electrolyte membranes as well as their applications

in flow batteries, particularly all-vanadium redox flow batteries. Various aspects of polymer electrolyte membranes including functional requirements, characterization methods, materials screening and preparation strategies, transport mechanisms, and commercialization progress are presented. Finally, perspectives for future trends on research and development of polymer electrolyte membranes with relevance to flow batteries are highlighted.

**Keywords:** Flow batteries; Polymer electrolyte membranes; Materials screening; Preparation and characterization methods; Transport mechanisms; Commercialization

## 1. Introduction

The continuous usage of inefficient (fossil) fuels in tandem with the ever-increasing and energy-consuming activities in the present society has led to severe energy crisis and environmental pollution, thereby necessitating the needs to deploy unconventional, yet efficient, energy sources. Renewable energy sources, such as wind and solar, have been widely recognized as sustainable alternatives towards achieving clean energy and reliable electricity generation.<sup>1-4</sup> However, due to the intermittent nature of these renewable energy sources, their grid applications for continuous and reliable power supply are still constrained.<sup>5-9</sup> To address this issue, several energy storage technologies including compressed air, pumped hydro, supercapacitors, and solid-state batteries have been developed over the years. However, the site-dependence and high financial implications of compressed air and pumped hydro, low storage capacity and high self-discharge rate of supercapacitors, thermal runaway effect and safety challenges of lithium-ion batteries, and short life cycle and inherent hazards of lead-acid batteries significantly limit the widespread and large-scale applications of these technologies.<sup>7, 10-14</sup> The quest to resolve these challenges therefore led to the revolution of electrochemical energy storage systems through the emergence of flow battery technology.

The various advantages of flow battery systems positioned them as one of the most promising technologies suitable for large-scale electrochemical energy storage applications. One of the major advantages of flow batteries is their independently tunable energy and power capacity. Unlike conventional batteries whose energy and power capacity are both dependent on the electrode properties, the energy capacity of flow batteries solely depends on the volume and

concentration of their electrolyte solution, while the power capacity is a function of the porous electrode geometry and the number of cells available in the stack.<sup>15, 16</sup> In addition, flow batteries exhibit short response time as they store electrical energy using two different types of redox couple as electroactive species. Structural design flexibility and long-term operation with cycling stability are some other advantages of flow batteries. Attracted by the above-mentioned advantages and other intriguing characteristics, different types of flow battery technology such as aqueous redox flow batteries (RFBs)<sup>17-24</sup>, hybrid flow batteries,<sup>25, 26</sup> organic flow batteries<sup>4, 27-36</sup> and semi-solid flow batteries<sup>37-39</sup> have been developed and investigated.<sup>40-44</sup>

A typical flow battery system, as shown in **Fig. 1**, comprises a cell, two external electrolyte tanks (for electrolytes storage), pumps (for electrolyte delivery into the cell), and other accessories.<sup>7, 16</sup> A single cell generally comprises a positive electrode and a negative electrode separated by a polymer electrolyte membrane. In terms of redox couples or battery chemistries, several types of flow batteries, including but not limited to all-vanadium redox flow battery (VRFB), zinc-bromine, iron-chromium, and polysulfide-bromine flow batteries have been proposed. Among them, the VRFB is the most well-studied and developed flow battery technology for large-scale energy storage due to the use of vanadium in its two electrolyte solutions. This therefore prevents cross-contamination of electrolytes, a major challenge, which is seemingly unavoidable in other flow battery chemistries. As a result of this unique feature, VRFBs boast of high round-trip efficiency, long operating life cycle (above 20 000 cycles),<sup>45</sup> low maintenance cost, low environmental footprint and toxicity, and effortless recycling of electrolytes compared to several other energy storage technologies.<sup>46-48</sup> VRFBs are, however, not without their challenges and shortcomings, such as degradation of materials and capacity, low power and energy density, and high capital cost, which currently limit the widespread application of this technology. Hence, more attention on the research and development on VRFBs materials such as fabrication of new membranes, advancing electrodes properties, and improving electrolyte composition are essentially required for performance enhancement, cost-effectiveness, and widespread commercialization.

Polymer electrolyte membrane is one of the key components in flow batteries which plays significant roles on the performance and cost of flow batteries. During the operation of a flow battery, membrane physically separates two half-cells, functionally conducts charge-carrier, minimizes cross-contamination, and prevents short-circuit.<sup>49,50</sup> However, it has been analyzed that polymer electrolyte membranes often claim over a quarter of the total capital cost of a flow battery system.<sup>51</sup> Hence, the selection and synthesis of membrane materials, as well as membrane designs and preparations, are crucially important for achieving a high-performance, and cost-effective flow battery. Up till now, several types of polymer electrolyte membrane have been developed for flow battery applications and are generally classified into: cation-exchange membranes, anion-exchange membranes, amphoteric-ion exchange membranes and porous membranes based on the type of fixed charges present in their matrix structures.<sup>52</sup> Thus, the identification, understanding and development of appropriate polymer electrolyte membranes that offer an optimal balance between performance and cost is currently one of major concerns for the global development of flow batteries. To date, a few review papers<sup>50,52-61</sup> have been published to summarize the various types of membranes that have been developed for use in flow batteries. Some of the previously published review papers, however, mainly focused on a specific type of membranes, for instance porous membranes<sup>50,55</sup> or anion-exchange membranes,<sup>57,62</sup> hence they did not capture other types of membrane employed in flow batteries. Elsewhere, Li et al.<sup>54</sup> discussed ion exchange membranes without including the amphoteric-ion exchange membranes. Even though a number of reviews<sup>52,58,59,61</sup> discussed the development of cation and anion-exchange membranes, amphoteric-ion exchange membranes, and porous membranes; detailed understanding on the transport phenomena, performance evaluations, cost and commercialization progress of these membranes were not considered. Shin et al.<sup>56</sup> also reviewed some membrane candidates appropriate for non-aqueous redox flow batteries. Apparently, discussions on materials selection for polymer electrolyte membranes are not sufficient in all these reviews. Other than this, the flow batteries have received increasing attentions and significant progress in recent years, particularly for membrane research and development. Consequently, a timely and contemporary review of polymer electrolyte membranes for flow batteries is of vital importance for information and

knowledge update. This article therefore presents a comprehensive review on the recent advances and developments of polymer electrolyte membranes and their applications in all-vanadium redox flow batteries.

## **2. The focus of the article**

The widespread commercialization of flow batteries still encounters some critical issues and challenges. Elimination of these lingering barriers demands a rudimentary understanding of the key material components, such as membrane, in flow battery systems. To this end, a comprehensive review on the latest advances and developments of polymer electrolyte membranes for flow batteries which covers several aspects on membrane research and development is needed. Hence, this article focuses on the various types of polymer electrolyte membrane employed in the design and operation of flow batteries, particularly for VRFBs. The characterization methods both at membrane and cell levels, state-of-the-art membrane materials with their properties and performances, and transport mechanisms of electroactive species and water across the polymer electrolyte membranes are discussed. The current advances and research outcomes on the development of these membranes are comprehensively reviewed towards stimulating rational designs and development of high-performance and cost-effective membranes. Strategies for enhancing the performance of these membranes, as well as their cost and commercialization progress at membrane- and battery-levels are presented. The remaining challenges and perspectives for future trends on the research and development of polymer electrolyte membranes with relevance to flow batteries are highlighted.

The remaining parts of this article are organized as follows: Section 3 states the functional requirements of polymer electrolyte membranes for flow battery applications. Section 4 presents the performance indicators at membrane- and cell- levels. Section 5 summarizes the various classifications of polymer electrolyte membrane and their preparation methods. Section 6 discusses the transport mechanisms through the membranes. Section 7 identifies the potential strategies for performance enhancement of membranes. Section 8 presents the cost at membrane- and battery-levels as well as the commercialization progress of flow battery technology. Finally, Section 9 highlights the remaining challenges and future perspectives

necessary for performance enhancement of polymer electrolyte membranes and flow battery systems.

### **3. Functional requirements**

Over the years, several types of flow battery have been proposed and studied. According to the types of electrolyte used and the structural design, flow battery technology can be primarily classified into aqueous, hybrid, organic, and semi-solid. The VRFB is the most developed aqueous RFB system and has received many successful installations and applications in several countries. It has also been widely studied and broadly investigated using different types of membrane. Hence, this section specifically highlights the functional requirements of membranes suitable for application in VRFBs. One of such requirements is high ionic conductivity. It has been widely reported that membranes with high ionic conductivity provide VRFBs with low ohmic loss,<sup>63</sup> which is crucially important towards reducing polarization loss under high current density operation.<sup>64</sup> In the meanwhile, low membrane permeability to electroactive species is also of paramount importance as it is closely related to vanadium-ion crossover phenomenon, which often leads to system capacity loss.<sup>65</sup> Hence, it is required of the membrane employed in VRFBs to be effectively selective to distinguish protons from vanadium ions, thereby maintaining a balanced ionic conductivity and vanadium-ion permeability for high coulombic efficiency and stable cycle performance.<sup>7, 50, 54, 66</sup> Moreover, the polymer electrolyte membrane for VRFBs should also be able to suppress the preferential transport of water between two half-cells for proper electrolyte balance, to avoid dilution/flooding and precipitation/over concentration of electrolyte solutions. A certain level of mechanical strength is another essential requirement for a membrane to be used in VRFBs. Such mechanical property would not only influences the assembling process of the battery, but also contributes to the system durability. Other essential requirements including thermal and chemical stabilities are also necessary for an ideal polymer electrolyte membrane in VRFBs to attain widespread applications and commercialization.<sup>46, 52</sup> All these functional requirements therefore significantly contribute to the performance of the membrane as well as the entire battery system as discussed in the following section.



## 4. Performance indicators

Polymer electrolyte membrane is an indispensable component in flow batteries, which not only separates the catholyte and the anolyte to prevent their mixing, but also provides channels for ionic transport to complete the electrical circuit and ensure electroneutrality. Nowadays, the most widely used polymer electrolyte membranes for flow batteries are the commercial Nafion series membranes,<sup>67</sup> which possess excellent proton conductivity and chemical stability. However, the high crossover rate of electroactive species and high cost of these membranes are major concerns influencing their application in flow batteries.<sup>68-70</sup> It is therefore of paramount importance to develop polymer electrolyte membranes that offer superior performance at membrane and cell levels while fulfilling affordable-cost requirement. To systematically and accurately characterize polymer electrolyte membranes, various methods have been developed and applied to evaluate their performance at both membrane- and cell-levels. In this section, the generally accepted methods and testing conditions for membrane characterizations with the typical reported value range of Nafion series are summarized.

### 4.1 Membrane level

#### 4.1.1 Ionic conductivity

As previously mentioned, one of the most important functions of a polymer electrolyte membrane in VRFBs is to provide pathways for charge carriers so as to complete the electrical circuit. Hence, ionic conductivity, which indicates the smooth transport of charge carriers through polymer electrolyte membranes, is considered as a major indicator for membrane performance evaluation. A high ionic conductivity therefore reveals that charge carriers can easily transport through the membrane, which in turn results to a high voltage efficiency. On the other hand, membranes with low ionic conductivity causes large internal resistance and thus limits the battery performance, especially at high discharging current densities. The electrochemical impedance spectroscopy is the most widely used method for evaluating the ionic conductivity ( $\sigma$ ) of membranes:<sup>71, 72</sup>

$$\sigma \text{ (S cm}^{-1}\text{)} = \frac{d}{RS} \quad (1)$$

where  $S$ ,  $d$ , and  $R$  represent the effective area, thickness of the membrane, and the impedance,

respectively. To date, several configurations, such as two-probe and four-probe systems as demonstrated in Refs.<sup>67, 73, 74</sup>, have been developed to determine the ionic conductivity of membranes used in VRFBs. It is worth mentioning that, while many studies conducted the ionic conductivity test of membranes in deionized water,<sup>75-77</sup> some have also performed the test in sulfuric acid<sup>67, 78</sup> or vanadium electrolyte<sup>79</sup> which is the actual scenario during the operation of VRFBs. Considering the real operating condition in VRFBs, the evaluation of membrane conductivity using vanadium electrolyte would provide substantial information relevant to membranes used in the battery system. The most widely used Nafion series membranes possess excellent ionic conductivity, which has been mostly reported to be within the range of 50-100 mS cm<sup>-1</sup>.<sup>67, 75, 80</sup> Therefore, to ensure rapid and smooth ionic transport via a membrane to be employed in a VRFB, such membrane is required to have a comparable ionic conductivity to that of the Nafion series.

#### 4.1.2 Water/Electrolyte uptake

The water uptake (WU) ratio of a polymer electrolyte membrane indicates its capability to absorb water. This is an important parameter for evaluating the performance of membranes such as Nafion as water uptake commonly leads to the dissociation of the ion pairs between the fixed ion exchange group and movable ions,<sup>81</sup> and therefore has a major influence on the membrane ionic conductivity and permeability. Considering the aqueous electrolyte environment within the cell, WU therefore plays significant roles on the performance of membranes used in VRFBs. The water uptake ratio of a membrane is not only influenced by the hydrophilic property of its polymer matrix and morphology, but also the density of polymer network.<sup>82</sup> Normally, the water uptake ratio is measured by first immersing a dry membrane into deionized water, afterwards the change in the membrane weight is calculated using:<sup>69, 83</sup>

$$\text{Water uptake(\%)} = \frac{W_w - W_d}{W_d} \times 100\% \quad (2)$$

where  $W_w$  and  $W_d$  are the weight of the wet and dry membrane, respectively. Many investigations have shown that an increase in the water uptake ratio of a membrane enhances its ionic conductivity as well as vanadium-ion permeability. However, this can also result in poor mechanical properties and stability of the membrane.<sup>84-86</sup> The Nafion series membranes have been tested and reported to have a water uptake ratio within 20-40 %.<sup>69, 76, 77</sup> While such

water uptake ratio facilitates the transport of protons through the membrane, the Nafion series membranes are exposed to high permeability of active species and undesired effects. Therefore, the membranes prepared for RFBs are desired to possess an optimized water uptake ratio in order to attain an optimal balance among other properties mentioned above. However, it is also worth to mention that, while many studies investigated the water uptake ratio of membranes, even for membranes applied in VRFBs, some researchers have examined the electrolyte uptake ratio of membrane.<sup>87</sup> The electrolyte uptake is measured using the same strategy as water uptake ratio while simply replacing the water with vanadium electrolyte solution. Considering the real operating condition in VRFBs, electrolyte uptake would provide better and substantial value relevant to membrane properties.

#### **4.1.3 Ion exchange capacity (IEC)**

Similar to the water uptake ratio, the ion exchange capacity (IEC) is another prominent parameter that influences the ionic conductivity and vanadium-ion permeability of polymer electrolyte membranes. IEC quantifies the ability of a membrane to provide paths for ions transport. This is primarily determined by the number of ion-exchange functional groups present in the polymer electrolyte membrane.<sup>88</sup> In VRFBs, insufficient ions transport across a membrane, as a result of low ion exchange capacity, leads to large ohmic loss and further limits the overall battery performance.<sup>89</sup> Hence, it is essential for the ion exchange membranes to possess high IEC so as to ensure superior battery performance. The IEC is often determined using titration method as described in Refs.<sup>90-92</sup> The aqueous solutions employed for IEC measurement of cation-exchange membranes and anion-exchange membranes are typically different. For cation-exchange membranes, the mostly used aqueous solutions for the IEC measurement are NaCl and NaOH. The measurement is conducted by weighing the dry membrane and then immersing it into NaCl solution for 24 hours to completely exchange H<sup>+</sup> in the membrane with Na<sup>+</sup>. After that, NaOH solution is used for titration to determine the amount of H<sup>+</sup> released from the membrane. The IEC of the cation-exchange membrane is thus calculated using:<sup>76, 93, 94</sup>

$$\text{IEC} = \frac{V_{\text{NaOH}} \times C_{\text{NaOH}}}{W_d} \quad (3)$$

where  $C_{NaOH}$  and  $V_{NaOH}$  represent the concentration and volume of NaOH solution used for titration, respectively, while  $W_d$  represents the weight of dry membrane.

On the other hand,  $NaNO_3$  and  $AgNO_3$  solutions are mostly used for determining the IEC of anion-exchange membranes. In this case, the anion-exchange membranes are first immersed into the  $NaNO_3$  solution for 24-48 hours to completely release  $Cl^-$  ions from the membrane. After this, the  $AgNO_3$  solution is used to titrate the released  $Cl^-$  ions. The IEC is thus calculated using:<sup>95, 96</sup>

$$IEC = \frac{V_{AgNO_3} \times C_{AgNO_3}}{W_d} \quad (4)$$

where  $C_{AgNO_3}$  and  $V_{AgNO_3}$  represent the concentration and volume of  $AgNO_3$  solution used for titration, respectively. It has been reported in literatures that the IEC of Nafion series membranes is between 0.85-0.95 mmol  $g^{-1}$ .<sup>76, 97, 98</sup> For the cation-exchange membranes, high IEC facilitates proton transport, even though it may also increase the permeability of active species across the membrane. It is thus important for the membranes employed in RFBs to possess a suitable IEC value that allows high ionic conductivity while reducing the crossover rate of electroactive species.

#### 4.1.4 Vanadium-ion permeability/diffusivity

The transport of vanadium ions through the polymer electrolyte membrane in a flow battery not only causes self-discharge, but also influences the cycling stability of the battery. In addition, it may also lead to membrane fouling, which generally occurs during long-term operation, especially for cation-exchange membranes. For vanadium-based electrolytes, two types of fouling mechanism have been reported, which are cation deposition on membrane surface and cation accumulation inside proton-conducting channels.<sup>99</sup> Such phenomena can further reduce ionic conductivity of membrane and also increase membrane resistance, which in turn result in the degradation of battery system. Many studies have shown that high crossover rate of vanadium ions through the membrane results in self-discharge, low coulombic efficiency, and poor cycle stability of the battery.<sup>100-102</sup> It is therefore crucial to examine the permeability of membranes to vanadium ions.

During the operation of VRFBs, the transport of different species including water, vanadium ions, and protons are highly coupled. Regarding the vanadium ions, not only  $\text{VO}^{2+}$  and  $\text{VO}_2^+$  ions transport through the membrane from the positive side to the negative side of the battery,  $\text{V}^{2+}$  and  $\text{V}^{3+}$  ions also transport through the membrane in the reverse direction. Hence, the comprehensive study of the permeabilities of each vanadium ion should be regarded with equal importance. Over the years, several studies have examined the permeabilities of these vanadium ions and each vanadium-ion has been reported with its diffusivity,<sup>101, 103, 104</sup> which is slightly different from that of other vanadium ions, attributed to their different ion sizes and carried charges.<sup>105</sup> Furthermore, it is also found that different studies have reported different values and trends for the permeability of these vanadium ions, which may be attributed to the different membrane compositions and structures in those studies.<sup>101, 106</sup> However, it is also worth to mention that, while some studies evaluated the membrane permeability of different vanadium ions, many studies still examined the vanadium-ion permeability of membrane using electrolyte containing only  $\text{VO}^{2+}$  ions, due to the fact that  $\text{VO}^{2+}$  ions possess the best stability in the open air and therefore allows the easy and precise concentration examination during permeability measurement. In more details, the vanadium-ion permeability test is commonly conducted using  $\text{VOSO}_4$  solution, where the membrane is first placed between two separate reservoirs each filled with  $\text{VOSO}_4$  and  $\text{MgSO}_4$  solution, respectively, as shown in **Fig. 2 (a)**. Thereafter, the solution samples are collected from the reservoir with  $\text{MgSO}_4$  solution at regular time-intervals to measure the concentration of  $\text{VO}^{2+}$  for calculation.<sup>107, 108</sup> The formula used for vanadium-ion permeability ( $P$ ) calculation is given as:<sup>109, 110</sup>

$$V_R \frac{dC_R(t)}{dt} = A \frac{P}{L} (C_L - C_R(t)) \quad (5)$$

where  $V_R$  is the solution volume of the compartment without  $\text{VO}^{2+}$  at the beginning and  $C_R(t)$  is the concentration of  $\text{VO}^{2+}$  in the compartment.  $C_L$  is the concentration of  $\text{VO}^{2+}$  in the other compartment containing  $\text{VO}^{2+}$  at the beginning.  $A$  and  $L$  are effective area and thickness of the membrane, respectively. Mostly, the Nafion series membranes have been reported to have a vanadium-ion permeability within the range of  $300\text{-}400 \times 10^{-8} \text{ cm}^2 \text{ min}^{-1}$ , which is relatively high and therefore results in fast capacity degradation during battery operation.<sup>91, 102</sup> In comparison, some modified Nafion membranes have been reported with much lower vanadium

ions permeability of  $< 100 \times 10^{-8} \text{ cm}^2 \text{ min}^{-1}$ .<sup>68, 111, 112</sup> However, it is worth noting that, for a membrane with a low crossover rate of vanadium ions, it may also possess a limited ionic conductivity, which further limits the voltage efficiency. Therefore, it is of vital importance to achieve an optimal balance between ionic conductivity and crossover rate of membranes. In essence, the ideal polymer electrolyte membrane for flow batteries is desired to simultaneously possess high ionic conductivity and low permeability of vanadium ions for performance improvement of both membrane and battery.

#### **4.1.5 Chemical stability**

The chemical stability of a polymer electrolyte membrane indicates its capability to withstand the extreme chemical environment within the cell of a battery system. It is essential for polymer electrolyte membranes used in flow batteries to possess superior chemical stability so as to minimize membrane degradation and ensure long-term cycling operation of the battery. As pointed out by previous studies, the oxidation of polymer is one of the major reasons for membrane degradation. For instance, in VRFBs, the corrosive electrolytes may react with the membrane which could result to side reactions during charge and discharge processes. Such reactions often reduce the concentration of electroactive species in the electrolyte and further lead to capacity loss. Apart from this, the degradation of the membrane due to severe oxidation by  $\text{VO}^{2+}$  ions in the electrolyte can also result in poor stability both for the membrane and the battery.<sup>113</sup> A detailed analysis of the degradation processes of sulfonated poly(sulfone) membranes in VRFB system was presented by Kim et al..<sup>114</sup> After 50 cycles of operation, utilizing the energy dispersive X-ray spectroscopy, a band with high vanadium and low sulfur content was observed on the membrane surface, which was found to correspond to the loss of sulfonate  $\text{SO}_2$  stretch as shown in a Raman spectroscopy. Such result demonstrated the chemical degradation of the membrane, while the cyclic formation of precipitates observed inside the membrane can also introduce mechanical stress, which could be a major degradation mode for aromatic membranes used in VRFBs.

The evaluation of the oxidative stability of a membrane is commonly conducted by immersing the membrane into an electrolyte solution of  $\text{VO}_2^+/\text{H}_2\text{SO}_4$ . Afterwards, the concentration

variation of the  $VO^{2+}$  in the solution at regular time intervals is examined. Following this, the amount of  $VO^{2+}$  obtained from the reduction of  $VO_2^+$  is used to analyze the oxidative stability of the membrane, mathematically expressed as:<sup>115</sup>

$$\text{Reduction rate(\%)} = \frac{c(VO^{2+})}{c(VO_2^+)} \times 100\% \quad (7)$$

where  $c(VO^{2+})$  represents the final concentration of  $VO^{2+}$  after the test and  $c(VO_2^+)$  represents the initial concentration of  $VO_2^+$  before the test. Nafion membranes have been reported to reduce 1 % of the  $VO_2^+$  to  $VO^{2+}$  after 21 days, thereby showing superior chemical stability.<sup>76</sup> In addition, the chemical stability of the membrane can also be determined by measuring the weight of the membrane both before and after immersing it into  $VO_2^+/H_2SO_4$  electrolyte solution to calculate the membrane weight loss as follows:<sup>115</sup>

$$\text{Weight loss(\%)} = \frac{W_b - W_a}{W_b} \times 100\% \quad (8)$$

where  $W_b$  and  $W_a$  represents the membrane weight before and after the chemical stability test, respectively. Through these results, membrane degradation can therefore be quantified. Other methods such as using the scanning electron microcopy (SEM) to monitor the morphological changes in membrane before and after the chemical test can also be employed to confirm the chemical stability of membrane structure.<sup>116</sup> The chemical stability of membrane in VRFBs is not only dependent on the oxidative stability of the membrane, but also relates to its hydrolytic stability considering the cell operating condition. Following this, membrane degradation caused by water in the electrolyte have also been reported.<sup>117</sup> This is due to the fact that water molecule can break the polymer chain and then significantly affect the mechanical strength of the membrane and even lead to the breakdown of the membrane structure.<sup>118</sup> For the hydrolytic stability test, the membrane is first immersed into hot water for a period of time, and then the changes of the membrane properties such as mechanical properties, morphology changes, conductivity, and weight loss are evaluated to assess the membrane stability.<sup>117, 119, 120</sup>

#### 4.1.6 Thermal stability

The thermal stability is another important criterion to be considered when evaluating

membrane performance. An increase in operating temperature has been severally reported as an effective method to enhance the performance of flow batteries. For example, the performance of a VRFB has been reported with a peak power density increment from 259.5 to 349.8 mW cm<sup>-2</sup> when the operating temperature was increased from 15 to 55°C.<sup>121</sup> Hence, it is essential for a polymer electrolyte membrane to possess excellent thermal stability which allows the battery to safely operate under wide operational temperature range. The thermal stability of membrane is commonly determined through the thermogravimetric test (TGA).<sup>93, 122</sup> During this test, the membrane is heated at rate of 10 °C min<sup>-1</sup> under nitrogen conditions while the membrane weight loss is recorded during the heating process to evaluate its thermal stability. The TGA results with a lower weight loss at higher temperature indicates a better thermal stability. Generally, for the Nafion series membranes, the major decomposition happens at temperature around 400-500°C with the final residue weight lower than 10 %.<sup>76, 80</sup> It is also worth to note that, as VRFBs would normally not operate under an operating temperature higher than 100 °C, it is more reasonable to investigate the thermal stability of membrane at temperatures below 100 °C, which therefore underscores the importance of investigating membrane shrinkage under high operating temperatures.<sup>123</sup>

#### **4.1.7 Mechanical property**

The mechanical strength of a membrane not only influences its long-term stability, but also plays a vital role during the preparation process as the membrane may undergo compression as well as stretching during fabrication. Generally, membranes with high mechanical strength have been reported to ease the assembling process of battery system and also increase the lifetime of batteries. It is worth to mention that the mechanical property of a polymer electrolyte membrane not only depend on intrinsic parameters such as the type of material used, but can also be affected by its thickness. To evaluate the mechanical property of membrane, tensile testing machine, as shown in **Fig. 2 (b)**,<sup>98</sup> is usually applied to determine the ultimate tensile strength of the membrane as well as its elongation at break.<sup>84, 109</sup> The test has been reported to be conducted with membrane under both dry and wet conditions.<sup>98, 112, 124, 125</sup> It is not only important for the membrane to be mechanically stable under dry condition so as to prevent rupture or damage during the fabrication and assembling process of battery system, but also of



equal importance for it to be stable under wet condition to ensure long-term stability of the battery. High ultimate tensile strength and elongation at break demonstrate a membrane with mechanical stability. For instance, the widely used Nafion membranes have been reported to possess a tensile strength within the range of 14-24 MPa with an elongation of 170-250 % under both wet and dry conditions.<sup>77, 80, 98, 112</sup> This could serve as a benchmark for assessing the mechanical properties of membranes to be used in flow batteries.

## 4.2 Cell level

While all the performance evaluation parameters discussed in **Section 4.1** allow the comprehensive characterization of the properties of polymer electrolyte membranes, it is also of vital importance to evaluate the ultimate performance of membranes when used in a flow battery system. Therefore, to evaluate membrane performance at the cell level, charge-discharge performance, long term stability, and self-discharge rate are commonly carried out.<sup>126,</sup>

127

### 4.2.1 Polarization curve

The polarization curve is one of the methods commonly employed to illustrate the relationship between voltage output and applied current density in flow batteries. In other words, the curve can be used to investigate the response of cell voltage with change in current to further provide information about the system performance.<sup>128</sup> Other than this, the contribution of different polarization losses including the activation loss, ohmic loss, and mass transport loss can be analyzed with a polarization curve (**Fig. 3**).<sup>129</sup> The activation loss, dominant at low current density region, is majorly influenced by the activation energy required to initiate the electrochemical reaction. The ohmic loss is attributed to the ohmic resistance of the cell components. The mass transport loss results from the consumed reactive species near the electrode surface, which is dominant at the high current density region where reactants are depleted.<sup>130, 131</sup> The shape of the polarization curve can also reveal the dominant overpotential limiting the cell performance. However, it should be noted that the polarization curve may not be able to provide sufficient information to identify the causes of these overpotentials. To perform the polarization test, the cell is usually charged to a state of charge (SOC) of ~50-100 .<sup>121, 132</sup> Then, the curve is obtained through recording and plotting the cell voltage at various

current densities to reveal the relationships between these parameters. With this, the power density curve can also be obtained by multiplying the cell voltage with the corresponding current density, from which the peak power density that can be delivered from the cell can be revealed.

#### **4.2.2 Charge-discharge performance**

Charge-discharge test is also an important method that is mostly used in evaluating the performance of membrane at cell level. This test is conducted by charging and discharging the cell at a fixed current, in order to examine the cell performance for energy storage and power generation under operation conditions that is very close to its real application. It is therefore considered as one of the most standard tests that can be used to evaluate the cell performance. For the charge-discharge cycle test, the discharge capacities and the charge-discharge profiles of the cell are the most important results for performance evaluation. While the discharge capacity indicates the highest amount of electric charge the cell can deliver, the charge-discharge profile reveals the charge and discharge voltage of the cell. The ideal polymer electrolyte membrane in flow batteries is desired to provide the cell with high and stable charge/discharge capacity, low charge voltage, and high discharge voltage. In VRFBs, the charge-discharge test is generally conducted using the battery testing system with a voltage range of ~0.7-1.7 V at a constant current density between ~20-100 mA cm<sup>-2</sup>.<sup>133-135</sup> Normally, for the VRFB using the Nafion series membranes and operating at 20-100 mA cm<sup>-2</sup>, the cell is able to achieve a voltage plateau of ~1.1-1.35 V during discharging and a voltage plateau of ~1.35-1.5 V during charging.<sup>67, 136, 137</sup>

#### **4.2.3 Coulombic, Voltage, and Energy efficiencies**

Apart from the charge-discharge profile, the coulombic, voltage, and energy efficiencies are three important efficiencies that are popularly used in evaluating the performance of batteries.<sup>138</sup> The coulombic efficiency is a performance indicator that evaluates the ratio of the discharge capacity to the charge capacity of a cell, while the voltage efficiency is an indicator for evaluating the overpotential losses during charging and discharging process. Many studies have shown that high coulombic efficiency can be mainly achieved when there is low

permeability of vanadium ions through the membrane, which further improves the capacity retention ability of the battery.<sup>127, 139</sup> On the other hand, high voltage efficiency is attributed to superior ionic conductivity of membrane and low internal resistance within the cell.<sup>68, 140</sup> Energy efficiency, which is commonly expressed as the product of coulombic efficiency and voltage efficiency, precisely indicates the overall performance of flow battery systems. The calculation of these three efficiencies are obtained using:<sup>141</sup>

$$CE = \frac{Q_{dis}}{Q_{cha}} \times 100\% \quad (9)$$

$$VE = \frac{V_{dis}}{V_{cha}} \times 100\% \quad (10)$$

$$EE = CE \times VE \quad (11)$$

where  $Q_{dis}$  and  $Q_{cha}$  represent discharge capacity and charge capacity of the cell, respectively. And  $V_{dis}$  and  $V_{cha}$  represent the mean discharge and charge voltage of the cell, respectively. Mostly, the Nafion membranes are reported to provide a coulombic efficiency of ~85-95 %, a voltage efficiency of ~80-95 %, and an energy efficiency of 70-85 % at ~20-100 mA cm<sup>-2</sup> when used in VRFBs.<sup>69, 136, 142</sup>

#### 4.2.4 Cycle stability

The cycle stability of a battery is also a key indicator for evaluating the performance of a membrane. During the operation of VRFBs, the inevitable crossover phenomenon of vanadium ions would result in imbalanced volume and concentration of electrolytes between the two sides of the battery system.<sup>67</sup> Such a phenomenon often results into capacity loss, consequently deteriorating the cycling stability of the battery, which however can be restored by remixing the electrolytes at both sides.<sup>67</sup> In comparison to this, there are also some irreversible capacity loss during long-term operation of the battery, such as the possible side reactions between electrolytes and cell components, and electrolyte leakage which could lead to irreversible loss of reactive species.<sup>143</sup> Even though the cycle stability is not solely dependent on the membrane performance, membrane still plays vital roles in determining the cycle stability of the cell. Generally, the cycle stability of cell is determined by using the same battery testing system as the charge-discharge tests, while mainly focusing on evaluating the stability of the cell performance after long-term operation.<sup>83, 85</sup> The test is conducted by charging and discharging

the cell at a fixed current density for many cycles to examine its capacity retention ability, which is calculated through dividing the discharge capacity of the cell at the last tested cycle by the value at the first tested cycle. The test results with more cycles and better capacity retention ability indicate a better cycle stability and prove the long-term operation capability of both the membrane and battery. For the VRFBs that employ Nafion series membranes, the capacity retention rate are mostly reported to be around 50 % to 90 % after 50-150 cycles.<sup>67, 68,</sup>

98

#### **4.2.5 Rate performance**

The rate performance test is employed in evaluating the charge-discharge performance of cell under various current densities, especially under high current densities, which is of paramount importance during practical applications. It is significant for achieving reduced system size and capital costs, as the cell needs to be operated at high current density and generate high power and efficiencies, which however are often limited by the large polarization loss with increasing of current density.<sup>144</sup> This polarization loss, in more detail, is closely related to the membrane conductivity, which thereby places high ionic conductivity of membrane as a major requirement so as to reduce ohmic loss and increase the efficiencies of the battery system under high current density operation. In addition, it also indicates the battery can provide high efficiencies at a wide range of current densities,<sup>145</sup> which thereby allows the battery to be applied under various working conditions. During the test, results including the discharge capacity, coulombic efficiency, voltage efficiency, and energy efficiency are recorded. High discharge capacity and efficiencies under high current density indicates a better rate performance of the membrane and cell. At a current density range of  $\sim 100\text{-}320\text{ mA cm}^{-2}$ , the VRFBs using the Nafion membranes has been reported to mostly achieve an energy efficiency of  $\sim 55\text{-}85\%$ , which thus greatly limit the operational current density range of the cell.<sup>67, 146, 147</sup>

#### **4.2.6 Self-discharge**

During the actual operation of a flow battery, the active species may inevitably transport through the membrane, which is also known as the vanadium-ion crossover phenomenon. Such process leads to imbalance of electrolyte volume and concentration, and further result to

capacity loss, which is also known as the self-discharge. In the characterization section at membrane level, the transport ability of vanadium ions through the membrane can be evaluated through the vanadium-ion permeability test. However, such testing environment is still slightly different from the actual conditions during charge-discharge processes of flow battery systems. Therefore, to determine the actual influence of vanadium ions transport across the membrane at cell-level, the self-discharge test is needed.

For VRFBs, the self-discharge test of the cell is mostly conducted by first charging the cell to SOC-50<sup>148, 149</sup> and then using the battery testing system to record the change in battery voltage while maintaining the circulating electrolyte. The self-discharge test ends when the open-circuit voltage of cell drops below 0.8 V. A long test duration indicates that the cell has low self-discharge rate. For VRFBs that employs Nafion series membrane, the test duration for evaluating self-discharge rate is generally between 30-60 hours.<sup>80, 125, 137</sup>

## **5. Membrane classifications and preparations**

As mentioned earlier, membrane is an indispensable component in RFBs not only to serve as medium for the transport of charge carriers but also to avoid the crossover of reactive species between two half-cells. Hence, various types of membrane have been developed and studied for the purpose of application in RFBs. These membranes, according to the functional groups attached and their major purpose, can be mainly categorized into cation-exchange membranes, anion-exchange membranes, amphoteric-ion exchange membranes, and porous membranes.

### **5.1 Cation-exchange membranes**

The cation-exchange membrane is the most well-developed and widely used in RFBs. In the pores of cation-exchange membranes, anionic functional groups are intrinsically attached on the polymer backbone to facilitate the transport cations as shown in **Fig. 4 (a)**. Based on the presence of anionic functional group, Nafion-based membranes and many other polymeric membranes are the common cation-exchange membranes commonly employed in RFBs. The latest development on these membranes are summarized and discussed in this section.

#### **5.1.1 Pure Nafion membranes**

The pure Nafion membranes, also known as Dupont's Nafion membranes, are the most widely

applied commercial cation-exchange membranes in flow batteries due to their excellent ionic conductivity and chemical stability. The attractive properties of pure Nafion membranes are established by their distinctive structures, where perfluorovinyl ether groups terminated with sulfonate groups are incorporated onto a stable tetrafluoroethylene (Teflon) backbone.<sup>54</sup> Over the years, different types of Nafion membrane have been produced by Dupont.<sup>67, 150</sup> These membranes have varied thicknesses and present different performances when assembled into flow batteries. This is due to the fact that membrane thickness plays a key role on influencing the membrane properties such as ionic conductivity and vanadium-ion permeability. Hence, to examine the influence of membrane thickness on the performance of a RFB, different types of Nafion membrane including Nafion 112, Nafion 1135, Nafion 115, and Nafion 117 have been used in VRFBs for performance comparison.<sup>67</sup> The obtained properties and performances of these membranes are summarized in **Table S1**. It was found that self-discharge rate, discharge capacity fading rate, and electrolyte volume change rate all reduce with increase in membrane thickness. In contrast, thin membranes presented high ionic conductivity and are thus considered to be more suitable for batteries operating under high current densities. Overall, results from the experimental study show that Nafion 115 membrane possesses the highest performance, among the four types of Nafion membranes investigated, due to its superior balance between ionic conductivity and vanadium ions permeability rendering it as the membrane option most suitable for application in VRFBs.

## **5.1.2 Modified Nafion membranes**

### **5.1.2.1 Combining with other polymers**

The utilization and performance of Nafion series membranes in flow batteries has been severally studied, however, the high capital cost of these membranes greatly restricts their wide applications. Therefore, a lot of research efforts have been made to reduce the amount of Nafion used during membrane preparation while maintaining their excellent performance.

Casting a thin layer of Nafion onto the surface of a polymer substrate has been considered as an effective modification method as it not only improves the membrane performance, but also reduces the cost of the membrane production due to the reduction in the amount of Nafion used

in the process. This method is conducted by pouring or spraying Nafion solution onto the surface of a polymer substrate.<sup>151</sup> The final composite membrane is obtained after the evaporation of the solvents. The membranes prepared by this method are reported to possess uniform thickness, flatness, and dimensional stability.<sup>59</sup> However, due to the relatively weak interaction between the casting layer and the substrate layer, the casting layer is reported to easily dissociate from the substrate layer, particularly after long-term operation, which therefore adversely affect the chemical stability of the membrane.<sup>59, 152</sup> Many studies have been conducted based on this idea while various materials including sulfonated poly(ether ether ketone) (SPEEK),<sup>140</sup> poly(ether sulfone) (PES),<sup>111</sup> polybenzimidazole (PBI),<sup>151</sup> and polytetrafluoroethylene (PTFE)<sup>112, 149</sup> have been cast with a thin layer of Nafion to improve both membrane and battery performances, many of which are summarized in **Table S2**.<sup>108, 110, 111, 151</sup> Among these reported membranes, one successful attempt that achieved low vanadium ions permeability was demonstrated by a PBI-based membrane coated with Nafion.<sup>151</sup> The PBI layer reduces vanadium ions permeability of the membrane, while the Nafion enhances the chemical stability of the membrane. It was found that this composite membrane finally exhibits an apparently reduced vanadium-ion permeability of  $1.95 \times 10^{-9} \text{ cm}^2 \text{ min}^{-1}$  (**Fig. 5 (a)**) and an improved energy efficiency of 76.84 % at  $100 \text{ mA cm}^{-2}$  compared to Nafion 115. Another commercial membrane named VANADion was also developed with this strategy of casting on substrates. The VANADion membrane is composed of a thin layer of Nafion and a porous substrate layer, as shown in **Fig. 5 (b)**, which contribute to the price reduction of the membrane. It has been studied by Zhou et al.<sup>108</sup> for its application in VRFBs. The membrane was reported to exhibit a higher energy efficiency of 76.2 % and electrolyte utilization efficiency of 68.4 % at  $240 \text{ mA cm}^{-2}$  compared to the Nafion 115 with an energy efficiency of 71.3 % and an electrolyte utilization of 54.1 % under the same condition. Such performance therefore place VANADion membrane in advantageous position for more applications in flow battery systems. Immersing a membrane into a Nafion solution is another method widely used for introducing a thin layer of Nafion onto a membrane. For instance, Tian et al.<sup>153</sup> fabricated a Daramic/Nafion composite membrane by soaking a microporous Daramic membrane in a 5 wt. % Nafion solution. The introduced Nafion partially blocked the pores of the membrane leading to a

reduced vanadium ions permeability, which in turn reduced the self-discharge rate and further achieved a longer self-discharge duration of over 1600 mins than the Daramic membrane with ~800 mins. With these results, introducing a thin layer of Nafion on the surface of a porous substrate has been proven to be an effective method for modifying Nafion membranes.

Other than the modification methods mentioned above, blending the Nafion resin with other polymers for membrane preparation is another effective method through which Nafion can be tightly combined with other polymers. Materials including PVDF,<sup>125</sup> PTFE,<sup>76</sup> and others<sup>154</sup> have been directly blended with Nafion to prepare composite membranes and they have all achieved improved performances.

One of the successful attempts which achieved an improved membrane performance was demonstrated by blending the highly crystalline and hydrophobic PVDF polymer with Nafion to fabricate PVDF/Nafion composite membrane. The modification process was not only found to successfully restrain the swelling behavior of the membrane but also improves the ions selectivity of the membrane.<sup>125</sup> In comparison to the recast-Nafion membrane, this composite membrane achieved higher coulombic efficiency of ~93-95 % at 40-80 mA cm<sup>-2</sup> (**Fig. 6 (a)**). With the same strategy, another study utilizing hydrophobic PTFE has also been conducted and a series of Nafion/PTFE blend membranes with various weight ratios were prepared.<sup>76</sup> The obtained composite membrane showed an improved chemical stability with stable cycle performance for over 50 cycles. Thus, the usage of hydrophobic polymers for Nafion modification was demonstrated as a promising method to prevent the crossover of vanadium ions through the membrane and also provide the membrane with better chemical stability. However, this approach may also reduce the ionic conductivity of the membrane due to the hydrophobic nature of the polymer introduced and further leads to a lower voltage efficiency.

Another strategy for combining Nafion with different polymers is to immerse the Nafion membrane into other polymers in order to obtain the Nafion-based composite membrane. Polymers such as (poly)pyrrole<sup>154, 155</sup> have been used to obtain Nafion-based composite membranes through this strategy, which was also found to successfully improve membrane properties and in turn provides the battery with improved performance. Elsewhere, Xi et al.<sup>102</sup>



have used polycation poly(diallyldimethylammonium chloride) (PDDA) and polyanion poly(sodium styrene sulfonate) (PSS) to prepare a multilayer barrier on the surface of Nafion membrane *via* the layer-by-layer self-assembly technique, as shown in **Fig. 6 (b)**. This powerful layer-by-layer technique is based on the adsorption of oppositely charged species onto the membrane alternately using the electrostatic attraction, which can freely control the composition and property of the membrane. In addition to this, it is environmentally friendly and with cost-effectiveness.<sup>156</sup> With the introduction of these barrier layers onto the membrane surface, improved coulombic efficiency of 97.6 % and energy efficiency of 83.9 % compared to the pristine Nafion membrane were obtained. Such a performance improvement is considered to be attributed to the covering of ion-transport pathways and the electrostatic repulsion effect, which further restrict vanadium-ion permeability of the membrane. The improved membrane performance achieved through this strategy, most of which are also summarized in **Table S2**,<sup>76, 125, 154, 157</sup> have proven that combining Nafion with other polymers is an effective solution to achieve a membrane with better cost-effectiveness and improved battery performance compared to pristine Nafion.

### 5.1.2.2 Combining with organic/inorganic materials

The high vanadium-ion permeability of Nafion membranes is one of the major factors hindering their wide application. Thus, much efforts have been invested to reduce vanadium-ion permeability of the Nafion membranes through blending them with various organic and inorganic materials. This idea was first inspired by the promising results obtained from direct methanol fuel cell, where inorganic materials have been proven to efficiently decrease methanol permeability through membrane, as the inorganic materials can block the hydrophilic regions of membranes.<sup>54</sup> Guided by this idea, silicalite,<sup>158</sup> amino-silica,<sup>68</sup> SiO<sub>2</sub>,<sup>97, 104, 159, 160</sup> TiO<sub>2</sub>,<sup>69</sup> delaminated AMH-3,<sup>161</sup> ZrO<sub>2</sub> nanotubes (ZrNT),<sup>100</sup> graphene oxide (GO),<sup>98, 162, 163</sup> fluorocarbon,<sup>80</sup> N,N-dimethylaminoethylmethacrylate,<sup>75</sup> and other materials<sup>77, 91, 142, 164-169</sup> are some of the organic/inorganic materials that have been integrated with Nafion to prepare composite membranes for use in VRFBs. A look at the performance and properties of some of these Nafion membranes recently modified through combining with organic/inorganic materials are summarized in **Table S3**<sup>98, 100, 137, 163, 164, 167-170</sup>. Some of these studies where

significant improvement in battery performance was achieved are discussed in detail below.

One of the techniques that have been employed in introducing organic/inorganic materials into the Nafion membranes is the layer-by-layer self-assembly technique, as discussed above.<sup>137</sup> Lu et al.<sup>79</sup> applied this technique and obtained a novel Nafion-based polymer-inorganic composite membrane. The polycation chitosan (CS) and negatively charged phosphotungstic acid (PWA) were introduced onto the surface of Nafion membrane layer-by-layer. The introduction of CS-PWA multilayers greatly reduced vanadium-ion permeability of the membrane while showing a negligible impact on its proton conductivity. It is considered that the vanadium ion permeability of this membrane is mainly reduced by the multi-layered structure, while the proton conducting PWA helps to retain the ionic conductivity of the membrane. The battery using this membrane exhibits high coulombic (~80 %) and energy efficiencies (~75 %) and long self-discharge duration of ~70 hours compared to a battery using the pristine Nafion membrane, which only possesses a coulombic efficiency of ~77 %, an energy efficiency of ~71 % and a self-discharge duration of ~50 hours. In addition to the fabrication method, the material used also plays a key role in determining the membrane performance. It is suggested that after the modification, the top-layer of the multilayered membrane should exhibit excellent chemical stability and ion conductivity, so as to ensure long-term battery stability and effective ion transport. In the meanwhile, the number of layers and thickness of each layer should also be carefully adjusted so as to ensure proper thickness to achieve lower membrane resistance and vanadium crossover rate at the same time.<sup>54</sup>

GO is a material that has attracted a lot of attention worldwide due to its special two-dimensional layered structure. It has been introduced into Nafion to fabricate a series of GO/Nafion composite membranes with various GO contents.<sup>162</sup> It was found that, after the introduction of GO, the proton conductivity and vanadium ions permeability of the composite membrane decreased, which are attributed to the reduced value of inter-planar space dimension. In order to further maximize the vanadium ions barrier effect of GO, Su et al.<sup>98</sup> therefore designed and prepared an ultra-thin Nafion/GO composite layer on the surface of Nafion membrane using the spin coating method with GO nanosheets in parallel to the surface of

membrane, as shown in **Fig. 6 (c)**. Compared to Nafion 212, this GO/Nafion composite membrane exhibited a reduced vanadium-ion permeability and the batteries using it has been reported to achieve an improved coulombic efficiency of 92.9-98.8 % at 20-100 mA cm<sup>-2</sup>. The membrane also showed an improved balance between vanadium ions permeability and proton conductivity which resulted in an 88.5 % capacity retention ability after 50 cycles.

Other than the GO, catalysts have also been introduced into Nafion membrane for modification. The electrocatalyst tungsten trioxide/super activated carbon was sprayed onto the surface of Nafion membrane to obtain a catalyst coated membrane (CCM).<sup>136</sup> It was found that, the introduction of this catalyst layer on the membrane surface reduces the reaction over-potential due to the excellent electrochemical reactivity of the catalyst, which further results in a voltage efficiency of 85.9 % and an energy efficiency of 81.2 % at 120 mA cm<sup>-2</sup> while the battery with pristine Nafion membrane only presented a voltage efficiency of 81.3 % and an energy efficiency of 76.9 %. Apart from the improved efficiencies offered by the CCM, the membrane also showed an excellent stability with no obvious drop in energy efficiency for 300 cycles.

Utilizing the methods and materials discussed in this section, the modified Nafion-based membranes facilitated the performance improvement of batteries, even at low cost. However, the real application of all these modified Nafion-based membranes is still being held back as their performances are yet to satisfactorily meet the requirements for actual application. One of the major limitations is the poor capacity retention ability of these membranes after a long-term operation. Therefore, these Nafion-based membranes still require further studies before their real applications. More intensified efforts on efficient modifications of Nafion membranes are also needed.

### **5.1.3 Other polymeric cation-exchange membranes**

Although the Nafion membranes can provide an acceptable battery performance for flow batteries, their high cost has greatly restricted the large-scale application of flow batteries. Therefore, many efforts have been devoted into the preparation of new polymeric cation-exchange membranes that could compete with or replace the Nafion membranes. Materials including SPEEK,<sup>70, 85, 94, 124, 148, 171-205</sup> sulfonated polyimide (SPI),<sup>107, 206-222</sup> sulfonated poly

(fluorenyl ether ketone) (SPFEK),<sup>71, 223-227</sup>, PTFE,<sup>84, 228-231</sup> PES,<sup>232-234</sup> PVDF,<sup>103, 235, 236</sup> sulfonated poly(phthalazinone ether ketone) (SPPEK),<sup>141, 237, 238</sup> and many others have been used for membrane preparation and their performance have been examined. Many of these materials are discussed in the following sections together with their performance and limitations.

### **5.1.3.1 Sulfonated poly(ether ether ketone) (SPEEK)-based**

SPEEK, as a sulfonated aromatic polymer, has drawn a lot of attention for membrane preparation in VRFBs due to its low cost, ease of preparation and superior chemical and thermal stabilities.<sup>124</sup> Unlike the structure of Nafion, SPEEK has a less hydrophobic backbone and less acidic sulfonic acid group and therefore leads to a weaker separation between hydrophobic and hydrophilic region. Such a different microstructure hence results in a narrower ion channels and has been proven to exhibit a lower methanol crossover rate when applied in direct methanol fuel cells, in comparison to Nafion series.<sup>52</sup> Therefore, the SPEEK is regarded as a promising candidate for cation-exchange membrane fabrication and have been extensively applied and studied in VRFBs. The properties of SPEEK are highly dependent on the degree of sulfonation (DS).<sup>200, 202, 205</sup> The SPEEK-based membranes with high DS always possess a better ion-conductivity and IEC, although they also show high vanadium-ion permeability and poor mechanical stability which limits their real applications.<sup>171</sup> To gain a better performance and render the SPEEK feasible for real application, a lot of modification methods have been carried out. The major modification methods including the combination of SPEEK with other polymers<sup>85, 94, 171-174</sup>, and the addition of additives<sup>124, 148, 175-178, 196-199</sup> have been successfully reported to improve the performance of SPEEK-based membranes.

As discussed above, one of the major factors hampering the real application of the SPEEK-based membrane with high DS is its poor mechanical strength. Therefore, in order to improve the mechanical properties of SPEEK-based membranes, the hydrophobic PVDF polymer, which has superior mechanical strength, has been introduced into SPEEK to prepare a series of SPEEK/PVDF blend membranes with various mixing mass ratios.<sup>94</sup> The results indicated that, the mass ratio of the PVDF in the blend membrane would influence its water uptake,

swelling behavior, IEC, and proton conductivity, which finally resulted in a satisfactory balance between proton conductivity and vanadium-ion permeability and also achieved stable cycle performance for 80 cycles. Beyond enhancing the mechanical properties, a thin layer of polydopamine (PDA) has been coated on the SPEEK membrane and was found to improve both the chemical stability and thermal stability of pristine SPEEK membrane.<sup>172</sup> It further reveals that, the coated PDA layer can as well effectively function as a block layer to drastically reduce the vanadium-ion permeability of the membrane.

Other than combining with other polymers, addition of additives has also been studied and proven to be an effective method. GO is a well-studied material.<sup>199</sup> Kong et al. used the p-phenylene diamine-functionalized graphene oxide (PPD-GO) and combined it with SPEEK for membrane preparation.<sup>178</sup> It was pointed out that, the interfacial interaction between -NH<sub>2</sub> groups from PPD-GO and -SO<sub>3</sub>H groups from SPEEK positively influenced the water uptake ratio and swelling behavior of the composite membrane to ultimately achieve higher coulombic efficiency of 96.9 % and an energy efficiency of 82.8 % at 30 mA cm<sup>-2</sup> compared to Nafion 117 as shown in **Fig. 7 (a)**. In the meanwhile, long self-discharge duration of 56 hours and stable performance up to 100 cycles were also achieved. In an attempt to achieve an improved balance between vanadium ions permeability and proton conductivity, ethylenediamine functionalized GO was later synthesized and introduced into the SPEEK matrix to fabricate a membrane for VRFBs.<sup>148</sup> It was found that the introduced N-based functionalized graphene oxide (GO-NH<sub>2</sub>) successfully restrained the permeability of vanadium ions due to its layered structures and the Donnan exclusion effect. The membrane also shows high ionic conductivity with the narrow pathway provided for proton transport due to the electrostatic interaction between -SO<sub>3</sub>H groups and N-base groups on the GO nanosheets. With this composite membrane, an improved battery performance with an energy efficiency of 89.5 % at 50 mA cm<sup>-2</sup> and capacity retention of 92 % after 100 cycles was achieved (**Fig. 7 (b)**). It is thus apparent that the introduction of functionalized nanofillers into other polymers is an effective modification method suitable for enhancing their interfacial interaction and further leads to an improved battery performance. In summary, the SPEEK-based membranes have been modified by various methods and materials to provide them with improved performance, with most of

the recent results summarized in **Table S4**.<sup>70, 148, 174-196</sup> However, more application of the SPEEK-based membrane is still being hindered as a result of its poor cyclic stability and limited energy efficiency especially under high operating current densities.

### 5.1.3.2 Sulfonated polyimide (SPI)-based

Sulfonated polyimide (SPI), as a kind of non-fluorinated aromatic polymer, possesses good chemical and mechanical properties at low cost. It has been widely investigated for cation-exchange membrane fabrication and has been applied in VRFBs with most of the performance achieved summarized in **Table S5**.<sup>211-220</sup>

Among these developed SPI-based membranes, one of the successful attempts to effectively block the permeation of vanadium ions was demonstrated by the SPI/chitosan (CS) composite membranes, which was prepared using an immersion and self-assembly method.<sup>107</sup> Due to the crosslinking of CS and sulfuric acid during membrane preparation and the blocked micropores by CS layer, the crossover of vanadium ions through the membrane was significantly restrained. The same research group further conducted another experiment to investigate the effect of infiltration time with CS solution and thereafter prepared a series of SPI/CS composite membranes with different infiltration time.<sup>222</sup> A longer infiltration time during membrane preparation would attach more CS molecules onto SPI, which has been proven to significantly influence the proton conductivity, vanadium ions permeability, and mechanical and chemical stabilities of the membrane. Through adjusting the infiltration time, the membrane with the optimum modification time presented a balance between proton conductivity and vanadium ions permeability to successfully achieve a coulombic efficiency of 97.8 % and an energy efficiency of 88.6 % at 40 mA cm<sup>-2</sup>, demonstrating the modification time to be an important factor towards determining the membrane performance.

In addition, additives including ZrO<sub>2</sub>,<sup>206</sup> boehmite (AlOOH),<sup>207</sup> TiO<sub>2</sub>,<sup>90</sup> and sulfonated molybdenum disulfide (s-MoS<sub>2</sub>)<sup>239</sup> have also been added into the SPI to prepare various composite membranes to yield improved performances. For instance, s-MoS<sub>2</sub> was found to exhibit a blocking effect on vanadium ions.<sup>239</sup> This composite SPI/s-MoS<sub>2</sub> membrane, was also found to have an improved ionic conductivity due to the unique two-dimensional structure and

the sulfonated groups of s-MoS<sub>2</sub>. In comparison to the VRFBs assembled with Nafion 117, the battery assembled with SPI/s-MoS<sub>2</sub> presented a much lower self-discharge rate with a self-discharge duration of 193 hours. In an attempt to enhance the antioxidant ability of SPI-based membranes, TiO<sub>2</sub>, a mesoporous material has been studied for membrane preparation.<sup>90</sup> After the introduction of TiO<sub>2</sub>, the composite membrane was found to also achieved an improved ionic conductivity, however with high vanadium-ion permeability. Nonetheless, compared to Nafion 117, this composite membrane still achieved a higher energy efficiency of 83.2-67.61 % at 20-80 mA cm<sup>-2</sup> with a stable performance for 50 cycles, due to its improved chemical stability. In summary, although the modified SPI-based membranes showed an improvement on battery performance compared to the pristine SPI membrane, their proton conductivity and cycle stability still need to be further improved so as to hasten their real application.

#### **5.1.3.3 Sulfonated poly (fluorenyl ether ketone) (SPFEK)-based**

Sulfonated poly (fluorenyl ether ketone) (SPFEK), due to its low-cost and low vanadium ions permeability, is considered as a suitable substitute material for Nafion membranes. The pristine SPFEK membrane prepared through casting method was studied for its application in VRFBs,<sup>227</sup> which was found to present a low vanadium ions permeability and self-discharge rate compared to Nafion 117. However, the energy efficiency of the VRFBs using SPFEK membrane is only ~50 % which is too low for real application. Therefore, the SPFEK has been extensively studied and modified for cation-exchange membrane preparation to ensure better ionic conductivity and mechanical strength during its applications. The performance and properties of recently prepared SPFEK-based membranes are summarized in **Table S6**.<sup>71, 223-226</sup>

To enhance the proton conductivity of SPFEK-based membrane, Chen et al.<sup>224</sup> blended fluorinated SPFEK with the 3-aminopropyltriethoxysilane to prepare a F-SPFEK-APTES composite membrane. It was found that the fluorinated SPFEK successfully improved the membrane proton conductivity in comparison to the pristine SPFEK membrane. Moreover, after the introduction of 3-aminopropyltriethoxysilane, the vanadium ions permeability of the composite membrane was reduced in comparison to the F-SPFEK membrane due to the

Donnan effects between vanadium ions and the cationic groups of APTES. Overall, the cell using the F-SPFEK-APTES composite membrane finally achieved a coulombic efficiency of 80.4 % at 50 mA cm<sup>-2</sup>. To block the crossover of vanadium ions more effectively, the layer-by-layer deposition technique as discussed in Section 5.1.2.1 was then applied for modification by depositing the PDDA and PSS onto this SPFEK membrane repeatedly.<sup>226</sup> It was found that, utilizing this technique, the modified membrane successfully demonstrated a coulombic efficiency of 82.1 % at 30 mA cm<sup>-2</sup>. However, it is worth to mention that, even though the SPFEK-based membranes have indeed shown an improved battery performance after these modifications, they are still far from the real applications primarily due to their poor balance between proton conductivity and vanadium-ions permeability. Hence, it is important for the properties of SPFEK-based membranes to be carefully adjusted before they can truly achieve a superior battery performance.

#### 5.1.3.4 Polytetrafluoroethylene (PTFE)-based

Polytetrafluoroethylene (PTFE), as a polymer with superior chemical and mechanical stability, was widely used for membrane preparation in fuel cells at first.<sup>84</sup> Attracted by its great performance in fuel cells, more and more studies have begun to apply the PTFE-based membranes in flow batteries, whose performances are summarized in **Table S7**.<sup>84, 228-231</sup> One widely studied modification of PTFE is to produce a composite membrane of PTFE and SPEEK,<sup>84, 228, 229</sup> and among them, a study was conducted to analyze the effects of solvents on the membrane performance through preparing a series of SPEEK/PTFE composite membranes utilizing three different solvents.<sup>229</sup> The SPEEK was dissolved into N-methyl-2-pyrrolidone (NMP), N,N'-dimethylacetamide (DMAc), and DMF separately and then cast onto the PTFE-base membranes to obtain the final composite membranes. It was found that the membrane prepared with NMP achieved high proton conductivity due to the ease of NMP removal, while the membrane prepared with DMF showed low vanadium-ion permeability and the membrane that used DMAc presented the best mechanical strength. Hence, it is revealed that the solvents had a great influence on the membranes' physicochemical properties which can further affect the battery performance. Overall, the VRFBs assembled with the SPEEK/DMF/PTFE membranes presented the best performance with an energy efficiency of 91.2 % at 40 mA cm<sup>-2</sup>



<sup>2</sup>. However, while these SPEEK modified PTFE-based membranes have shown improved battery performance, the studies regarding the PTFE-based membranes are still limited. The incorporation of more suitable materials can therefore be a potential direction for future studies.

#### **5.1.3.5 Poly(ether sulfone) (PES)-based**

Poly(ether sulfone) (PES), with its excellent mechanical stability, has been widely used for membrane fabrication and applied in separation process like ultrafiltration and nanofiltration.<sup>240, 241</sup> It has also been used in the preparation of cation-exchange membranes and employed in VRFBs with its achieved performance summarized in **Table S8**.<sup>232-234</sup>

For instance, sulfonated poly(ether sulfone) (SPES) and SPEEK have been employed for membrane fabrication in a previous study.<sup>233</sup> The obtained membrane was reported to eventually exhibit improved mechanical stability and high water uptake ratio. Compared to the battery with Nafion 212, the battery using this SPES/SPEEK membrane achieved a higher coulombic efficiency of 98 % and energy efficiency of 85 % at 50 mA cm<sup>-2</sup>. However, similar to other aromatic polymer-based ion-exchange membranes, one of the major problems of PES is its poor chemical stability. Therefore, to improve the membrane stability, a strategy to isolate the ion-exchange groups from polymer backbone has been demonstrated.<sup>232</sup> After the detachment, the ion-exchange group was then reconstructed by fixing the phosphotungstic acid (TPA) into alkaline poly(vinyl pyrrolidone) (PVP) and the VRFB assembled with this membrane presented a coulombic efficiency of 99.36 % and an energy efficiency of 81.61 % at 140 mA cm<sup>-2</sup> which are higher than those of Nafion 115, as shown in **Fig. 8 (a)**. In the meanwhile, the membrane also exhibited a superior chemical stability and showed a stable cycle performance for over 1200 cycles. However, while some of these PES-based membranes have indeed shown great potential for further applications, it is still necessary for them to attain improved conductivity while maintaining their low vanadium-ions permeability for high energy efficiency at high operating current density.

#### **5.1.3.6 Poly(vinylidene fluoride) (PVDF)-based**

Poly(vinylidene fluoride) (PVDF), a hydrophobic polymer, has drawn a lot of attentions and been widely used for membrane fabrication in recent years. It possesses excellent mechanical,

thermal and chemical stabilities which ensure long-term stabilities for membranes and batteries. However, the hydrophobic nature of PVDF limits its ionic conductivity when employed in VRFBs due to the presence of aqueous electrolyte. To enhance the performance of a PVDF-based membrane, various materials have been grafted onto it to prepare the cation-exchange membrane. This technique, utilizing radiation sources such as electron-beam and  $\gamma$ -rays, allows ionic chemical groups or free radicals to be induced onto the polymer, to achieve the combination of properties and advantages of the various materials.<sup>59</sup> The performances and properties of PVDF-based membranes recently employed in VRFBs are summarized in **Table S9**,<sup>103, 235, 236</sup> while some of the prominent studies are discussed below.

One of the examples of utilizing the grafting technique for PVDF-based membrane performance improvement is carried out through the electron-beam-induced pre-irradiation grafting technique, which successfully grafted the styrene (St) and maleic anhydride (MAN) onto the commercially obtained PVDF.<sup>235</sup> During the experiment, it was found that the required dose during the membrane preparation can be reduced effectively through adding the MAN during the preparation process. Compared to Nafion 117, the obtained membrane possessed higher IEC and ionic conductivity with a much lower vanadium-ion permeability. However, the performance study of this membrane on battery-level is insufficient as no charge-discharge tests were reported. In comparison to this, in another study conducted by Luo et al.<sup>103</sup> more cell-level tests were reported. They prepared a poly(vinylidene fluoride)-graft-poly(styrene sulfonic acid) (PVDF-g-PSSA) membrane utilizing a solution grafting method. It was found that, this PVDF-based membrane exhibits low vanadium-ion permeability and adequate chemical stability, to achieve an excellent capacity retention ability with no obvious capacity drop for about 250 cycles as shown in **Fig. 8 (b)**. Moreover, the battery using PVDF-g-PSSA presented higher coulombic efficiency of ~75-90 % at 10-60 mA cm<sup>-2</sup> and energy efficiency of 75.8 % at 30 mA cm<sup>-2</sup> than the ones with Nafion 117.

However, it should be noted that, while the above mentioned studies have proven grafting as a promising method for membrane performance improvement, the radiation techniques such as UV and plasma always require specific reactors, which demands high capital and energy

costs.<sup>59</sup> Moreover, in order to further improve the membrane and system performance, the grafting yields, as a crucial factor, requires careful adjustment during membrane fabrication. This is because while high grafting yields (GY) can lead to high IEC and membrane conductivity, it could also result in polymer degradation and further reduces the battery lifetime.<sup>54</sup> Hence, for the PVDF-based membranes, further studies to carefully adjust the grafting yields and material compositions are still needed before it can truly achieve a better trade-off between membrane conductivity and vanadium ions permeability.

#### **5.1.3.7 Sulfonated poly(phthalazinone ether ketone) (SPPEK)-based**

Sulfonated poly(phthalazinone ether ketone) (SPPEK) is a polymer considered to possess the level of chemical, mechanical and thermal stabilities required in a membrane. Attributed to the rigid unsymmetrical phthalazinone moiety contained in its backbone, the polymer has a high glass transition temperature and a low swelling ratio.<sup>238</sup> With these compelling properties, the SPPEK has been successfully applied for fabrication of membranes used in VRFBs. However, similar to other sulfonated aromatic polymers such as SPEEK, the performance of the pristine SPPEK membrane with high DS is unsatisfactory, therefore various modification methods have been applied for performance enhancement as well as further applications. Most of these prepared membranes with their respective performance are summarized in **Table S10**.<sup>141, 237,</sup>

238

In order to improve the proton conductivity of SPPEK-based membrane, Wang et al.<sup>237</sup> applied hydrothermal method to fabricate a SPPEK/WO<sub>3</sub> hybrid membrane. The introduction of the hydrated WO<sub>3</sub> fillers successfully improved the water uptake of the membrane, which further improved the proton conduction channels and resulted in an enhanced membrane proton conductivity and a slightly higher energy efficiency of 78.6 % when compared with Nafion 117 at a current density of 50 mA cm<sup>-2</sup>. However, influenced by the increased proton conductivity of membrane, its vanadium ions permeability also increased which further lead to a larger self-discharge rate compared with the pristine SPPEK membrane. Other than introducing inorganic materials, a better performance of the SPPEK-based membranes was achieved by a membrane fabricated using a series of sulfonated poly(phthalazinone ether ketone)s containing pendant

phenyl moieties (SPPEK-Ps).<sup>141</sup> The sulfonic functional groups on the side chain of the SPEEK-Ps are considered to improve the proton conductivity of the membrane, while its mechanical strength was also observed to be relatively stable even after the membrane was treated with 1.5 M VO<sup>2+</sup> and 3 M H<sub>2</sub>SO<sub>4</sub> solution for 60 days. The VRFBs assembled with this membrane achieved a comparable performance with Nafion 115 with an energy efficiency of 83 % at 60 mA cm<sup>-2</sup>, as shown in **Fig. 9 (a)**. In summary, the SPPEK-based membranes provide the battery with a lot of improved performance, even though their capacity retention ability and rate performance still require further enhancement in the future. The SPPEK could be a promising candidate for real application in the future after further modification.

#### 5.1.3.8 Other polymers-based

Other than the materials mentioned above, many other materials including the poly(aryl ether ketone) (PAEK),<sup>242-244</sup> sulfonated poly (arylene ether),<sup>245</sup> poly(p-phenylene),<sup>246</sup> sulfonated poly (diallyl-bisphenol ether ether ketone),<sup>247</sup> polysulfone (PSF),<sup>248-250</sup> poly(fluorenyl ether ketone sulfone)s,<sup>251</sup> poly(propene)<sup>252, 253</sup> and others<sup>120, 254-263</sup> have also been used in membrane preparation. Here, the performance of these membrane materials for application in VRFBs are discussed.

In one of these studies, a PAEK-based membrane with long aliphatic pendant sulfonated groups was prepared towards obtaining a membrane suitable for application in VRFBs.<sup>242</sup> It was found that the long aliphatic side chains can protect the membrane from vanadium ions, which not only ensure a low vanadium-ions permeability, but also enhance the chemical stability of the membrane. Such design hence allows the composite membrane with a stable performance for 100 cycles achieving a capacity retention rate of ~55 %. In another work, a membrane with better chemical stability was demonstrated using a synthesized poly(p-phenylene)-based copolymers with controlled molecular weights.<sup>246</sup> It was found that, due to the rigid polymer structure, this obtained membrane not only achieved a stable and high efficiency for over 100 cycles at 50 mA cm<sup>-2</sup>, but further achieves a capacity retention rate of 43 % after 1000 cycles as shown in **Fig. 9 (b)**.

Other than these materials mentioned above, the importance of DS on the membrane

performance has again been proven by another material.<sup>87, 247</sup> A series of membranes using crosslinkable sulfonated poly (diallyl-bisphenol ether ether ketone) membranes with various DS were prepared, which were later employed and tested in VRFBs.<sup>247</sup> It was found that the ionic conductivity of the membrane is greatly influenced by the DS, while the vanadium-ion permeability is affected by both the membrane thickness and DS. Compared to Nafion 115, the obtained membrane presented a much lower vanadium-ion permeability with a higher coulombic efficiency of 98 % at 50 mA cm<sup>-2</sup> and a lower self-discharge rate. In addition, the membrane also achieved a stable performance for 900 hours.

In summary, many different materials have been employed for the purpose of preparing cation-exchange membranes for flow batteries. However, there are still no suitable cation-exchange membrane with excellent battery performance and facile production method that can completely replace or compete with the commercial Nafion membranes. Therefore, more efforts are still needed towards the development of suitable cation-exchange membranes other than the Nafion membranes.

## 5.2 Anion-exchange membranes

Anion-exchange membrane is another type of polymer electrolyte membrane that have received considerable attentions for application in flow batteries due to the beneficial ion selectivity of the membrane.<sup>264</sup> Unlike the cation-exchange membranes, anion-exchange membranes are made up of fixed cationic groups on the polymer backbone to effectively restrict the transport of vanadium ions which in turn leads to improved coulombic efficiency of battery system, as shown in **Fig. 4 (b)**. As a result of this, the anion-exchange membranes have been employed in a number of investigations and studies in VRFBs. However, the wide application of anion-exchange membranes in flow battery systems is hindered by poor ionic conductivity and chemical stability. A lot of research efforts have been put into the development of anion-exchange membranes for flow batteries through the development and investigations of various materials such as polysulfone (PSF),<sup>86, 126, 264-272</sup> poly(phthalazinone ether ketone) (PPEK),<sup>95</sup> poly(phthalazinone ether ketone ketone) (PPEKK),<sup>273, 274</sup> poly(aryl ether ketone) (PAEK),<sup>275-278</sup> PES,<sup>279, 280</sup> poly(flourenyl ether),<sup>281</sup> PBI,<sup>282, 283</sup> polyvinyl chloride,<sup>96</sup> poly(phenylene),<sup>284</sup>

PE,<sup>285</sup> poly(phenyl sulfone),<sup>92</sup> poly(arylene ether sulfone) (PAES),<sup>286</sup> and many others.<sup>60, 83, 101, 105, 287-301</sup> In the following sections, we discussed in detail some of the prominent materials for anion-exchange membranes that have achieved superior battery performance.

### 5.2.1 Polysulfone (PSF)-based

As discussed earlier, polysulfone (PSF) is a polymer well known for its mechanical, thermal and chemical stabilities suitable for the preparation of membranes. It has therefore also been used to prepare some anion-exchange membranes<sup>86, 126, 264-272</sup> for VRFBs. Some of these PSF-based anion-exchange membranes recently reported are summarized in **Table S11**.<sup>86, 269-272</sup> Among these previously reported studies, two of them where extremely high coulombic efficiency was achieved due to superior blocking effects towards vanadium ions are discussed below.

In one of these studies, the cross-linking strategy was employed during the membrane preparation, which is regarded as one of the common modification methods to create reinforced structure which offers high mechanical stability. This fabricated PSF/PVDF membrane was crosslinked via the cation- and dication-forming reactions, which was then proven to possess well-balanced properties.<sup>265</sup> The membrane was further found to achieve a much lower self-discharge rate, compared to the Nafion membranes, with a stable coulombic efficiency of 99 % for more than 900 cycles as shown in **Fig. 10 (a)**, demonstrating its compelling performance. In another study, PVDF was added into quaternized PSF, as presented in **Fig. 10 (b)**.<sup>86</sup> It was observed that due to the Donnan exclusion effect between the fixed anion-exchange groups and vanadium ions, the vanadium ions are effectively blocked by the composite membrane. Furthermore, the swelling behavior of the membrane was also greatly suppressed due to the crystallization of PVDF. Consequently, this PSF-based anion-exchange membrane achieved a coulombic efficiency of ~100 %. However, it is worth to note that, while the PSF-based membranes show superior performance and great potential for future applications, their ionic conductivity are not as good as the commercial Nafion membranes. Therefore, studies to address this particular limitation of PSF-based anion-exchange membranes, while also maintaining their battery performance especially under high operating current densities are

much required.

### 5.2.2 Poly(aryl ether ketone) (PAEK)-based

Poly(aryl ether ketone) (PAEK) is another kind of polymer that has been used for anion-exchange membrane development and has been studied and reported for their application in VRFBs, as summarized in **Table S12**.<sup>275-278</sup> Among all of these studies, the introduction of long aliphatic imidazolium groups onto PAEK for anion-exchange membrane preparation was demonstrated to achieve an improved battery performance and capacity retention ability.<sup>278</sup> The attached positively charged imidazolium groups, with their chemical stability, were majorly employed to provide the membrane with improved oxidative stability and reduced vanadium ions permeability. The resulting membrane thus presented a decrease in energy efficiency from ~87 to 78 % as the operating current density increases from 40 to 100 mA cm<sup>-2</sup>, which are much higher than the performance of Nafion 117. Furthermore, the battery using this PAEK-based membrane showed a capacity retention ability of ~84 % after 100 cycles, justifying the stability of this polymer and its promising potentials for membrane preparation suitable for more applications beyond the VRFBs. However, similar to most of the anion-exchange membranes, one of the major problems of the PAEK-based anion-exchange membrane is its poor conductivity, which results in limited voltage efficiency thereby restraining the energy efficiency of the battery especially at high operating current densities. Hence, further studies to improve the conductivity of the PAEK-based membranes while effectively blocking vanadium-ions therefore remains one of the major research directions in the future.

### 5.2.3 Other polymers-based

Other than PSF and PAEK, many other materials have also been used for anion-exchange membranes preparation.<sup>83, 279, 281, 286</sup> Some of these materials and their performance when used in VRFBs are discussed in this section.

Fumasep FAP series from Fumatech GmbH is one of the most widely employed commercial AEMs in flow batteries. A number of research works have therefore examined the performance of these types of membrane in the operations of VRFBs.<sup>101, 106, 302, 303</sup> In comparison to Nafion 112 (CE: 93 %, VE: 87 % and EE: 81 %), FAP-450 has been reported to achieve higher CE

(98 %), lower VE (84 %), and a comparable EE (82 %) when operated at  $40 \text{ mA cm}^{-2}$ .<sup>303</sup> Such performance therefore indicates that the commercial FAP-450 AEM is able to effectively suppress the crossover of vanadium ions while it allows an easy transport of anions. However, in order to further minimize the vanadium ions permeability of this commercial AEM, the sol-gel synthesis method has been applied to modify a FAP membrane using silica nanoparticles. The prepared silica nanocomposite membrane was demonstrated to further hinder the permeation of vanadium ions, which in turn leads to a longer self-discharge duration. As a result, the membrane further achieved a 9 % higher CE with a 5 % higher EE compared to the pristine FAP membrane.<sup>101</sup> However, this FAP membrane even after modification is still found to present lower VE compared to the Nafion series especially at high operating current density as a result of its limited ionic conductivity. This therefore restricts the operating current density range of FAP membranes.

Other than the commercial FAP membranes, imidazolium-based structures, due to their high ionic conductivity and chemical stability, has been introduced into PAES for membrane preparation for performance improvement.<sup>286</sup> The obtained membranes were assembled into VRFBs and the test results showed that, compared to Nafion 117, the fabricated membranes achieved a slight lower voltage efficiency of 75.6 % with a much higher coulombic efficiency of 96.1 % at  $120 \text{ mA cm}^{-2}$ , demonstrating the addition of imidazolium-based structures as a potential strategy to achieve better conductivity for the anion-exchange membranes.

Other than the relatively low voltage efficiency as a result of the low membrane ionic conductivity, poor chemical stability is another lingering issue that hinders the real application of anion-exchange membranes. In order to improve the chemical stability of anion-exchange membranes, Zeng et al.<sup>83</sup> therefore prepared a pyridinium-functionalized cross-linked anion-exchange membrane with chemical inertness backbone. Due to the internal cross-linking networks of the membrane and the Donnan exclusion effect, the permeation of  $\text{VO}^{2+}$  ions through the membrane is greatly hampered, while its chemical stability is greatly improved. The membrane further presented an improved balance between the ionic conductivity and vanadium-ion permeability to attain a coulombic efficiency of ~98-99 % and voltage efficiency



of ~92-77.5 % at 100-250 mA cm<sup>-2</sup>. Furthermore, it reveals a cycle stability of operating for 537 cycles at 200 mA cm<sup>-2</sup> with a capacity decay rate of 0.037 % per cycle, as shown in **Fig. 11 (a)**. Another example demonstrating an anion-exchange membrane with extremely superior chemical stability was achieved by a PES-PVP blend anion-exchange membrane.<sup>279</sup> The combination of PVP and PES successfully retains the advantages of each material to provide the membrane with mechanical stability, hydrophilicity, and low vanadium-ion permeability. The battery assembled with the obtained PES-PVP membrane achieved a coulombic efficiency of 99 % at a rate of 50 C and operated for 26,000 cycles thereby validating its excellent stability as shown in **Fig. 11 (b)**.

In summary, the anion-exchange membranes have received a number of investigations and studies in the last decade to showcase their applications and performance improvement in flow battery technology. However, for the anion-exchange membranes to be widely applied, further experimental studies are still needed. Not only the ionic conductivity and chemical stability of anion-exchange membrane need further improvement, but also the fabrication methods and financial cost of the membrane need to be addressed.

### **5.3 Amphoteric-ion exchange membranes**

To date, several materials and fabrication methods have been developed to enhance the application of cation-exchange and anion-exchange membranes in flow battery systems. However, some lingering deficiencies of these membranes have also been pointed out. For instance, the cation-exchange membranes generally suffer from high vanadium-ion permeability, while the anion-exchange membranes are of low ionic conductivity. Thus, in order to achieve a membrane that combines the advantageous properties of these two membranes - high ionic conductivity and restricted transport of vanadium ions, the idea of attaching both anionic and cationic functional groups onto a membrane backbone has been proposed and named the amphoteric-ion exchange membrane. The amphoteric-ion exchange membrane, shown in **Fig. 4 (c)**, therefore combines the advantages of cation and anion-exchange membranes while minimizing their respective drawbacks. Some of the various materials that have been utilized in the preparation of amphoteric-ion exchange membranes for

VRFBs include PVDF,<sup>304-307</sup> poly(ethylene-co-tetrafluoroethylene) (ETFE),<sup>308, 309</sup> SPEEK,<sup>310-312</sup> PE,<sup>313</sup> and other materials<sup>127, 314-318</sup>.

### 5.3.1 Poly(vinylidene fluoride) (PVDF)-based

Poly(vinylidene fluoride) (PVDF), as discussed earlier, is a widely used polymer for membrane preparation. It has also been reported for the preparation of amphoteric-ion exchange membranes.<sup>305-307</sup> The performance and properties of prominent PVDF-based amphoteric-ion exchange membranes recently reported are summarized in **Table S13**<sup>304-307</sup> while some of these materials that have seemingly contributed to the improvement of battery performances are discussed in this section.

In an attempt to provide the PVDF-based membranes with low vanadium ions permeability, St and dimethylaminoethyl methacrylate were grafted onto PVDF film using the  $\gamma$ -irradiation technique for amphoteric-ion exchange membrane preparation.<sup>304</sup> The obtained amphoteric-ion exchange membrane was found to maintain the battery voltage over 1.2 V for 68 hours proving its low vanadium-ion permeability, which was attributed to the Donnan exclusion effect between the cation groups and the vanadium ions. Elsewhere, sodium styrene sulfonate (SSS) and N,N-dimethylaminoethyl methacrylate have also been successfully grafted into the PVDF film using this technique, followed by protonation process to obtain an amphoteric-ion exchange membrane.<sup>307</sup> It was found that the increasing composition of N,N-dimethylaminoethyl methacrylate can reduce vanadium-ion permeability of the membrane, which in turn enables the prepared membrane to achieve a low self-discharge rate and allows the VRFB to be maintained at an OCV higher than 1.4 V for 85 hours as shown in (**Fig. 12 (a)**). However, while the  $\gamma$ -irradiation technique can introduce ion functional groups into the membrane, it can also potentially result in their non-uniform distribution. Hence, to allow a more uniform distribution of ion-exchange groups, the radiation grafting technique and solution phase inversion method has been combined for membrane preparation (**Fig. 12 (b)**).<sup>305</sup> During the preparation, the PVDF powder was firstly grafted with St and dimethylaminoethyl methacrylate and then fabricated into a membrane through the solution phase inversion method. This membrane, after sulfonation and protonation treatment, becomes the final amphoteric-ion

exchange membrane needed. It was found that, the membrane prepared with the combination of radiation grafting technique and solution phase inversion method resulted in a uniform grafting throughout the membrane structure. This therefore provides the membrane with a higher conductivity compared to the amphoteric-ion exchange membranes prepared through performing grafting directly on the PVDF film. However, this also increases the vanadium ions permeability of the membrane. In summary, the PVDF has been proven to be a polymer with great potential for the preparation of amphoteric-ion exchange membrane, while its modification especially through grafting technique needs further attentions to ensure uniformity of ion-exchange group distribution for improved battery performance.

### **5.3.2 Other polymers-based**

Other than the aforementioned materials, other materials such as polysulfone (PS),<sup>316</sup> SPEEK,<sup>310, 311</sup> and PPEK<sup>314, 315</sup> have also been used for the preparation of amphoteric-ion exchange membrane. One of these studies examined the effects of GY during the preparation process, which is an important factor that determines the membrane performance.<sup>308</sup> The radiation-induced grafting technique was employed during the membrane preparation process while both anionic and cationic groups were successfully introduced into the poly(ethylene-co-tetrafluoroethylene) (ETFE) film. Through controlling the GY during the preparation process, vanadium-ion permeability and ionic conductivity of the fabricated membrane can be easily adjusted. The obtained optimal amphoteric-ion exchange membrane showed a reduced vanadium ions permeability compared to cation-exchange membranes and an improved ionic conductivity than anion-exchange membranes. As a result, the VRFB assembled with the obtained amphoteric-ion exchange membranes attained a coulombic efficiency of 95.6 % and an energy efficiency of 87.9 % at 40 mA cm<sup>-2</sup>. Elsewhere, an improved battery performance was reported to be demonstrated by a SPEEK and quaternized poly(ether imide) (QAPEI) composite amphoteric-ion exchange membrane.<sup>312</sup> The introduction of QAPEI was found to greatly improved the selectivity of the amphoteric-ion exchange membrane. Moreover, it was found that the membrane possessed a high degree of micro-phase separate structure which is considered to facilitate ion transport. This obtained composite membrane presented higher efficiencies than both the pristine SPEEK and Nafion 115 membranes with a coulombic

efficiency of 96.1 % and an energy efficiency of 88.45 % at 50 mA cm<sup>-2</sup> as shown in **Fig. 13**.

However, the amphoteric-ion exchange membrane is still far from real application up till now. This is mainly attributed to the following reasons: i) the preparation of these membranes always involves complex preparation procedures making them unsuitable for mass production; and ii) the performance of the batteries utilizing these membranes are still unsatisfactory especially under high charge-discharge current densities. Thus, more efforts are still required towards the preparation and development of amphoteric-ion exchange membranes suitable for wide application in flow batteries.

#### **5.4 Porous membranes**

Even though several types of polymer electrolyte membrane have been proposed and developed for application in flow batteries, their high cost and complicated preparation procedures still hinder their wide applications and thus require further investigations for improvement. The porous membrane guided by the idea of separating the protons and other cations *via* the size exclusion effect has therefore attracted a lot of attentions and investigations.<sup>319</sup> It is worth to note that porous membranes for VRFBs has received a considerable research attention, particularly by Huamin Zhang and his research group.<sup>320-328</sup> The ideal porous membrane requires a well-defined ion-transport channel that promotes easy transport of protons while hindering the transport of other metal ions, thereby providing the battery with high efficiencies. The working principle of a porous membrane when employed in VRFBs is illustrated in **Fig. 4 (d)**. Researchers have used various materials such as PBI,<sup>74, 326, 328-336</sup> PES,<sup>240, 241, 319, 320, 322-324, 337-343</sup> polyacrylonitrile (PAN),<sup>325, 344, 345</sup> porous glass,<sup>346-349</sup> PSF,<sup>327, 350-352</sup> PVDF,<sup>116, 321, 353, 354</sup> and others<sup>145, 355</sup> using various preparation methods to obtain porous membranes.

##### **5.4.1 Polybenzimidazole (PBI)-based**

Polybenzimidazole (PBI) is a type of heterocyclic polymers well known for its high glass transition temperature, superior thermal, mechanical and chemical stabilities<sup>336</sup>. These properties therefore make it suitable for applications in an acidic and corrosive electrolyte environment such as VRFBs.<sup>74, 139, 334</sup> While PBI has been widely studied and investigated for

the preparation of porous membranes for flow batteries, the major challenge of the pristine PBI membranes is poor proton conductivity.

To enhance their proton conductivity, PBI membranes are commonly treated with strong acid, so that the imidazole group on PBI backbone could be protonated and form the acid-based complex which is conductive for proton transport. Moreover, the positively charged imidazole group can also repel the vanadium ions by Donnan effect, limiting the vanadium ions permeability. Zhao et al.<sup>139</sup> first studied the application of PBI membrane in VRFB in 2015, after the development of a PBI porous membrane for application in fuel cells. They have deeply investigated the ionic conductivity, vanadium-ion permeability, chemical stability and battery performance of the sulfuric-doped PBI porous membrane, to demonstrate the PBI membrane as a promising candidate suitable for flow battery operation. However, while the acid treatment could improve the proton conductivity of PBI membrane, its conductivity was still relatively low, thereby leading to limited voltage efficiency at high operating current densities. To further improve the performance of PBI-based membrane in VRFBs, a lot of experimental studies have therefore been conducted to modify the membrane and some positive results have been achieved.

One of the successful efforts to efficiently improve the proton conductivity of PBI-based membrane was conducted by Chen et al.<sup>330</sup> where they introduced pyridine groups into the PBI membrane. The pyridine groups and imidazole rings inside the PBI forms the dual proton transport channels, which is expected to effectively enhance the proton transport across the membrane. Moreover, the positively charged acid-doped pyridine and imidazole groups was found to repel the vanadium-ions to achieve low vanadium ions permeability while still exhibiting its high ion conductivity. Utilizing this method, a coulombic efficiency of 99 % and a voltage efficiency of ~80 %, were obtained which are even higher than those of Nafion 115 membrane. Furthermore, the membrane also demonstrates a stable performance for 600 cycles.

Another strategy to control the balance between proton conductivity and vanadium-ions permeability is by modifying the morphology of porous membranes. Huamin Zhang and his research group have notably performed extensive studies on controlling the morphology of PBI

membranes for performance improvement.<sup>326, 328, 335</sup> In 2016, they first prepared a sponge-like porous PBI membrane using the typical vapor induced phase inversion method.<sup>328</sup> Such membrane morphology was found to effectively create multiple barriers to vanadium ions, which hence limits the permeability of vanadium ions and thereby results in high ions selectivity. The obtained membrane finally achieved an astonishing stable operation of over 13000 cycles at a current density ranging from 80 to 120 mA cm<sup>-2</sup>, presenting an energy efficiency of ~80% as shown in **Fig. 14 (a)**, successfully demonstrating the excellent chemical stability of the prepared membrane. Considering the difficulties associated with the traditional vapor-induced phase separation method, the research group later developed a nonsolvent-induced phase separation method for the preparation of porous PBI membrane. During this phase separation process, the membrane morphology can be controlled by altering the concentrations of the salt solution, which is environmentally friendly and suitable for mass production.<sup>326</sup> It was found that the porous membrane could achieve the balance between vanadium ions permeability and ionic conductivity through appropriate optimization of membrane morphology. Moreover, the structure was found to possess high stability, which enables the fabricated membrane to achieve a similar stable operation for 10000 cycles, with an energy efficiency of ~80 % at 160 mA cm<sup>-2</sup>, as shown in **Fig. 14 (b)**.

Considering the recent applications of PBI-based membranes in VRFBs as summarized in **Table S14**,<sup>74, 326, 328-336</sup>, these compelling performances have suggested efficient direction for PBI improvement, thereby promoting the PBI as a promising candidate for preparing porous membranes for viable applications in the future. It is worth to note that while some of the modification methods can improve the proton conductivity of PBI, they may on the other hand affect other properties of the membrane, such as ions selectivity and mechanical strength. Hence, further investigations are still required to achieve an optimal balance between the various properties.

#### **5.4.2 Poly(ether sulfone) (PES)-based**

Poly (ether sulfone) (PES), with its excellent chemical and mechanical stability, has been widely used for membrane preparation as well as in separation processes such as ultrafiltration

and nanofiltration.<sup>240</sup> A summary of the properties and performance of the recently reported PES-based porous membranes is presented in **Table S15**.<sup>241, 319, 320, 322, 337-342</sup> Among the PES-based membranes, tuning the membrane pores is one of the most common strategies with the aim to obtain an optimal trade-off between vanadium-ion permeability and proton conductivity. Some of such cases where this strategy was utilized and achieved satisfactory battery performance are discussed in this section.

Hydrophilic PVP was incorporated into PES for membrane morphology adjustment, which results in a membrane with more pores and bigger pore size distribution.<sup>240</sup> After the modification of the membrane morphology, it was found that the membrane achieved a voltage efficiency of 82-85 % at 80 mA cm<sup>-2</sup> and a stable performance for 150 cycles, demonstrating that the pore size and pore distribution play an important role in influencing the performance of porous membranes. In another attempt for pore structure modification, a series of porous PES/SPEEK membranes with a structure made of hydrophobic porous PES matrix and interconnected hydrophilic small pores were prepared.<sup>319</sup> It was found that with the introduction of SPEEK, the membrane with a more uniform pore structure and improved ionic conductivity was achieved. After solvent treatment, the polymer chains were reorganized, which led to the shrinkage of membrane pores to achieve low vanadium-ion permeability with improved ion selectivity. The VRFBs assembled with this membrane finally present a coulombic efficiency of 99 % and an energy efficiency of over 91 % at 80 mA cm<sup>-2</sup> as shown in **Fig. 15 (a)**.

Apart from blending with other polymers, the PES membrane can also be modified by introducing hydrophilic layers onto the pore and surface of the membrane to create well-defined ions transport channels and therefore result to high ionic conductivity. Xu et al.<sup>323</sup>, for the first time, introduced multilayered PDDA and poly (acrylic acid) (PAA) complexes on the inner pore and surface of the PES/SPEEK membrane through a solvent-responsive layer-by-layer assembly technique as shown in **Fig. 15 (b)**. After the modification, the pore size of the membrane decreased while its hydrophilicity improved, to indicate its ions selectivity and conductivity improvement. Moreover, by placing the PES/SPEEK-based membrane in various

solvents (isopropanol, methanol and ethylene glycol) so as to swell before introducing other polymers, it was proved that the swelling effect of solvent can adjust the free volume of polymer and provide more opening space for the deposition of other layers on the membrane pores. The obtained membrane successfully achieved an improved balance between vanadium-ion permeability and ionic conductivity thereby exhibiting an improved performance at various charge/discharge current densities.

With these achieved performance and properties, the PES-based porous membrane is therefore considered to possess great potential to achieve real application after further improvement. Specifically, future studies should focus more on providing the membrane with better balance between ionic conductivity and vanadium-ions permeability.

#### 5.4.3 Polyacrylonitrile (PAN)-based

Other than the PES and PBI, polyacrylonitrile (PAN) is another material that has been commonly used for porous membranes preparation. Some of their properties and performances in VRFBs are summarized in **Table S16**.<sup>325, 344, 345</sup> To understand the properties of PAN-based nanofiltration membrane, the pore sizes of the membrane have been tuned and investigated using strategies such as adjusting polymer concentration and adding volatile cosolvents.<sup>344</sup> The experimental results revealed that the decrement of pore sizes leads to an increase in ion selectivity. The VRFBs assembled with the obtained membrane achieved an energy efficiency of 76 % at 80 mA cm<sup>-2</sup>. Using another method, the same research team modified the PAN-based membrane in order to reduce the membrane pore size while maintaining its ionic conductivity. They therefore introduced various silica contents into the pores and surface of another PAN-based nanofiltration membrane *via in situ* hydrolysis of tetraethylorthosilicate (TEOS).<sup>325</sup> It was found that after the introduction of silica, the ion selectivity of the membrane is greatly enhanced, thereby results in an improved energy efficiency of 79 % at 80 mA cm<sup>-2</sup>. It was also found that, for the rate performance, the membrane with the optimized hydrolysis treatment is reported to exhibit a coulombic efficiency of 91-98 % at current densities of 40-80 mA cm<sup>-2</sup>, as shown in **Fig. 16 (a)**.

Apart from the modifications as discussed above, the coating of microporous polymer on PAN



for membrane fabrication has also been examined and proven to be an effective method. The PIM-1 polymer, which is the first generation polymer possessing the intrinsic microporosity has been coated onto PAN ultrafiltration membrane for membrane preparation.<sup>345</sup> With the small pore size and water molecules inside the membrane, the membrane showed a higher permeation rate for protons than vanadium ions. Following this, the VRFB equipped with PIM-1/PAN showed extremely high energy efficiency of ~98.7 % at a low current density of 1 mA cm<sup>-2</sup>, and maintained the energy efficiency above 85 % within the low current density ranging from 1 to 40 mA cm<sup>-2</sup>, which outperforms the Nafion series as shown in **Fig. 16 (b)**. While such results prove the potential of involving inherent microporosity materials for membrane fabrication, it is worth to emphasize that, due to the high resistance of this particular membrane, large ohmic loss is a key limitation for its cell-level performance, especially when operating at high current densities. Hence, up till now, the relatively poor ionic conductivity of the PAN-based membranes is still one of the lingering challenges before achieving their real applications, which therefore requires more research attentions.

#### **5.4.4 Porous glass-based**

Porous glass is another notable material that has been used for porous membrane fabrication. Some major studies on the application of porous glass membranes in VRFBs are summarized in **Table S17**.<sup>346-349</sup> The usage of porous glass for membrane preparation allows the modification of pore sizes and pore surface to reduce the crossover of vanadium ions. The porous glass membrane can be obtained by modifying the pristine non-porous glass via the specific heat treatment with suitable acidic and alkaline leaching steps. After the treatment, the modified membrane can generally maintain superior chemical and thermal stability as a result of the high ratio of silica composition.<sup>347, 356</sup> Furthermore, such material possesses large geometrical flexibility and allows manufacturing of various shapes and with thickness down to 150 μm.<sup>347</sup>

The first application of porous glass for membrane preparation was reported by Fang et al. in 2003,<sup>346</sup> where Vycor glass with a pore size of around 4.5 nm was used. The investigations on the membrane showed that it advantageously possesses low vanadium ions permeability. During the discharge tests carried out, the porous glass membrane was found to maintain a

coulombic efficiency of ~97 % with an open circuit voltage of about 1.5 V for over 72 h, indicating the negligible self-discharge effect due to the low crossover of vanadium ions. However, the ohmic resistance of this membrane was still relatively high, which hence limited the voltage efficiency of the system. Later, Mögelin et al.<sup>349</sup> investigated series of porous silica glass membranes with pore sizes ranging from 2 to 50 nm and thickness of 300 and 500  $\mu\text{m}$ . While a smaller pore size can effectively limit the crossover of vanadium ions through the membrane, the transport of protons is more likely to be hindered, which could reduce the ionic conductivity of the membrane. Overall, the membrane with an optimal pore size (8 nm) achieved the highest energy efficiency of 76.3 % at 20  $\text{mA cm}^{-2}$ . Besides, porous glass membrane also shows stability at high operating temperatures, as it possesses adequate thermal tolerance due to the rigid and non-swelling pore structure.<sup>348</sup>

While these advantages show great prospects for porous glass membranes for further applications in flow battery systems, the membrane still has its own shortcomings such as low ionic conductivity, and poor mechanical stability. In an attempt to improve the ionic conductivity of the membrane, the pore surface of a porous glass membrane was modified with sulfonic acid groups.<sup>347</sup> However, while the involvement of sulfonic acid groups was supposed to facilitate protons transport through the membrane, the pores of the membrane were observed to be blocked which in turn reduce the ion conducting channels. Consequently, satisfactory improvement in the ionic conductivity of the membrane was not achieved even after these modifications. In this case, further studies are therefore still required to fully address the poor ionic conductivity of the porous glass membranes, while their poor mechanical stability is another barrier that should also be considered for further investigations.

#### **5.4.5 Other polymers-based**

Other materials including PVDF,<sup>116, 353, 354</sup> PSF,<sup>350-352</sup> and many others<sup>145, 327, 355</sup> have also been used for the preparation of porous membranes. Among these materials, the use of PVDF for porous membrane has been reported to enhance battery performance to certain level as discussed below.

As introduced in previous sections, PVDF is a polymer with excellent mechanical, chemical

and thermal stabilities. Its application for preparing porous membrane for VRFBs was first reported by Zhang and his research group.<sup>116</sup> They fabricated a PVDF-based ultrafiltration membrane using the phase inversion method. Owing to the hydrophobic membrane pore walls and the effects of pore constriction, the membrane achieved a coulombic efficiency of 95 % and an energy efficiency of 78.6 % at a current density of 80 mA cm<sup>-2</sup>. In addition, the membrane attained a stable operation for 1000 cycles due to the excellent chemical stability of PVDF thereby providing the VRFB with improved stability. However, due to the hydrophobic nature of the PVDF polymer, poor ionic conductivity plays an important role in limiting the battery performance. Hence, in order to ease the proton transport through the membrane, a highly hydrophilic poly(vinyl pyrrolidone) (PVP) layer was introduced into the pores and onto the surface of PVDF membrane *via* cross-linking reaction and grafting polymerization with a solvent swelling pre-treatment.<sup>321</sup> The modified PVDF membrane combined the compelling properties of different materials together, and thus exhibited adequate chemical and mechanical stability after over 300 charge-discharge cycle tests. Moreover, as expected a high energy efficiency of 83.3 % was achieved at the same current density (80 mA cm<sup>-2</sup>) demonstrating its improved battery performance. Hence, with the comparable battery-level performance of PVDF-based membrane and its much lower cost against those of the conventional Nafion membranes, the PVDF-based membrane is considered as a potential substitute to Nafion in the future. Based on all of these results, the porous membranes have been proven suitable to contribute to the performance improvement of flow batteries. However, before their real applications in the future, further studies especially on their performances under high charge-discharge current densities are still needed, which should be regarded as one of the major research focus on porous membranes.

## 5.5 Summary

In this section, the different types of membrane that have been developed for VRFBs, based on the major materials used, have been divided into different sub-sections and extensively discussed. Following this, a comprehensive table (**Table 1**) summarizing the major membrane-materials discussed and their performance is presented. It can be seen that, among the various Nafion series membranes, the commercial Nafion 115 membrane,<sup>67</sup> have been reported to

possess the best balance between its various properties to produce excellent performance in VRFBs with an energy efficiency of 54 % at 320 mA cm<sup>-2</sup> and a capacity retention ability of 50 % after 152 cycles. Another commercial membrane, named, VANADion<sup>108</sup> has been reported to achieve a higher energy efficiency of ~72 % at the same current density with a capacity retention ability of ~93.2% after 85 cycles operation compared to the commercial Nafion 115 membrane. Other than the Nafion-based membranes, SPEEK is another material that has been mostly studied for its usage in the fabrication of cation-exchange membranes and have achieved notable performance in VRFBs. One of the SPEEK-based cation-exchange membranes<sup>191</sup> has been reported to present the best performance, with an energy efficiency of 80.1 % at a current density of 180 mA cm<sup>-2</sup>, while another SPEEK-based membrane<sup>192</sup> is reported to achieve an outstanding operation stability of 1000 cycles with a capacity retention ability of ~60 %. However, while some of the cation-exchange membranes have been reported to achieve an impressive performance on some levels, the major downside of most cation-exchange membranes still remains the high vanadium ions permeability. This needs to be significantly reduced while simultaneously maintaining its high ionic conductivity to ensure high capacity retention ability after long-term operation and high energy efficiency under high operating current density range.

For the anion-exchange membranes, PSF has been pointed out as the material with the most promising potential for further study. One of the membranes prepared using this material achieved an energy efficiency of ~78 % at a current density of 180 mA cm<sup>-2</sup>,<sup>270</sup> while another PSF-based membrane successfully operated for an astonishing 6000 cycles.<sup>272</sup> The anion-exchange membranes have been commonly reported to possess high capacity retention ability due to their low vanadium ions permeability. However, one of their major drawbacks remains poor ionic conductivity, which should be addressed through further studies so as to attain high voltage efficiency under a wide operating current density range.

Regarding the amphoteric-ion exchange membranes and porous membranes, it may be difficult to point out the membrane material with the most promising potential for further applications due to the limited studies that have been carried out on these materials. Nonetheless, the PBI

and PES seem to be the dominant materials for the preparation of porous membranes at present. It is also worth to note that a particular PBI-based porous membrane has successfully demonstrated a stable operation with a capacity retention ability of 68 % after 1350 cycles,<sup>328</sup> and a PES-based porous membrane has been reported to exhibit an energy efficiency of 80% at a current density of 260 mA cm<sup>-2</sup> with a capacity retention of 93% for 100 cycle operation.<sup>338</sup> These results achieved from these materials, particularly for porous membranes, provide an insight that better and improved performance could be attained with further investigations. Moreover, the methods to accurately tune the concentration of anion-exchange groups and cation-exchange groups in an amphoteric-ion exchange membrane as well as tune the pore sizes and pore structure for a porous membrane still require further investigations. Such methods would definitely play important roles in determining the membrane performance towards obtaining the ideal membrane suitable for VRFBs.

**Table 1.** Performances of membranes according to the major materials used.

Membrane Type	Membrane name	Functional group(s)	Ionic conductivity (mS·cm <sup>-1</sup> )	VO <sup>2+</sup> permeability (10 <sup>-7</sup> cm <sup>2</sup> min <sup>-1</sup> )	WU (%)	IEC (mmol g <sup>-1</sup> )	Mechanical property <sup>a</sup>	Thermal stability <sup>b</sup>	Chemical stability <sup>c</sup>	EE (%) (current density (mA cm <sup>-2</sup> ))	Self-discharge duration (hours)	Life stability testing <sup>d</sup>	Ref.	
Cation-exchange membrane	Nafion-based	Nafion 115	-SO <sub>3</sub> H	~100	/	32.1±2.2	0.87±0.02	/	/	/	~54% (320)	22	50% (152)	67
		B20N10	-SO <sub>3</sub> H	111	0.02	23.6	/	/	/	/	76.84% (100)	/	80.2% (300)	151
		VANADion	-SO <sub>3</sub> H	/	127	/	/	/	/	/	~72% (320)	/	~93.2% (85)	108
		HPPY-N212	-SO <sub>3</sub> H	~53	/	/	/	/	/	/	~76% (150)	/	90	154
		Nafion-NdZr (1%)/[P-S] <sub>2</sub>	-SO <sub>3</sub> H	73.7	1 x 10 <sup>-3</sup>	21.3	0.891	/	900°C (~100%)	/	~76% (140)	513.7	80.1% (200)	169
	SPEEK-based	SPEEK-15	-SO <sub>3</sub> H	/	/	43.63	/	68.78 MPa 23.33%	800°C (~45%)	~2.7% (325 h)	80.1% (180)	/	350	191
		S/CNT@PDA	-SO <sub>3</sub> H	97.7	8.7	43.3	/	39.4 MPa 76.3%	700°C (23.2%)	/	71.2% (240)	/	~60% (1000)	192
	SPI-based	CSPI-DMDA (1:1)	-SO <sub>3</sub> H	39.2	0.93	31.2	1.52	28.6 MPa 13%	700°C (~49%)	/	~71% (240)	103	1000	218
	SPFEK-based	SPFEK-[PDDA/PSS] <sub>2</sub>	-SO <sub>3</sub> H	23.8	1.16	44.5	/	/	/	/	/	80	/	226
	PTFE-based	SE3/P	-SO <sub>3</sub> H	42.6	7.1	29.8	/	49.5 MPa	/	/	~78% (100)	/	82.8% (200)	228
		SPEEK/PTFE	-SO <sub>3</sub> H	/	/	/	/	39.47 MPa 36.89%	/	/	83.7 ± 1% (80)	27	700	84
	PES-based	PES-IEC	PVP; TPA	/	~0.58	14.60	/	29.17 MPa	/	/	~75% (160)	90	60.1% (200)	232
	PVDF-based	PVDF-g-PSSA-co-PMAc	-SO <sub>3</sub> H; -COOH	~80	0.73	~28	2.56	/	/	/	/	33	/	235
	SPPEK-based	SPPEK-P-90	-SO <sub>3</sub> H	/	/	23.2	1.51	71 MPa 18%	800°C (~44%)	/	80% (80)	290	100	141

Membrane Type		Membrane name	Functional group(s)	Ionic conductivity (mS·cm <sup>-1</sup> )	VO <sup>2+</sup> permeability (10 <sup>-7</sup> cm <sup>2</sup> min <sup>-1</sup> )	WU (%)	IEC (mmol g <sup>-1</sup> )	Mechanical property <sup>a</sup>	Thermal stability <sup>b</sup>	Chemical stability <sup>c</sup>	EE (%) (current density (mA cm <sup>-2</sup> ))	Self-discharge duration (hours)	Life stability testing <sup>d</sup>	Ref.
Anion-exchange membrane	PSF-based	PSf-c-PTA-1.4	-NR <sub>3</sub>	20.4	2.57	36.7	1.71	32.5 MPa 8%	/	/	~78% (180)	58	~77% (50)	270
		CMPSF-72	Imidazole group	/	/	/	1.51	/	~825°C (~61%)	/	~75% (160)	/	6000	272
	PAEK-based	PAEK-API 2.0	Imidazole group	~5.2	1.91	/	1.43	9.04 MPa 87.7%	/	/	~78% (100)	/	~84% (100)	278
Amphoteric-ion exchange membrane	PVDF-based	AIEM (A, DOG=42.7%)	-SO <sub>3</sub> H; -NR <sub>3</sub> <sup>+</sup> ;	~67	0.53	~14.5	/	/	/	/	/	85	/	307
Porous membrane	PBI-based	B-PBI	Imidazole group; pyridine group	/	2.7 x 10 <sup>-2</sup>	~9.5	/	/	800°C (~28%)	/	~80% (160)	/	600	330
		PBI-68	Imidazole group	/	/	/	/	/	/	/	~74% (200)	/	68% (1350)	328
	PES-based	IP2-0.15	-COOH	269	0.73	/	/	/	/	/	80% (260)	/	93% (100)	338
		m30-24	-SO <sub>3</sub> H	/	/	/	/	/	800°C (~59%)	/	78.32% (200)	/	~85.3% (100)	319
	PAN-based	PIM-1/PAN	\	/	/	/	/	/	/	/	85% (40)	/	100	345
	Porous glass-based	VPG	\	28.5	/	/	/	/	/	/	77.3% (40)	240	~68% (40)	348

a: Tensile strength (MPa) and Elongation at break (%)

b: Terminal testing temperature of the TGA test and corresponding weight loss (%)

c: Reduction of VO<sub>2</sub><sup>+</sup> (%) and testing time of the chemical stability test

d: Capacity retention ability (%) and cycle number

## 6. Transport mechanisms

As mentioned earlier, polymer electrolyte membrane, as an integral component of a flow battery system not only provide pathways for ionic transport, but also prevents cross-contamination of electrolytes. During the operation of VRFBs, vanadium ions ( $V^{2+}$ ,  $V^{3+}$ ,  $VO^{2+}$ ,  $VO_2^+$ ), protons, and water, all possess the tendency to be transferred across the membrane through various mechanisms which consequently result to the complex mass transport and highly coupled transport processes within the battery system. This complex transport phenomena therefore leads to concentration and volume imbalance between the two electrolytes, self-discharge, and undesired side reactions which in turn significantly affect the cycling processes and efficiencies of VRFBs. In this section, the transport phenomena of vanadium ions, protons, and water through polymer electrolyte membranes are discussed.

### 6.1 Proton transport

Proton ( $H^+$ ) is one of the positive charges present in VRFB electrolytes resulting from the dissociation of sulfuric acid in the electrolytes. More importantly, protons are the major charge-carriers which moves across the membrane, particularly for the cation-exchange membranes, during charge and discharge processes to achieve charge balance between the electrolytes and also to complete the electrical circuit in the cell.<sup>54, 285, 295, 357</sup> The direction of proton flux across a cation-exchange membrane is dependent on the charge and discharge process, and therefore influences the volume of anolyte and catholyte of the VRFB. In more detail, protons as major charge-carrying species move from the negative side of VRFBs to the positive side during a discharge process to ensure electroneutrality, but in the reverse direction during charging conditions.

For cation-exchange membranes like Nafion and other sulfonated membranes, there are two major mechanisms, namely Grotthuss and Vehicular, that contribute to proton transport across these membranes.<sup>61, 358</sup> Grotthuss mechanism is the dominant proton transport mechanism and it involves the transport of protons at the center of membrane pores resulting from the hydrogen bond network of water molecules in the channels of the membrane.<sup>61</sup> The vehicular mechanism, on the other hand, refers to proton transport by correlated ion-pair motion, which allows the



transport of protons along the sidewalls of the membrane pores. Consequently, the proton conductivity of membranes can be greatly enhanced by increasing the pore sizes of membrane. However, such a design may also result in high vanadium-ion permeability and water transport which in turn leads to poor battery performance.

In summary, as proton transport is significant in tandem with water and vanadium-ion transport, it is therefore essential for membranes used in VRFBs to effectively distinguish vanadium ions from protons. Generally, the ideal polymer electrolyte membrane suitable for VRFB operations should selectively limit vanadium-ion permeability while allowing the ease transport of protons.

## 6.2 Vanadium-ion transport

The continuous circulation of electrolytes during the operation of VRFBs and the concentration difference of vanadium ions between the two half-cells inevitably leads to the transport of vanadium ions across the membrane to the opposite compartment, even though, it is desirable for this crossover process not to take place.<sup>49</sup> Vanadium ions crossover consequently triggers self-discharge, side reactions, and capacity loss. The transport of vanadium ions across polymer electrolyte membranes varies with the ionic exchange groups attached to the membrane.<sup>359, 360</sup> For instance, a typical cation-exchange membrane readily gives pathways to positively charged ions, primarily because the membrane composition contains negatively charged groups, such as  $-\text{COO}^-$ ,  $-\text{PO}_3\text{H}^-$  and  $-\text{SO}_3^-$ . On the other hand, the anion-exchange membranes contain positively charged groups, like  $-\text{NH}_3^+$ ,  $-\text{SR}_2^+$  and  $-\text{NRH}_2^+$ , in their matrix and therefore allow the transport of anions while restricting the transport of cations.<sup>360</sup> Besides the attached groups on the membrane, the morphology and structure of polymer electrolyte membranes also influence the transport of metal cations.<sup>361</sup> In this section, vanadium-ion crossover in cation-exchange membranes and porous membranes are discussed. Generally, the various mechanisms that contribute the transport of vanadium ions through membranes are diffusion, migration, and convection. These transport mechanisms are influenced and determined by different factors. Diffusion mechanism is majorly determined by the concentration gradient of vanadium ions; migration mechanism is largely influenced by the potential gradient of electrolytes; and convection is primarily driven by pressure gradient of the electrolytes.<sup>49, 362</sup>

To investigate the processes and effects of vanadium-ion transport mechanisms in cation-exchange membranes, as well as the dominant mechanisms in VRFBs under various operating conditions, several computational and numerical studies have been carried out. Knehr et al.<sup>363</sup> developed a model to investigate the transport of vanadium ions through the membrane used in a VRFB. The three aforementioned transport mechanisms were all taken into consideration in the study. It was pointed out that, diffusion, convection and migration influence the rate and direction of vanadium-ion transport across the membrane during charging and discharging processes based on the operating conditions of the numerical study. The study further shows that the net vanadium-ion transport occurs from the positive to the negative half-cell during charging process and then reversed during discharging process. In another study, the influence of different membrane thicknesses on these transport mechanisms were later numerically investigated.<sup>364</sup> Their results showed that the membranes with a thinner thickness present a higher crossover flux indicating that the ease of vanadium ions transport through membranes is closely related to the thickness of the membrane as shown in **Fig. 17 (a)**. Besides membrane thickness, the degradation of membrane also enhances the crossover of vanadium ions through the membrane.

To compare the transport mechanisms in different types of cation-exchange membrane, Nafion 117 and sulfonated Radel membranes were studied using numerical model.<sup>365</sup> The results indicated that vanadium-ion transport through Nafion 117 was predominated by diffusion. While vanadium-ion transport through sulfonated Radel membrane was reported to be mostly dominated by convection as a result of low vanadium-ion permeability and high ionic conductivity of the membrane. The study also showed that, in the s-Radel membrane, the direction of convection changes during the charging and discharging process, while it maintained the same direction in Nafion membranes. This therefore shows that the transport processes of vanadium ions in different membranes may not be generally the same.

Other than the cation-exchange membranes, Zhou et al.<sup>366</sup> also developed a numerical model to investigate the three transport mechanisms of vanadium ions through a porous membrane made of pore size of about 45 nm. Operation parameters including the electrolyte flow rate

showed a great influence on the crossover rate through the porous membrane. After the numerical analysis, transport of vanadium ions by convection was discovered as the dominant transport mechanism in the porous membrane. In addition, their results further indicated vanadium-ion crossover via convection can be reduced if the pore size of the membrane is below 15 nm, while the vanadium ion crossover resulting from diffusion and migration modes can be reduced if the pore size is about 2 nm.

In summary, the direction of vanadium species crossover through membrane due to diffusion is the same during both charging and discharging processes while the direction of migration changes,<sup>367</sup> as shown in **Fig. 17 (b)**. For different operating conditions and membranes, it is also important to take all these mechanisms into consideration when analyzing the contribution of each mechanism to the transport of vanadium ions as they may not always be the same.

### **6.3 Water transport**

The transfer of water through the polymer electrolyte membrane is of vital importance as it greatly influences electrolyte volume change and the overall performance of flow batteries. Water crossover may lead to imbalance between the volume of electrolytes, thereby resulting in the dilution/flooding of one electrolyte and at the same time leading to more concentration/precipitation of the other electrolyte solution.<sup>49, 368-371</sup> Apparently, this usually result in the capacity loss as well as operational difficulties in flow battery systems.

In VRFBs, water is produced in the positive side during discharge while consumed during charge. Skyllas-Kazacos and her research team<sup>368</sup> for the first time investigated water transport in VRFBs after an unequal level of electrolytes in the two half-cells were observed in their previous studies.<sup>295, 372</sup> Various mechanisms were reported to be responsible for water transport across the membrane. First, the diffusion of water (bound water) along with the crossover of electroactive species. Water molecules have been reported to accompany vanadium ions as the later transport through the membrane during the charge and discharge operations of a VRFB.<sup>370</sup> Second is water concentration difference between the two half-cells.<sup>373</sup> Third, water transfer across membrane by electro-osmotic drag. This is the water dragged alongside proton transport through the membrane as the protons move to maintain electroneutrality and complete the

internal electric circuit in the cell.<sup>371, 374</sup> Water transport by electro-osmotic drag from proton flux has been reported to transfer more volume of water across the membrane in comparison to vanadium ions crossover.<sup>374</sup> Water transport through the membrane also occurs via osmosis. This is as a result of the osmotic pressure gradients between the two half-cells, which could exist due to the difference in the viscosity of the catholyte and anolyte.<sup>373</sup> In a VRFB, the viscosity of the catholyte is usually greater than the anolyte which leads to pressure gradient across the membrane.<sup>375</sup> This therefore underlines the convective water transport towards the negative half-cells in cation-exchange membranes, irrespective of charging or discharging condition. Generally, electro-osmosis water drag via proton flux and diffusion of water are considered to predominantly influence electrolyte imbalance as they both majorly contribute to electrolyte volume change, and in turn influence concentration difference of electrolytes on both sides of VRFBs. However, Jeong and Jung<sup>373</sup> mentioned that, if equal number of protons move across the membrane during a cycling process, the electroosmotic drag would not contribute to electrolytes imbalance.

Generally, the rate and direction of water transport are determined by the nature and properties of membranes, electrolyte compositions, and SOC. Hence, when a cation-exchange membrane is employed in VRFBs, a significant volume of water moves from the negative half-cell to the positive half-cell during the battery operations, which is attributed to the large volume of water (hydration water) that accompanies  $V^{2+}$  and  $V^{3+}$  transport from the negative side. However, water transport occurs in the reverse direction when an anion exchange membrane is used.<sup>61, 376</sup> As for the SOC, Sukkar and Skyllas-Kazacos<sup>370</sup> investigated the effects of SOC on water transport in cation-exchange membranes. Their results indicated that from SOC-100 to SOC-0, water moves towards the positive half-cell at first and then reverses the direction at about SOC-50 and then maintains the new direction till SOC-0. The study further revealed that at high SOCs, the rate of water crossover has negligible effect on the system operations while it becomes significant when the battery reaches over-discharge state.

In order to further understand the contribution of different mechanisms of water transport in a cation-exchange membrane employed in a VRFB, a model on water transport was recently

developed.<sup>369</sup> The model thoroughly considered the water produced during the redox reactions at the positive electrode, the side reactions and three water transfer mechanisms namely electro-osmotic drag (EOD), water diffusion, and vanadium-ion crossover with bound water. The illustration and contributions of these water transfer mechanisms are shown in **Fig. 18 (a)**. Specifically, the contribution of the different mechanisms of water transport when the battery is operated at a current density of  $60 \text{ mA cm}^{-2}$ , is shown in **Fig. 18 (b)** and **(c)**. It was further concluded that when the battery is operated at a low current density or after longer charge-discharge duration, the difference between the anolyte and catholyte volumes significantly increases. A more recent numerical analysis on water transport revealed that electro-osmosis water drag via proton flux and diffusion have the major influence on water transport across cation-exchange membranes.<sup>373</sup> Electro-osmosis water drag by protons was further predicted and presented as the dominant water transport mechanism due to the fact that the direction of the water flux resulting from electro-osmosis water drag via proton is the same as the direction of ionic current through the membrane.

In summary, various factors are responsible for water crossover through the membranes employed in VRFBs. For different polymer electrolyte membranes and working conditions, the dominant water transport mechanism may change. Even though water transport across the membrane could be associated with some challenges including capacity degradation, it is worth noting that the complete prevention of water crossover might not be practicably achievable. The reason is that, for polymer electrolyte membranes especially cation-exchange membranes, the transport of protons is always accompanied by water transport. As such, the complete prevention of water transport will consequently hinder the flow of protons across the membrane and result in high internal resistance in the battery system. Therefore, it is of vital importance for the membrane to ensure an optimized water transport ability so as to achieve an appropriate balance between proton conductivity and low vanadium-ion permeability.

## **7. Performance-enhancing strategies for membranes**

A number of strategies have been developed and applied to enhance the performance of membranes towards achieving significant performance improvement in flow batteries.

Irrespective of the membrane preparation method or materials, there are various enhancement strategies that can be applied to improve the performance of both membrane and battery. Some of these strategies include adjusting the DS,<sup>200, 204</sup> blending/compositing with other polymers,<sup>174, 233</sup> and tuning pore structural parameters,<sup>285, 295, 377</sup>. Thus, this section briefly discusses some of these performance-enhancing strategies that have shown significant improvement on the cycle stability, self-discharge rate and voltage, coulombic and energy efficiencies of flow batteries.

### **7.1. Adjusting sulfonation degree**

Degree of sulfonation (DS) indicates the amount of sulfonic acid groups contained in a membrane. Hence, this is closely related to the IEC of the membrane and therefore plays a key role in influencing the ionic conductivity of the membrane. DS can be adjusted by using methods such as varying the time and temperature of the reaction during membrane preparation so as to obtain a desired DS and associated membrane properties.<sup>52</sup> Many studies have attempted to adjust the DS of various materials during membrane preparation process towards improving the membrane performance.<sup>200, 220</sup>

SPEEK, as one of the most widely utilized materials for cation-exchange membranes preparation have been deeply investigated regarding the influence of DS on the properties of the SPEEK-based membranes. The investigation revealed that the increment of DS of the SPEEK increases its proton conductivity, water uptake ratio and IEC.<sup>203</sup> However, it also leads to increase in vanadium-ion crossover and subsequently reduces the mechanical strength of the membrane. Other than the SPEEK, the effects of DS on the fluorene-containing poly(arylene ether sulfone)s have also been evaluated.<sup>72</sup> It was found that, similar to the SPEEK membranes, the resulting membranes with high DS also showed improved proton conductivity and low mechanical strength.

It should be noted that the influence of DS on different polymers may not always be the same. For example, research on the SPI and polyvinyl alcohol (PVA) blending membrane revealed that, while the increase of DS provides the membrane with high proton conductivity and crossover rate of vanadium ions, unlike SPEEK membranes, its mechanical strength was found

to increase, due to the improved dispersion of SPI in the blend membranes, which therefore results in a less stress convergence during mechanical property test.<sup>209</sup> Therefore, for specific membrane compositions, the optimized DS needs to be specifically analyzed according to different application requirements. These results proved that adjusting the DS of membrane is an effective method that has great influence on the ion conductivity, crossover rate, and mechanical properties of membranes. However, for different materials, the effects of DS are not necessarily the same. Generally, a high DS would increase the proton conductivity and vanadium ions crossover of a membrane.

## 7.2. Blending/compositing with other polymers

Blending/compositing with other polymers is another important method that is widely used for enhancing the performance of polymer electrolyte membrane.<sup>240, 253</sup> Various polymers have been composited with other polymers to obtain different membranes including cation-exchange, anion-exchange, amphoteric-ion exchange and porous membranes.<sup>265, 319, 321</sup> Through compositing various polymers during the preparation process, the merits of different polymers can be combined while the drawbacks could be compensated for each other and therefore form a polymer electrolyte membrane that is more suitable for flow batteries.

For example, the introduction of hydrophobic PVDF into SPEEK membrane was reported to restrain the swelling nature of pristine SPEEK.<sup>174</sup> The obtained SPEEK/PVDF composite membrane was found to exhibit a much lower ion permeability than Nafion 117 and achieved a better cell performance with reduced self-discharge rate. Other than PVDF, the combination of PAN and SPEEK has also been investigated, where the properties of the composite membrane with varied mass ratios are shown in **Table 2**.<sup>85</sup> The water uptake ratio and vanadium-ion permeability of the membrane were effectively reduced as a result of the hydrogen bonding between SPEEK and PAN and the acid-base interaction of ionic cross-linking. Compared to Nafion 117, this composite membrane finally provides the battery with improved coulombic and energy efficiencies.

Beyond using only two types of polymer during membrane preparation, the combination of more polymers has also been studied and proven as an effective method. For instance, Wang et

al.<sup>226</sup> deposited the positively charged polyelectrolyte PDDA and negatively charged PSS on SPFEK membrane layer-by-layer fabricate a PDDA/PSS-SPFEK composite membrane. With the introduction of the PDDA/PSS bilayer, the chemical stability of the membrane was greatly improved, and its vanadium-ion permeability was also reduced, compared to the pristine SPFEK membrane.

**Table 2.** Data of physicochemical properties, mechanical properties, VO<sup>2+</sup> permeability, and ion selectivity of Nafion 117, SPEEK, and SPEEK/PAN membranes.<sup>85</sup> Reproduced with permission. Copyright 2014, American Chemical Society.

Membranes	Water uptake (%)	Swelling ratio (%)	IEC (mmol g <sup>-1</sup> )	Proton conductivity (mS cm <sup>-1</sup> )	Breaking strength (Mpa)	Elastic modulus (Mpa)	Percentage elongation (%)	VO <sup>2+</sup> permeability (10 <sup>-7</sup> cm <sup>2</sup> s <sup>-1</sup> )
Nafion 117	37 ± 1	20 ± 1	0.93 ± 0.01	36.2 ± 1.0	19.1 ± 0.3	189 ± 7	149 ± 3	37.7 ± 0.4
SPEEK	365 ± 18	109 ± 1	2.24 ± 0.01	19.5 ± 0.3	20.1 ± 0.3	696 ± 15	97 ± 2	76.6 ± 2.6
S/PAN-5%	183 ± 7	52 ± 1	2.12 ± 0.01	18.6 ± 0.4	22.2 ± 0.4	749 ± 19	91 ± 3	48.4 ± 0.8
S/PAN-10%	120 ± 4	34 ± 1	2.00 ± 0.01	17.5 ± 0.3	23.8 ± 0.5	805 ± 20	79 ± 4	29.9 ± 0.2
S/PAN-15%	69 ± 2	21 ± 1	1.89 ± 0.01	16.3 ± 0.4	25.9 ± 0.7	959 ± 21	57 ± 2	17.8 ± 0.1
S/PAN-20%	58 ± 1	16 ± 1	1.78 ± 0.01	15.0 ± 0.3	28.3 ± 1.1	1043 ± 29	41 ± 1	11.3 ± 0.1
S/PAN-25%	51 ± 1	14 ± 1	1.67 ± 0.01	13.4 ± 0.2	32.9 ± 1.5	1148 ± 25	32 ± 1	7.7 ± 0.1

Other than cation-exchange membranes, compositing different polymers is also considered as an effective method for the performance improvement of other types of membranes. For instance, a series of anion-exchange membranes was prepared by pore-filling the PE substrate with poly(4-vinylbenzyl chloride) followed by amination with pyridyl functional groups.<sup>285</sup> It is found that, with the increasing content of divinylbenzene in this composite membrane, the cross-linking between polymers increased, which further lead to a more dense membrane structure and thereby preventing the crossover of vanadium ions. The optimized membrane finally possessed an improved conductivity with a lower vanadium-ion permeability compared to Nafion 117. The VRFBs assembled with the obtained membranes presented a 5.4 % higher energy efficiency than the ones assembled with Nafion 117.

With these results, blending/compositing different polymers is hence proved to be an effective method for preparing high-performance membrane. However, it is important to carefully adjust



the content ratio between the different polymers so as to ensure that the membrane achieve adequate balance among properties for better performance.

### **7.3. Tuning pore structural parameters**

The pore structures of polymer electrolyte membranes such as pore size and porosity have been proven to greatly influence the transport of species within the membrane.<sup>342</sup> Membranes with large pore sizes would ease species transport and further provide the batteries with low internal resistance and high voltage efficiency. However, membranes with a large pore size may also result in severe crossover of vanadium ions which in turn reduce the capacity retention ability of the battery. Therefore, tuning the pore sizes of membranes to appropriate dimension can greatly influence the performance of the membranes and flow batteries. Especially for the porous membranes, the pore sizes are considered to be one of the most important parameters that can be tuned to improve their performance.<sup>322, 325</sup>

Many methods have been proposed for tuning pore structure. One of the pore adjustment strategies is through blending different polymers. Chen et al.<sup>342</sup> combined the SPEEK with PES to fabricate a series of symmetric spongy porous membranes. It was found that, with the increment of SPEEK content, the pore size of this composite membrane can be enlarged, thereby validating that the content ratio between different polymers in a composite membrane has significant effect on the adjustment of membrane pore structure. Overall, by adjusting the pore structure, the obtained optimal membrane with 13 % of SPEEK successfully provide the battery with stable cell performance for more than 200 cycles. Another successful demonstration for pore structure control was achieved by Peng et al.<sup>378</sup> by introducing an ultra-thin defect free skin layer onto the surface of PBI-based porous membranes. In their study, the adjustment of the porosity and pore size was achieved by varying the porogen content, while it was found that, with the porogen content increased to 200 wt.%, the membrane achieved the best balanced performance with a coulombic efficiency of 99 % and an energy efficiency of 82.3 % at 80 mA cm<sup>-2</sup>. However, it was also found that, over increasing the porogen content has a negative effect on the capacity retention ability of the membrane, as shown by the cycle performance test conducted. Hence, it has been proven that the membrane pore structure has

notable impact on the membrane performance. Thus, the pore structure and sizes of membrane are of vital importance towards determining membrane performance, as well as an effective strategy for membrane and battery performance improvement.

#### **7.4. Tuning geometric parameters and designs**

The performance of polymer electrolyte membranes can be significantly enhanced by tuning the geometric parameters and designs of the membranes. A lot of studies have shown that the geometric parameters of membranes such as the thickness have several impacts on the membrane properties such as ionic conductivity and mechanical strength, and are therefore considered to be one of the most effective methods for performance improvement.<sup>84, 379</sup>

Membrane thickness is an important geometric parameter that has significant influence on the performance of both membrane and battery. The effect of the thickness of SPEEK membranes on the performance has been deeply investigated by a series of SPEEK membranes with thickness ranging from 30-150  $\mu\text{m}$ .<sup>380</sup> The results showed that the thickness of membrane largely influences the charge and discharge voltage profile of the battery, as membrane thickness is one of the parameters that determine the ohmic resistance of the membrane. In the meanwhile, with the increase of membrane thickness, the vanadium ions permeability is found to decrease, while, the thicker membrane would result in a large resistance, and thereby lead to low voltage efficiency.

Other than the membrane thickness, tuning the membrane structure design is another effective method for performance improvement. A novel sandwich-structure membrane proposed by Yu et al. has proven this idea.<sup>194</sup> Utilizing the hydrophilic porous PTFE and SPEEK, a novel PTFE/SPEEK/PTFE membrane was fabricated. With the introduction of PTFE layer on both sides of the SPEEK membrane, the external damages from electrolytes, electrodes and sealing materials were successfully prevented which hence provides the membrane with better chemical stability. It was found that, with this novel design, the membrane with an appropriate thickness of PTFE presented an excellent capacity retention ability after running for more than 1000 cycles as shown in **Fig. 19**. Hence, tuning the geometric parameters and designs of membranes are typical effective methods that can improve the performance of membranes.

However, it is worth to emphasize that for different membrane compositions and designs, the required optimal thickness is not necessarily the same and should be adjusted individually.

### **7.5. Adding inorganic materials**

Similar to blending/compositing with other polymers during membrane preparation process, adding inorganic materials is another effective and widely-used method that improves the membrane performance.<sup>98, 325</sup> It has been proven in direct methanol fuel cells that the incorporation of inorganic materials to membranes can help alleviate methanol crossover.<sup>54</sup> Hence, in an attempt to restrict the vanadium ions permeation effectively, researchers have followed this idea and developed membranes for VRFBs through adding various inorganic materials.

Carbon-based inorganic materials have been widely employed for membrane preparation. In section 5, the involvement of GO, which is a famous material with special two-dimensional layered structure has been extensively discussed as an additive in the fabrication of various composite membranes with improved performances.<sup>210</sup> In addition to that, nano carbon-based materials have also been used for membrane fabrication. The short-carboxylic multi-walled carbon nanotube (SCCT) is an inorganic material which exhibited excellent electrochemical activity and durability. It has been successfully embedded into SPEEK matrix to fabricate the SPEEK/SCCT membrane.<sup>198</sup> The introduction of SCCT offers the composite membrane with a high electro-catalytic activity, which in comparison to Nafion 212 also exhibited higher mechanical strength and lower vanadium-ion permeability, as shown in **Fig. 20**.

Other than carbon-based materials, different types of nano oxides have also been used as additive for membrane preparation. The introduction of Al<sub>2</sub>O<sub>3</sub>, SiO<sub>2</sub>, and TiO<sub>2</sub><sup>175</sup> into the SPEEK is an example. It was found that the introduction of these inorganic particles into polymers can improve the mechanical property of the membrane while suppressing the crossover of vanadium ions as the inorganic particles could serve as barrier. The battery test results showed that in comparison to Nafion 117, the fabricated composite membrane exhibited a much better cycle stability.

In summary, adding inorganic particles into other polymers for membrane preparation could therefore be regarded as an effective performance-enhancing technique. It is also worth to note that the concentration of these inorganic particles inside the membrane may be an important factor that could influence the overall membrane performance.

## **8. Cost and commercialization**

High capital cost is one of the crucial factors hampering the wide application of flow batteries.<sup>141, 175, 255</sup> To realize the actual application of flow batteries, several cost analysis have been carried on their structural components so as to identify and reduce the major sources of the high cost. In the meanwhile, attracted by the impressive performance of flow battery technology, some large-scale commercial systems have been constructed and developed to validate their practicality.<sup>381, 382</sup>

### **8.1 Cost**

The high initial cost of flow battery is one of the major concerns holding back its widespread commercialization. The cost of flow battery system is closely related to the set-up of the system, which is determined by the requirement of the power and storage capacity. In 2004, Joerissen et al.<sup>383</sup> comprehensively analyzed the cost of a VRFB as an electrical energy storage system based on lab-scale cell experiments. Results from the analysis showed that for a 2 kW/30 kWh system, the cost of VRFB is expected to be slightly lower than €30000. Their results also indicated that the cost of a VRFB system is very sensitive to the market price of  $V_2O_5$  such that a reduction in price of  $V_2O_5$  is expected to reduce the cost of VRFB.

In order to further analyze the relationship between the performance and cost of flow battery, Viswanathan et al.<sup>384</sup> later developed a cost and performance model for flow battery. The model has been used to regulate the operating parameters of the battery system in order to maximize the efficiency of the system while minimizing the capital cost. Considering VRFB, the model results showed that the battery using the sulfuric acid-based electrolyte incurs a higher cost than the system using mixed acid-based electrolyte. For VRFB system using mixed acid electrolyte, the cost of  $V_2O_5$  takes 8 and 43 % of the total cost, for the system with an energy size of 0.25 MWh and 4 MWh, respectively. While the cost for the membrane in these systems

takes 44 and 27 %, respectively. The results indicated that the major cost of the entire flow battery system largely depends on the cost of membrane and electrolyte preparation. To analyze the cost of an optimized VRFB system, another model has been developed by Crawford et al.<sup>385</sup> The results showed that the optimized system is estimated to have a system cost < \$ 350 kWh<sup>-1</sup> for 4-h application. While, it was also suggested that the cost could be reduced to 160 kWh<sup>-1</sup> when the production scale becomes larger. Furthermore, the costs of different types of flow battery system have also been compared in order to identify the optimal flow battery suitable for commercialization. Zeng et al.<sup>51</sup> investigated the application of large-scale electrical energy storage using VRFB and iron-chromium RFB and also analyzed the capital cost of both flow batteries. It was revealed that for a 1 MW-8h system, the capital cost of a VRFB is \$ 229 kW h<sup>-1</sup>, while an iron-chromium RFB goes for \$ 194 kW h<sup>-1</sup>. According to their study, one of the major contributors to the high cost of VRFB is the electrolyte as it accounts for about 53 % of the total cost while the membrane takes almost 20 % of the total cost. Different from VRFBs, the component with the highest cost in iron-chromium RFB is the membrane as it takes 38 % of the total cost while that of the electrolyte is 9 %. Thus, while the electrolyte cost varies a lot for different flow battery systems, the cost of membrane is always high and requires substantial reduction.

With the cost analysis of flow battery system, the cost of the membranes and the electrolyte are identified as the most important factors that hinder wide application of flow batteries. It is believed that, reduction in the cost of membranes will accelerate the wide application of flow battery systems.

## **8.2 Commercialization**

### **8.2.1 Membrane level**

The polymer electrolyte membranes that are commercially available and commonly employed in flow battery systems are still very limited. The most widely used commercial polymer electrolyte membranes come from the Dupont including the Perfluorinated Nafion series (e.g., Nafion 115, Nafion 117, Nafion 211, Nafion 212 etc.). These membranes possess adequate stability and provide flow batteries with satisfactory performance. However, the Nafion

membranes are very expensive and possess low selectivity of protons to other ions which therefore limit their wide application. To compensate for this, various methods have been employed for membrane modification to enhance their electrochemical properties. Notwithstanding, a reduced cost of Nafion membrane materials coupled with improved transport properties would go a long way in the market widespread of VRFB. Other than the Nafion membranes, another type of commercial membrane named VANADion, has also been used in flow batteries and shows compelling performance. The VANADion membrane is made of a micro-porous layer together with a thin Nafion layer. VANADion 20 and VANADion 20L are the two available types of VANADion membranes on Nafionstore Ion Power Nafion™ Store website.<sup>381, 382</sup> In addition to these cation exchange membranes, some of the common commercial anion-exchange membranes developed by Fumasep have also been summarised and compared as shown in **Table 3**.

**Table 3.** Summary and comparison of commercial membranes.

S/No	Membrane type	Size	Cost	Typical thickness (µm)	Basis weight (g/m <sup>2</sup> )	Ref.
1	Nafion 115	0.30 x 0.30 m	\$165.00	127	250	382
		0.41 x 1.23 m	\$773.00			
2	Nafion 117	0.30 x 0.30 m	\$200.00	183	360	382
		0.41 x 1.23 m	\$1,004.00			
3	Nafion 211	0.305 x 0.305 m	\$130.00	25.4	50	382
		0.305 x 1 m	\$369.00			
		0.305 x 5 m	\$970.00			
4	Nafion 212	0.305 x 0.305 m	\$ 135.00	50.8	100	382
		0.305 x 1 m	\$419.00			
		0.305 x 5 m	\$1,360.00			
5	VANADion 20	0.30 x 0.30 m	\$105.00	254	/	381
6	VANADion 20L	0.30 x 0.30 m	\$215.00	254	/	381
7	Fumasep® FAP-420-PE	0.10 x 0.10 m	\$17.00	20	25-38	386
		0.20 x 0.30 m	\$50.00			
8	Fumasep® FAP-450	0.10 x 0.10 m	\$19.00	50	75-85	386
		0.20 x 0.30 m	\$63.00			
9	Fumasep® FAS-30	0.10 x 0.10 m	\$16.00	30	35-44	386
		0.20 x 0.30 m	\$43.00			
10	Fumasep® FAA-3-PK-75	0.10 x 0.10 m	\$21.00	70-80	70-90	386
		0.20 x 0.30 m	\$72.00			
11	Fumasep®	0.10 x 0.10 m	\$21.00	130	100-130	386

	FAB-PK-130	0.20 x 0.30 m	\$72.00			
		0.20 x 0.30 m	\$72.00			

### 8.2.2 Battery level

In 1993, the first VRFB system developed by the University of New South Wales, conducted its first field trial in a Solar House in Thailand and since then more and more efforts have been put into the commercialization of this particular flow battery to further validate and improve their practical applications.<sup>387</sup> Later, in 1996, a 200 kW/800 kWh VRFB system was installed by Mitsubishi Corporation for load-leveling at Kashima-Kita Electric Power.<sup>6</sup> In 2005, another 4 WM/6 MWh VRFB system was installed at Subaru Wind Farm for electrical energy storage by Sumitomo Electric Industries.<sup>388</sup> Following these successful installations and commercial applications, more and more large-scale VRFB systems have been installed at various locations across the globe including Japan, Europe and the U.S.A. Some of these installations are summarized in **Table 4**.

**Table 4.** Summary of some successful installations of large-scale VRFB systems at different locations

S. No	Installation site/country	Company/project name	Year	Power output	Energy	Energy eff.	Ref.
1	Thai Gypsum Solar Demonstration House, Thailand	University of New South Wales, Australia	1993	1.6-5 kW	12 kWh	/	45, 387
2	Kashima-Kita Electric Power, Japan	Mitsubishi Chemicals	1996	200 kW	800 kWh	/	6, 388
3	Tasumi Sub-station, Kansai Electric	Sumitomo Electric Industries	1996	450 kW	900 kWh	/	388
4	Renewable Energy Dynamics Technology Ltd.	Camco Clean Energy	2000	5kW/20 kW	20kWh/100 kWh	/	46
5	Kansai Electric, Japan	Sumitomo Electric Industries	2000	200 kW	1.6 MWh	/	388
6	Stellenbosch University, South Africa	VRB Power	2001	250 kW	500 kWh	/	388
7	Tottori Sanyo Electric, Japan	Sumitomo Electric Industries	2001	1.5 MW	1.5 MWh	/	388
8	Hokkaido Electric Power Wind farm, Japan	Sumitomo Electric Industries	2001	170 kW	1 MWh	/	45
9	CESI, Milan, Italy	Sumitomo Electric Industries	2001	42 kW	90 kWh	/	388
10	Gwansei Gakuin University, Japan	Sumitomo Electric Industries	2001	500 kW	5 MWh	/	388
11	High-Tech factory, Japan	Sumitomo Electric Industries	2003	500 kW	2 MWh	/	388
12	Hydro Tasmania on King Island	Pinnacle VRB	2003	250 kW	1 MMWh	/	388
13	Pacific Corp in Moab, USA	VRB Power	2004	250 kW	2 MWh	/	54
14	J Power, Subaru wind farm, Tomahae, Japan	Sumitomo Electric Industries	2005	4 MW	6 MWh	/	388
15	Australia	V-Fuel	2005	5 kW-50kW	/	/	46
16	Some Hill wind farm, Donegal, Ireland	Tapbury Management and Sustainable Energy Ireland	2006	2 MW	12 MWh		45
17	Different commercial batteries in Thailand	Cellenium Company Limited	2008	10-50 kW	/	/	389
18	Germany	Gildemeister	2010	10 kW/1 MW	40kWh/4 MWh	/	46
19	Dalian EV Charging Station	Dalian Institute of Chemical Physics and Rongke Power, China	2010	260 kW	5 MWh		45



S. No	Installation site/country	Company/project name	Year	Power output	Energy	Energy eff.	Ref.
20	U.S.A.	California Public Utilities Commission	2011	100 kW	300 kWh	/	45
21	Zhangbei, China	Prudent Energy Corporation	2011	500 kW	1 MWh	/	45
22	Austria	Gildemeister, Germany	2014	/	300 kWh	/	45
23	U.S.A.	Imergy, Silicon Valley	2015	250 kW	1 MWh	/	45
24	Pullman, Washington, USA	UniEnergy Technologies	2015	1 MW	4 MWh	/	45
25	China	Golden Energy Fuel Cell Co., Ltd	2003	2.5 kW/4MW	3.75 kWh/ 32 MWh		46
26	China	Golden Energy Century Limited	2011	2.5kW/5 kW	40 kWh		46
27	China	Pan-tang Group Pang-zhi-hua Iron and Steel Research Institute	/	0.25-0.9 kW	24Wh dm <sup>-3</sup>	/	389
29	Australia	National Energy Research Development Council	/	1.33 kW	0.7 kWh	72-90 %	389
30	Austria	Austrian Motor and Expressway Operator	/	1 kW	50 kWh	/	389
31	Australia, and Canada	Telepower Australia pty. and Vantack Technology Corp	/	250 kW	520 kWh	82-85 %	389
32	Australia	Department of Resources and Energy, Australia	/	1 kW	5 kWh	/	389
33	Gongju, South Korea	Samyoung	/	50 kW	0.1 MWh	/	390
34	China	National 863 programme of China	/	1 kW	/	78 %	389
35	Kongens Lyngby, Denmark	RISO Syslab Redox flow battery	/	15 kW	0.1 MWh	/	390
36	Sumba, Indonesia	Sumba Island Microgrid Project	/	400 kW	0.5 MWh	/	390
37	Evora, Portugal	PVCROPS Evora	/	5 kW	0.1 MWh	/	390
38	Vierakker, Netherlands	Fotonenboer't Spieker Photon Farm Project		10 kW	0.1 MWh	/	390

## 9. Remaining challenges and perspectives

Flow batteries, with their independently tunable power and energy storage capacity, are considered as one of the most promising electrochemical systems for large-scale electrical energy storage. Coupled with their compelling features and advantages, they have therefore increasingly attracted global attention. However, the unsatisfactory performance and high capital cost of polymer electrolyte membrane, one of the major components in flow batteries, remain a major concern towards achieving the wide application of flow battery systems. This therefore justifies the need for further studies on performance improvement as well as cost effectiveness of membranes, especially under high charge/discharge current densities and extreme operating conditions.

The Nafion membranes, as the most widely used commercial membrane, possess a number of advantages and have therefore attracted several applications in large-scale systems. However, their wide applications still suffer from high crossover rate of electroactive species in addition to its high cost. Though much efforts have been made to design and prepare more polymer electrolyte membranes suitable for flow batteries to achieve improved battery performance; without doubt, some challenges still remain. The requirements for an ideal polymer electrolyte membrane for all-vanadium redox flow batteries can be summarized as follows: i) it should possess an optimal balance between ionic conductivity and vanadium-ion permeability to achieve high-power density and excellent cycle retention ability; ii) it should possess adequate chemical, mechanical, and thermal stabilities to withstand extreme assembling and operating conditions; and iii) it should be affordable so as to fulfill the needs for large-scale application and usage.

Although different types of membrane have been developed over the years, yet, it is still somewhat difficult to obtain a membrane that can fulfill all the aforementioned requirements. In other words, the ideal performance of the available membranes is being limited by various challenges. For instance, the major challenge of cation-exchange membranes is high vanadium-ions permeability which has negative impacts on the capacity retention ability of battery system. For anion-exchange membranes, the prominent challenge has been its poor ionic conductivity,

which greatly restricts the voltage efficiency of the battery. Though amphoteric-ion exchange membrane has a great prospect to achieve effective ions selectivity, however, its complicated fabrication method and poor accuracy of adjusting the concentrations of anion-exchange groups and cation-exchange groups mostly hinder the potential performance of this particular membrane. Similarly, challenges on how to accurately adjust pore size while ensuring a hydrophilic pore structure, so as to ease proton transport, confronts the porous membranes.

To address and overcome many of these challenges towards obtaining ideal polymer electrolyte membranes for flow batteries, some directions for further investigations are given here. Firstly, the development and widespread application of more porous membranes is a viable solution. Here, the pore structure of the membrane such as the pore size and porosity need to be carefully adjusted. For instance, the pore size of the membrane is often required to be adjusted within a range larger than the molecular size of protons while at the same time smaller than the vanadium ions inside the electrolyte. With this design, the ease of proton transport through the membrane can be assured while remarkably restricting the transport of vanadium ions. However, it is worth mentioning that tuning the pore size to this range may still limit the battery performance to certain level, especially as tuning can potentially limit the ionic conductivity of the membrane. The introduction of charged groups into the pores of the porous membrane could be a potential solution. However, the amount to be used needs to be carefully controlled so as to minimize its impact on vanadium-ion permeability.

For the ion exchange membranes including cation-exchange membranes, anion-exchange membranes, and amphoteric-ion exchange membranes, major strategies for performance improvement should include further modifications of membranes using currently reported materials, especially the ones with compelling properties. In addition to this, development of other novel materials with backbone of excellent chemical stability and simultaneous conductivity for cations or anions. In summary, further development and study on polymer electrolyte membranes should concentrate on but not limited to: i) the development of ion-exchange membranes with excellent balance between ionic conductivity and vanadium-ion permeability through tuning the material composition, improving the preparation procedures,

optimizing membrane thickness and pore size distribution; and ii) the development of porous membranes with appropriate pore structure. In addition, further studies and investigations on polymer electrolyte membranes suitable for other types of flow battery systems such as hybrid, organic and semi solid flow batteries should be exploited and developed. With the recognition of the various challenges confronting the performance of polymer electrolyte membranes, the promising directions highlighted above are considered useful to facilitate further investigations for performance improvement, even at low cost, to achieve widespread applications of these membranes in flow batteries.

### Acknowledgements

The work described in this paper was fully supported by a grant from the Research Grant Council of the Hong Kong Special Administrative Region, China (Project No. T23-601/17-R).

### References

1. S. M. Hwang, J. S. Park, Y. Kim, W. Go, J. Han, Y. Kim and Y. Kim, Rechargeable Seawater Batteries-From Concept to Applications, *Adv. Mater.*, 2019, **31**, 1804936.
2. M. Z. Jacobson, M. A. Delucchi, M. A. Cameron and B. V. Mathiesen, Matching demand with supply at low cost in 139 countries among 20 world regions with 100% intermittent wind, water, and sunlight (WWS) for all purposes, *Renew. Energ.*, 2018, **123**, 236-248.
3. S. Chu, Y. Cui and N. Liu, The path towards sustainable energy, *Nat. Mater.*, 2017, **16**, 16.
4. B. Huskinson, M. P. Marshak, C. Suh, S. Er, M. R. Gerhardt, C. J. Galvin, X. Chen, A. Aspuru-Guzik, R. G. Gordon and M. J. Aziz, A metal-free organic-inorganic aqueous flow battery, *Nature*, 2014, **505**, 195.
5. D. Larcher and J. M. Tarascon, Towards greener and more sustainable batteries for electrical energy storage, *Nat. Chem.*, 2015, **7**, 19.
6. A. Shibata and K. Sato, Development of vanadium redox flow battery for electricity storage, *Power Eng. J.*, 1999, **13**, 130-135.
7. G. L. Soloveichik, Electrochemistry: Metal-free energy storage, *Nature*, 2014, **505**, 163.
8. J. P. Barton and D. G. Infield, Energy storage and its use with intermittent renewable energy, *IEEE Trans. Energy Convers.*, 2004, **19**, 441-448.
9. X. Shi, X. Huo, Y. Ma, Z. Pan and L. An, Energizing Fuel Cells with an Electrically Rechargeable Liquid Fuel, *Cell Rep. Phys. Sci.*, 2020, **1**, 100102.
10. S. Hameer and J. L. van Niekerk, A review of large-scale electrical energy storage, *Int. J. Energy Res.*, 2015, **39**, 1179-1195.
11. H. Chen, T. N. Conga, W. Yang, C. Tan, Y. Li and Y. Ding, Progress in electrical energy

- storage system: A critical review, *Prog. Nat. Sci.*, 2009, **19**, 291-312.
12. G. L. Soloveichik, Battery technologies for large-scale stationary energy storage, *Annu. Rev. Chem. Biomol. Eng.*, 2011, **2**, 503-527.
  13. M. Li, J. Lu, Z. Chen and K. Amine, 30 years of lithium - ion batteries, *Adv. Mater.*, 2018, **30**, 1800561.
  14. A. González, E. Goikolea, J. A. Barrena and R. Mysyk, Review on supercapacitors: technologies and materials, *Renew. Sust. Energ. Rev.*, 2016, **58**, 1189-1206.
  15. M. Skyllas-Kazacos, M. H. Chakrabarti, S. A. Hajimolana, F. S. Mjalli and M. Saleem, Progress in flow battery research and development, *J. Electrochem. Soc.*, 2011, **158**.
  16. A. Z. Weber, M. M. Mench, J. P. Meyers, P. N. Ross, J. T. Gostick and Q. Liu, Redox flow batteries: a review, *J. Appl. Electrochem.*, 2011, **41**, 1137-1164.
  17. K. Ma, Y. Zhang, L. Liu, J. Xi, X. Qiu, T. Guan and Y. He, In situ mapping of activity distribution and oxygen evolution reaction in vanadium flow batteries, *Nat. Commun.*, 2019, **10**, 1-11.
  18. M. Park, I.-Y. Jeon, J. Ryu, H. Jang, J.-B. Back and J. Cho, Edge-halogenated graphene nanoplatelets with F, Cl, or Br as electrocatalysts for all-vanadium redox flow batteries, *Nano Energy*, 2016, **26**, 233-240.
  19. M. Park, I. Y. Jeon, J. Ryu, J. B. Baek and J. Cho, Exploration of the Effective Location of Surface Oxygen Defects in Graphene - Based Electrocatalysts for All - Vanadium Redox - Flow Batteries, *Adv. Energy Mater.*, 2015, **5**, 1401550.
  20. M. Park, J. Ryu, Y. Kim and J. Cho, Corn protein-derived nitrogen-doped carbon materials with oxygen-rich functional groups: a highly efficient electrocatalyst for all-vanadium redox flow batteries, *Energy Environ. Sci.*, 2014, **7**, 3727-3735.
  21. S. Rudolph, U. Schröder and I. Bayanov, On-line controlled state of charge rebalancing in vanadium redox flow battery, *J. Electroanal. Chem.*, 2013, **703**, 29-37.
  22. S. Rudolph, U. Schröder, R. Bayanov, K. Blenke and I. Bayanov, Optimal electrolyte flow distribution in hydrodynamic circuit of vanadium redox flow battery, *J. Electroanal. Chem.*, 2015, **736**, 117-126.
  23. A. Orita, M. Verde, M. Sakai and Y. Meng, The impact of pH on side reactions for aqueous redox flow batteries based on nitroxyl radical compounds, *J. Power Sources*, 2016, **321**, 126-134.
  24. Y. Wu, P. Zhu, X. Zhao, M. Reddy, S. Peng, B. Chowdari and S. Ramakrishna, Highly improved rechargeable stability for lithium/silver vanadium oxide battery induced via electrospinning technique, *J. Mater. Chem. A*, 2013, **1**, 852-859.
  25. M. Park, E. S. Beh, E. M. Fell, Y. Jing, E. F. Kerr, D. De Porcellinis, M. A. Goulet, J. Ryu, A. A. Wong and R. G. Gordon, A high voltage aqueous zinc-organic hybrid flow battery, *Adv. Energy Mater.*, 2019, **9**, 1900694.
  26. M. G. Verde, K. J. Carroll, Z. Wang, A. Sathrum and Y. S. Meng, Achieving high efficiency and cyclability in inexpensive soluble lead flow batteries, *Energy Environ. Sci.*, 2013, **6**, 1573-1581.
  27. D. G. Kwabi, K. Lin, Y. Ji, E. F. Kerr, M. A. Goulet, D. De Porcellinis, D. P. Tabor, D. A. Pollack, A. Aspuru-Guzik and R. G. Gordon, Alkaline quinone flow battery with long lifetime at pH 12, *Joule*, 2018, **2**, 1894-1906.
  28. Y. Ji, M. A. Goulet, D. A. Pollack, D. G. Kwabi, S. Jin, D. De Porcellinis, E. F. Kerr, R.

- G. Gordon and M. J. Aziz, A phosphonate - functionalized quinone redox flow battery at near - neutral pH with record capacity retention rate, *Adv. Energy Mater.*, 2019, **9**, 1900039.
29. K. Lin, Q. Chen, M. R. Gerhardt, L. Tong, S. B. Kim, L. Eisenach, A. W. Valle, D. Hardee, R. G. Gordon and M. J. Aziz, Alkaline quinone flow battery, *Science*, 2015, **349**, 1529-1532.
  30. K. Lin, R. Gómez-Bombarelli, E. S. Beh, L. Tong, Q. Chen, A. Valle, A. Aspuru-Guzik, M. J. Aziz and R. G. Gordon, A redox-flow battery with an alloxazine-based organic electrolyte, *Nat. Energy*, 2016, **1**, 1-8.
  31. Y. Li, J. Sniekers, J. Malaquias, X. Li, S. Schaltin, L. Stappers, K. Binnemans, J. Franssaer and I. F. Vankelecom, A non-aqueous all-copper redox flow battery with highly soluble active species, *Electrochim. Acta*, 2017, **236**, 116-121.
  32. M. R. Gerhardt, L. Tong, R. Gómez - Bombarelli, Q. Chen, M. P. Marshak, C. J. Galvin, A. Aspuru - Guzik, R. G. Gordon and M. J. Aziz, Anthraquinone derivatives in aqueous flow batteries, *Adv. Energy Mater.*, 2017, **7**, 1601488.
  33. Z. Yang, L. Tong, D. P. Tabor, E. S. Beh, M. A. Goulet, D. De Porcellinis, A. Aspuru - Guzik, R. G. Gordon and M. J. Aziz, Alkaline benzoquinone aqueous flow battery for large - scale storage of electrical energy, *Adv. Energy Mater.*, 2018, **8**, 1702056.
  34. M. O. Bamgbopa, N. Pour, Y. Shao-Horn and S. Almheiri, Systematic selection of solvent mixtures for non-aqueous redox flow batteries—vanadium acetylacetonate as a model system, *Electrochim. Acta*, 2017, **223**, 115-123.
  35. M. O. Bamgbopa, Y. Shao-Horn and S. Almheiri, The potential of non-aqueous redox flow batteries as fast-charging capable energy storage solutions: demonstration with an iron—chromium acetylacetonate chemistry, *J. Mater. Chem. A*, 2017, **5**, 13457-13468.
  36. W. Li, E. Kerr, M. A. Goulet, H. C. Fu, Y. Zhao, Y. Yang, A. Veysal, J. H. He, R. G. Gordon and M. J. Aziz, A long lifetime aqueous organic solar flow battery, *Adv. Energy Mater.*, 2019, **9**, 1900918.
  37. M. Duduta, B. Ho, V. C. Wood, P. Limthongkul, V. E. Brunini, W. C. Carter and Y. M. Chiang, Semi - Solid lithium rechargeable flow battery, *Adv. Energy Mater.*, 2011, **1**, 511-516.
  38. X. Chen, B. J. Hopkins, A. Helal, F. Y. Fan, K. C. Smith, Z. Li, A. H. Slocum, G. H. McKinley, W. C. Carter and Y. M. Chiang, A low-dissipation, pumpless, gravity-induced flow battery, *Energy Environ. Sci.*, 2016, **9**, 1760-1770.
  39. Y. Zhu, T. M. Narayanan, M. Tułodziecki, H. Sanchez-Casalongue, Q. Horn, L. Meda, Y. Yu, J. Sun, T. Regier and G. H. McKinley, High-energy and high-power Zn-Ni flow batteries with semi-solid electrodes, *Sustain. Energy Fuels*, 2020.
  40. G. L. Soloveichik, Flow batteries: current status and trends, *Chem. Rev.*, 2015, **115**, 11533-11558.
  41. M. Park, J. Ryu, W. Wang and J. Cho, Material design and engineering of next-generation flow-battery technologies, *Nat. Rev. Mater.*, 2016, **2**.
  42. P. Leung, X. Li, C. Ponce de León, L. Berlouis, C. T. J. Low and F. C. Walsh, Progress in redox flow batteries, remaining challenges and their applications in energy storage, *RSC Adv.*, 2012, **2**.
  43. W. Wang, Q. Luo, B. Li, X. Wei, L. Li and Z. Yang, Recent progress in redox flow

- battery research and development, *Adv. Funct. Mater.*, 2013, **23**, 970-986.
44. O. C. Esan, X. Shi, Z. Pan, X. Huo, L. An and T. Zhao, Modeling and Simulation of Flow Batteries, *Adv. Energy Mater.*, **10**, 2000758.
  45. M. Ulaganathan, V. Aravindan, Q. Yan, S. Madhavi, M. Skyllas-Kazacos and T. M. Lim, Recent advancements in all-vanadium redox flow batteries, *Adv. Mater. Interfaces*, 2016, **3**.
  46. Á. Cunha, J. Martins, N. Rodrigues and F. P. Brito, Vanadium redox flow batteries: a technology review, *Int. J. Energy Res.*, 2015, **39**, 889-918.
  47. M. Guarnieri, P. Mattavelli and G. Petrone, Vanadium redox flow batteries, *IEEE Trans. Ind. Electron.*, 2016, **10**, 20-31.
  48. C. Ding, H. Zhang, X. Li, T. Liu and F. Xing, Vanadium flow battery for energy storage: Prospects and challenges, *J. Phys. Chem. Lett.*, 2013, **4**, 1281-1294.
  49. L. Dai, Y. Jiang, W. Meng, H. Zhou, L. Wang and Z. He, Improving the electrocatalytic performance of carbon nanotubes for VO<sub>2</sub><sup>+</sup>/VO<sub>2</sub><sup>+</sup> redox reaction by KOH activation, *Appl. Surf. Sci.*, 2017, **401**, 106-113.
  50. W. Lu, Z. Yuan, Y. Zhao, H. Zhang, H. Zhang and X. Li, Porous membranes in secondary battery technologies, *Chem. Soc. Rev.*, 2017, **46**, 2199-2236.
  51. Y. K. Zeng, T. S. Zhao, L. An, X. L. Zhou and L. Wei, A comparative study of all-vanadium and iron-chromium redox flow batteries for large-scale energy storage, *J. Power Sources*, 2015, **300**, 438-443.
  52. H. Prifti, A. Parasuraman, S. Winardi, T. M. Lim and M. Skyllas-Kazacos, Membranes for redox flow battery applications, *Membranes*, 2012, **2**, 275-306.
  53. S. Hosseiny and M. Wessling, in *Advanced membrane science and technology for sustainable energy and environmental applications*, Elsevier, 2011, pp. 413-434.
  54. X. Li, H. Zhang, Z. Mai, H. Zhang and I. Vankelecom, Ion exchange membranes for vanadium redox flow battery (VRB) applications, *Energy Environ. Sci.*, 2011, **4**.
  55. X. Wei, B. Li and W. Wang, Porous Polymeric Composite Separators for Redox Flow Batteries, *Polym. Rev. (Philadelphia, PA, U. S.)*, 2015, **55**, 247-272.
  56. S. H. Shin, S. H. Yun and S. H. Moon, A review of current developments in non-aqueous redox flow batteries: characterization of their membranes for design perspective, *RSC Adv.*, 2013, **3**.
  57. S. Maurya, S. H. Shin, Y. Kim and S. H. Moon, A review on recent developments of anion exchange membranes for fuel cells and redox flow batteries, *RSC Adv.*, 2015, **5**, 37206-37230.
  58. T. N. L. Doan, T. K. A. Hoang and P. Chen, Recent development of polymer membranes as separators for all-vanadium redox flow batteries, *RSC Adv.*, 2015, **5**, 72805-72815.
  59. Y. Shi, C. Eze, B. Xiong, W. He, H. Zhang, T. Lim, A. Ukil and J. Zhao, Recent development of membrane for vanadium redox flow battery applications: A review, *Appl. Energy*, 2019, **238**, 202-224.
  60. S. Yun, J. Parrondo and V. Ramani, Composite anion exchange membranes based on quaternized cardo-poly (etherketone) and quaternized inorganic fillers for vanadium redox flow battery applications, *Int. J. Hydrogen Energy*, 2016, **41**, 10766-10775.
  61. B. Schwenzer, J. Zhang, S. Kim, L. Li, J. Liu and Z. Yang, Membrane development for vanadium redox flow batteries, *ChemSusChem*, 2011, **4**, 1388-1406.

62. L. Zeng, T. Zhao, L. Wei, H. Jiang and M. Wu, Anion exchange membranes for aqueous acid-based redox flow batteries: Current status and challenges, *Appl. Energy*, 2019, **233**, 622-643.
63. R. A. Elgammal, Z. Tang, C. N. Sun, J. Lawton and T. A. Zawodzinski, Species uptake and mass transport in membranes for vanadium redox flow batteries, *Electrochim. Acta*, 2017, **237**, 1-11.
64. H. Jiang, J. Sun, L. Wei, M. Wu, W. Shyy and T. Zhao, A high power density and long cycle life vanadium redox flow battery, *Energy Stor. Mater.*, 2020, **24**, 529-540.
65. L. Gubler, Membranes and separators for redox flow batteries, *Current Opinion in Electrochemistry*, 2019, **18**, 31-36.
66. Z. Yang, J. Zhang, M. C. Kintner-Meyer, X. Lu, D. Choi, J. P. Lemmon and J. Liu, Electrochemical energy storage for green grid, *Chem. Rev.*, 2011, **111**, 3577-3613.
67. B. Jiang, L. Wu, L. Yu, X. Qiu and J. Xi, A comparative study of Nafion series membranes for vanadium redox flow batteries, *J. Membr. Sci.*, 2016, **510**, 18-26.
68. C. H. Lin, M. C. Yang and H. J. Wei, Amino-silica modified Nafion membrane for vanadium redox flow battery, *J. Power Sources*, 2015, **282**, 562-571.
69. N. Wang, S. Peng, D. Lu, S. Liu and Y. Liu, Nafion/TiO<sub>2</sub> hybrid membrane fabricated via hydrothermal method for vanadium redox battery, *J. Solid State Electrochem.*, 2012, **16**, 1577-1584.
70. D. Mu, L. Yu, L. Liu and J. Xi, Rice paper reinforced sulfonated poly(ether ether ketone) as low-cost membrane for vanadium flow batteries, *ACS Sustain. Chem. Eng.*, 2017, **5**, 2437-2444.
71. Y. Wang, S. Wang, M. Xiao, D. Han and Y. Meng, Preparation and characterization of a novel layer-by-layer porous composite membrane for vanadium redox flow battery (VRB) applications, *Int. J. Hydrogen Energy*, 2014, **39**, 16088-16095.
72. D. Chen, S. Wang, M. Xiao and Y. Meng, Synthesis and properties of novel sulfonated poly(arylene ether sulfone) ionomers for vanadium redox flow battery, *Energy Convers. Manag.*, 2010, **51**, 2816-2824.
73. C. H. Lee, H. B. Park, Y. M. Lee and R. D. Lee, Importance of proton conductivity measurement in polymer electrolyte membrane for fuel cell application, *Ind. Eng. Chem. Res.*, 2005, **44**, 7617-7626.
74. T. Luo, B. Dreusicke and M. Wessling, Tuning the ion selectivity of porous poly (2, 5-benzimidazole) membranes by phase separation for all vanadium redox flow batteries, *J. Membr. Sci.*, 2018, **556**, 164-177.
75. J. Ma, S. Wang, J. Peng, J. Yuan, C. Yu, J. Li, X. Ju and M. Zhai, Covalently incorporating a cationic charged layer onto Nafion membrane by radiation-induced graft copolymerization to reduce vanadium ion crossover, *Eur. Polym. J.*, 2013, **49**, 1832-1840.
76. X. Teng, C. Sun, J. Dai, H. Liu, J. Su and F. Li, Solution casting Nafion/polytetrafluoroethylene membrane for vanadium redox flow battery application, *Electrochim. Acta*, 2013, **88**, 725-734.
77. X. Teng, J. Dai and J. Su, Effects of different kinds of surfactants on Nafion membranes for all vanadium redox flow battery, *J. Solid State Electrochem.*, 2014, **19**, 1091-1101.
78. L. Ding, X. Song, L. Wang and Z. Zhao, Enhancing proton conductivity of



- polybenzimidazole membranes by introducing sulfonate for vanadium redox flow batteries applications, *J. Membr. Sci.*, 2019, **578**, 126-135.
79. S. Lu, C. Wu, D. Liang, Q. Tan and Y. Xiang, Layer-by-layer self-assembly of Nafion-[CS-PWA] composite membranes with suppressed vanadium ion crossover for vanadium redox flow battery applications, *RSC Adv.*, 2014, **4**, 24831-24837.
  80. X. Teng, J. Dai, J. Su and G. Yin, Modification of Nafion membrane using fluorocarbon surfactant for all vanadium redox flow battery, *J. Membr. Sci.*, 2015, **476**, 20-29.
  81. M. A. Izquierdo-Gil, V. Barragán, J. Villaluenga and M. Godino, Water uptake and salt transport through Nafion cation-exchange membranes with different thicknesses, *Chem. Eng. Sci.*, 2012, **72**, 1-9.
  82. V. Barragán and M. Pérez-Haro, Correlations between water uptake and effective fixed charge concentration at high univalent electrolyte concentrations in sulfonated polymer cation-exchange membranes with different morphology, *Electrochim. Acta*, 2011, **56**, 8630-8637.
  83. L. Zeng, T. S. Zhao, L. Wei, Y. K. Zeng and Z. H. Zhang, Highly stable pyridinium-functionalized cross-linked anion exchange membranes for all vanadium redox flow batteries, *J. Power Sources*, 2016, **331**, 452-461.
  84. W. Wei, H. Zhang, X. Li, Z. Mai and H. Zhang, Poly(tetrafluoroethylene) reinforced sulfonated poly(ether ether ketone) membranes for vanadium redox flow battery application, *J. Power Sources*, 2012, **208**, 421-425.
  85. Z. Li, W. Dai, L. Yu, L. Liu, J. Xi, X. Qiu and L. Chen, Properties investigation of sulfonated poly(ether ether ketone)/polyacrylonitrile acid-base blend membrane for vanadium redox flow battery application, *ACS Appl. Mater. Interfaces*, 2014, **6**, 18885-18893.
  86. J. Ren, Y. Dong, J. Dai, H. Hu, Y. Zhu and X. Teng, A novel chloromethylated/quaternized poly (sulfone)/poly (vinylidene fluoride) anion exchange membrane with ultra-low vanadium permeability for all vanadium redox flow battery, *J. Membr. Sci.*, 2017, **544**, 186-194.
  87. N. Wang, S. Peng, Y. Li, H. Wang, S. Liu and Y. Liu, Sulfonated poly(phthalazinone ether sulfone) membrane as a separator of vanadium redox flow battery, *J. Solid State Electrochem.*, 2012, **16**, 2169-2177.
  88. P. Kundu, K. Dutta, P. Kumar, R. Bharti, V. Kumar and P. Kundu, *Polymer electrolyte membranes for microbial fuel cells: Part A. Nafion-based membranes*, Elsevier: Amsterdam, The Netherlands, 2018.
  89. E. Moukheiber, G. De Moor, L. Flandin and C. Bas, Investigation of ionomer structure through its dependence on ion exchange capacity (IEC), *J. Membr. Sci.*, 2012, **389**, 294-304.
  90. J. Li, Y. Zhang and L. Wang, Preparation and characterization of sulfonated polyimide/TiO<sub>2</sub> composite membrane for vanadium redox flow battery, *J. Solid State Electrochem.*, 2014, **18**, 729-737.
  91. X. Teng, Y. Zhao, J. Xi, Z. Wu, X. Qiu and L. Chen, Nafion/organically modified silicate hybrids membrane for vanadium redox flow battery, *J. Power Sources*, 2009, **189**, 1240-1246.
  92. B. Zhang, E. Zhang, G. Wang, P. Yu, Q. Zhao and F. Yao, Poly (phenyl sulfone) anion

- exchange membranes with pyridinium groups for vanadium redox flow battery applications, *J. Power Sources*, 2015, **282**, 328-334.
93. T. Sadhasivam, H. T. Kim, W. S. Park, H. Lim, S. K. Ryi, S. H. Roh and H. Y. Jung, Low permeable composite membrane based on sulfonated poly (phenylene oxide)(sPPO) and silica for vanadium redox flow battery, *Int. J. Hydrogen Energy*, 2017, **42**, 19035-19043.
  94. Z. Li, J. Xi, H. Zhou, L. Liu, Z. Wu, X. Qiu and L. Chen, Preparation and characterization of sulfonated poly (ether ether ketone)/poly (vinylidene fluoride) blend membrane for vanadium redox flow battery application, *J. Power Sources*, 2013, **237**, 132-140.
  95. S. Zhang, C. Yin, D. Xing, D. Yang and X. Jian, Preparation of chloromethylated/quaternized poly (phthalazinone ether ketone) anion exchange membrane materials for vanadium redox flow battery applications, *J. Membr. Sci.*, 2010, **363**, 243-249.
  96. S. Maurya, S. H. Shin, K. W. Sung and S. H. Moon, Anion exchange membrane prepared from simultaneous polymerization and quaternization of 4-vinyl pyridine for non-aqueous vanadium redox flow battery applications, *J. Power Sources*, 2014, **255**, 325-334.
  97. P. Trogadas, E. Pinot and T. F. Fuller, Composite, Solvent-Casted Nafion Membranes for Vanadium Redox Flow Batteries, *Electrochem. Solid-State Lett.*, 2012, **15**.
  98. L. Su, D. Zhang, S. Peng, X. Wu, Y. Luo and G. He, Orientated graphene oxide/Nafion ultra-thin layer coated composite membranes for vanadium redox flow battery, *Int. J. Hydrogen Energy*, 2017, **42**, 21806-21816.
  99. M. Vijayakumar, M. Bhuvaneshwari, P. Nachimuthu, B. Schwenzer, S. Kim, Z. Yang, J. Liu, G. L. Graff, S. Thevuthasan and J. Hu, Spectroscopic investigations of the fouling process on Nafion membranes in vanadium redox flow batteries, *J. Membr. Sci.*, 2011, **366**, 325-334.
  100. M. A. Aziz and S. Shanmugam, Zirconium oxide nanotube–Nafion composite as high performance membrane for all vanadium redox flow battery, *J. Power Sources*, 2017, **337**, 36-44.
  101. P. K. Leung, Q. Xu, T. S. Zhao, L. Zeng and C. Zhang, Preparation of silica nanocomposite anion-exchange membranes with low vanadium-ion crossover for vanadium redox flow batteries, *Electrochim. Acta*, 2013, **105**, 584-592.
  102. J. Xi, Z. Wu, X. Teng, Y. Zhao, L. Chen and X. Qiu, Self-assembled polyelectrolyte multilayer modified Nafion membrane with suppressed vanadium ion crossover for vanadium redox flow batteries, *J. Mater. Chem. A*, 2008, **18**, 1232-1238.
  103. X. Luo, Z. Lu, J. Xi, Z. Wu, W. Zhu, L. Chen and X. Qiu, Influences of permeation of vanadium ions through PVDF-g-PSSA membranes on performances of vanadium redox flow batteries, *J. Phys. Chem. B*, 2005, **109**, 20310-20314.
  104. J. Xi, Z. Wu, X. Qiu and L. Chen, Nafion/SiO<sub>2</sub> hybrid membrane for vanadium redox flow battery, *J. Power Sources*, 2007, **166**, 531-536.
  105. J. Qiu, M. Li, J. Ni, M. Zhai, J. Peng, L. Xu, H. Zhou, J. Li and G. Wei, Preparation of ETFE-based anion exchange membrane to reduce permeability of vanadium ions in vanadium redox battery, *J. Membr. Sci.*, 2007, **297**, 174-180.

106. G.-J. Hwang, S.-W. Kim, D.-M. In, D.-Y. Lee and C.-H. Ryu, Application of the commercial ion exchange membranes in the all-vanadium redox flow battery, *J. Ind. Eng. Chem.*, 2018, **60**, 360-365.
107. M. Yue, Y. Zhang and L. Wang, Sulfonated polyimide/chitosan composite membrane for vanadium redox flow battery: Membrane preparation, characterization, and single cell performance, *J. Appl. Polym. Sci.*, 2012, **127**, 4150-4159.
108. X. L. Zhou, T. S. Zhao, L. An, Y. K. Zeng and X. B. Zhu, Performance of a vanadium redox flow battery with a VANADion membrane, *Appl. Energy*, 2016, **180**, 353-359.
109. Z. Li, L. Le, L. Yu, W. Lei, J. Xi, X. Qiu and L. Chen, Characterization of sulfonated poly(ether ether ketone)/poly(vinylidene fluoride-co-hexafluoropropylene) composite membrane for vanadium redox flow battery application, *J. Power Sources*, 2014, **272**, 427-435.
110. X. Teng, J. Dai, F. Bi and G. Yin, Ultra-thin polytetrafluoroethene/Nafion/silica composite membrane with high performance for vanadium redox flow battery, *J. Power Sources*, 2014, **272**, 113-120.
111. Y. Li, X. Li, J. Cao, W. Xu and H. Zhang, Composite porous membranes with an ultrathin selective layer for vanadium flow batteries, *ChemComm*, 2014, **50**, 4596-4599.
112. X. Teng, J. Dai, F. Bi, X. Jiang, Y. Song and G. Yin, Ultra-thin polytetrafluoroethene/Nafion/silica membranes prepared with nano SiO<sub>2</sub> and its comparison with sol-gel derived one for vanadium redox flow battery, *Solid State Ion.*, 2015, **280**, 30-36.
113. T. Mohammadi and M. S. Kazacos, Evaluation of the chemical stability of some membranes in vanadium solution, *J. Appl. Electrochem.*, 1997, **27**, 153-160.
114. S. Kim, T. B. Tighe, B. Schwenzer, J. Yan, J. Zhang, J. Liu, Z. Yang and M. A. Hickner, Chemical and mechanical degradation of sulfonated poly(sulfone) membranes in vanadium redox flow batteries, *J. Appl. Electrochem.*, 2011, **41**, 1201-1213.
115. H. Yu, Y. Xia, H. Zhang, X. Gong, P. Geng, Z. Gao and Y. Wang, Improved chemical stability and proton selectivity of semi - interpenetrating polymer network amphoteric membrane for vanadium redox flow battery application, *J. Appl. Polym. Sci.*, 2021, **138**, 49803.
116. W. Wei, H. Zhang, X. Li, H. Zhang, Y. Li and I. Vankelecom, Hydrophobic asymmetric ultrafiltration PVDF membranes: an alternative separator for VFB with excellent stability, *Phys. Chem. Chem. Phys.*, 2013, **15**, 1766-1771.
117. P. P. Sharma, V. Yadav, S. Gahlot, O. V. Lebedeva, A. N. Chesnokova, D. N. Srivastava, T. V. Raskulova and V. Kulshrestha, Acid resistant PVDF-co-HFP based copolymer proton exchange membrane for electro-chemical application, *J. Membr. Sci.*, 2019, **573**, 485-492.
118. H. Wei and X. Fang, Novel aromatic polyimide ionomers for proton exchange membranes: Enhancing the hydrolytic stability, *Polymer*, 2011, **52**, 2735-2739.
119. H. Yu, Y. Xia, H. Zhang and Y. Wang, Preparation of sulfonated polyimide/polyvinyl alcohol composite membrane for vanadium redox flow battery applications, *Polym. Bull. (Berlin)*, 2020, 1-22.
120. Y. Xia, B. Liu and Y. Wang, Effects of covalent bond interactions on properties of polyimide grafting sulfonated polyvinyl alcohol proton exchange membrane for

- vanadium redox flow battery applications, *J. Power Sources*, 2019, **433**, 126680.
121. C. Zhang, T. S. Zhao, Q. Xu, L. An and G. Zhao, Effects of operating temperature on the performance of vanadium redox flow batteries, *Appl. Energy*, 2015, **155**, 349-353.
  122. J. G. Kim, S. H. Lee, S. I. Choi, C. S. Jin, J. C. Kim, C. H. Ryu and G. J. Hwang, Application of Psf-PPSS-TPA composite membrane in the all-vanadium redox flow battery, *J. Ind. Eng. Chem.*, 2010, **16**, 756-762.
  123. K. K. Jana, S. J. Lue, A. Huang, J. F. Soesanto and K. L. Tung, Separator Membranes for High Energy - Density Batteries, *ChemBioEng Reviews*, 2018, **5**, 346-371.
  124. Z. Li, W. Dai, L. Yu, J. Xi, X. Qiu and L. Chen, Sulfonated poly (ether ether ketone)/mesoporous silica hybrid membrane for high performance vanadium redox flow battery, *J. Power Sources*, 2014, **257**, 221-229.
  125. Z. Mai, H. Zhang, X. Li, S. Xiao and H. Zhang, Nafion/polyvinylidene fluoride blend membranes with improved ion selectivity for vanadium redox flow battery application, *J. Power Sources*, 2011, **196**, 5737-5741.
  126. M. S. J. Jung, J. Parrondo, C. G. Arges and V. Ramani, Polysulfone-based anion exchange membranes demonstrate excellent chemical stability and performance for the all-vanadium redox flow battery, *J. Mater. Chem. A*, 2013, **1**, 10458-10464.
  127. J. B. Liao, M. Z. Lu, Y. Q. Chu and J. L. Wang, Ultra-low vanadium ion diffusion amphoteric ion-exchange membranes for all-vanadium redox flow batteries, *J. Power Sources*, 2015, **282**, 241-247.
  128. J. Zhang, L. Zhang, H. Liu, A. Sun and R.-S. Liu, *Electrochemical Technologies for Energy Storage and Conversion, 2 Volume Set*, John Wiley & Sons, 2011.
  129. P. Alotto, M. Guarnieri and F. Moro, Redox flow batteries for the storage of renewable energy: A review, *Renew. Sust. Energ. Rev.*, 2014, **29**, 325-335.
  130. H. Wang, X.-Z. Yuan and H. Li, *PEM fuel cell diagnostic tools*, CRC press, 2011.
  131. J. Zhang, *PEM fuel cell electrocatalysts and catalyst layers: fundamentals and applications*, Springer Science & Business Media, 2008.
  132. H. R. Jiang, W. Shyy, M. C. Wu, L. Wei and T. S. Zhao, Highly active, bi-functional and metal-free B 4 C-nanoparticle-modified graphite felt electrodes for vanadium redox flow batteries, *J. Power Sources*, 2017, **365**, 34-42.
  133. L. Wei, T. S. Zhao, G. Zhao, L. An and L. Zeng, A high-performance carbon nanoparticle-decorated graphite felt electrode for vanadium redox flow batteries, *Appl. Energy*, 2016, **176**, 74-79.
  134. L. Wei, T. S. Zhao, L. Zeng, Y. K. Zeng and H. R. Jiang, Highly catalytic and stabilized titanium nitride nanowire array-decorated graphite felt electrodes for all vanadium redox flow batteries, *J. Power Sources*, 2017, **341**, 318-326.
  135. L. Zeng, T. Zhao and L. Wei, Revealing the performance enhancement of oxygenated carbonaceous materials for vanadium redox flow batteries: functional groups or specific surface area?, *Adv. Sustain. Syst.*, 2018, **2**.
  136. C. Yao, H. Zhang, T. Liu, X. Li and Z. Liu, Cell architecture upswing based on catalyst coated membrane (CCM) for vanadium flow battery, *J. Power Sources*, 2013, **237**, 19-25.
  137. L. Zhang, L. Ling, M. Xiao, D. Han, S. Wang and Y. Meng, Effectively suppressing vanadium permeation in vanadium redox flow battery application with modified Nafion

- membrane with nacre-like nanoarchitectures, *J. Power Sources*, 2017, **352**, 111-117.
138. Q. Wang, Z. Qu, Z. Jiang and W. Yang, Experimental study on the performance of a vanadium redox flow battery with non-uniformly compressed carbon felt electrode, *Appl. Energy*, 2018, **213**, 293-305.
  139. X. L. Zhou, T. S. Zhao, L. An, L. Wei and C. Zhang, The use of polybenzimidazole membranes in vanadium redox flow batteries leading to increased coulombic efficiency and cycling performance, *Electrochim. Acta*, 2015, **153**, 492-498.
  140. Q. Luo, H. Zhang, J. Chen, D. You, C. Sun and Y. Zhang, Preparation and characterization of Nafion/SPEEK layered composite membrane and its application in vanadium redox flow battery, *J. Membr. Sci.*, 2008, **325**, 553-558.
  141. L. Chen, S. Zhang, Y. Chen and X. Jian, Low vanadium ion permeabilities of sulfonated poly(phthalazinone ether ketone)s provide high efficiency and stability for vanadium redox flow batteries, *J. Power Sources*, 2017, **355**, 23-30.
  142. X. Teng, Y. Zhao, J. Xi, Z. Wu, X. Qiu and L. Chen, Nafion/organic silica modified TiO<sub>2</sub> composite membrane for vanadium redox flow battery via in situ sol-gel reactions, *J. Membr. Sci.*, 2009, **341**, 149-154.
  143. X. Z. Yuan, C. Song, A. Platt, N. Zhao, H. Wang, H. Li, K. Fatih and D. Jang, A review of all - vanadium redox flow battery durability: Degradation mechanisms and mitigation strategies, *Int. J. Energy Res.*, 2019, **43**, 6599-6638.
  144. L. Wei, T. S. Zhao, L. Zeng, X. L. Zhou and Y. K. Zeng, Copper nanoparticle-deposited graphite felt electrodes for all vanadium redox flow batteries, *Appl. Energy*, 2016, **180**, 386-391.
  145. X. Wei, Z. Nie, Q. Luo, B. Li, B. Chen, K. Simmons, V. Sprenkle and W. Wang, Nanoporous polytetrafluoroethylene/silica composite separator as a high-performance all-vanadium redox flow battery membrane, *Adv. Energy Mater.*, 2013, **3**, 1215-1220.
  146. J. Ye, D. Yuan, M. Ding, Y. Long, T. Long, L. Sun and C. Jia, A cost-effective nafion/lignin composite membrane with low vanadium ion permeation for high performance vanadium redox flow battery, *J. Power Sources*, **482**, 229023.
  147. Q. Wu, Y. Lv, L. Lin, X. Zhang, Y. Liu and X. Zhou, An improved thin-film electrode for vanadium redox flow batteries enabled by a dual layered structure, *J. Power Sources*, 2019, **410**, 152-161.
  148. S. Liu, D. Li, L. Wang, H. Yang, X. Han and B. Liu, Ethylenediamine-functionalized graphene oxide incorporated acid-base ion exchange membranes for vanadium redox flow battery, *Electrochim. Acta*, 2017, **230**, 204-211.
  149. X. Teng, J. Dai, J. Su, Y. Zhu, H. Liu and Z. Song, A high performance polytetrafluoroethene/Nafion composite membrane for vanadium redox flow battery application, *J. Power Sources*, 2013, **240**, 131-139.
  150. D. Chen, M. A. Hickner, E. Agar and E. C. Kumbar, Optimizing membrane thickness for vanadium redox flow batteries, *J. Membr. Sci.*, 2013, **437**, 108-113.
  151. S. M. Ahn, H. Y. Jeong, J. K. Jang, J. Y. Lee, S. So, Y. J. Kim, Y. T. Hong and T. H. Kim, Polybenzimidazole/Nafion hybrid membrane with improved chemical stability for vanadium redox flow battery application, *RSC Adv.*, 2018, **8**, 25304-25312.
  152. J. Saqib and I. H. Aljundi, Membrane fouling and modification using surface treatment and layer-by-layer assembly of polyelectrolytes: state-of-the-art review, *Journal of*

- Water Process Engineering*, 2016, **11**, 68-87.
153. B. Tian, C. W. Yan and F. H. Wang, Proton conducting composite membrane from Daramic/Nafion for vanadium redox flow battery, *J. Membr. Sci.*, 2004, **234**, 51-54.
  154. Q. Tan, S. Lu, Y. Lv, X. Xu, J. Si and Y. Xiang, Doping structure and degradation mechanism of polypyrrole–Nafion® composite membrane for vanadium redox flow batteries, *RSC Adv.*, 2016, **6**, 103332-103336.
  155. B. Schwenzer, S. Kim, M. Vijayakumar, Z. Yang and J. Liu, Correlation of structural differences between Nafion/polyaniline and Nafion/polypyrrole composite membranes and observed transport properties, *J. Membr. Sci.*, 2011, **372**, 11-19.
  156. S. S. Sha'rani, E. Abouzari-Lotf, M. M. Nasef, A. Ahmad, T. M. Ting and R. R. Ali, Improving the redox flow battery performance of low-cost thin polyelectrolyte membranes by layer-by-Layer Surface assembly, *J. Power Sources*, 2019, **413**, 182-190.
  157. T. Sadhasivam, K. Dhanabalan, P. T. Thong, J. Y. Kim, S. H. Roh and H. Y. Jung, Development of perfluorosulfonic acid polymer - based hybrid composite membrane with alkoxysilane functionalized polymer for vanadium redox flow battery, *Int. J. Energy Res.*, 2020, **44**, 1999-2010.
  158. R. Yang, Z. Cao, S. Yang, I. Michos, Z. Xu and J. Dong, Colloidal silicalite-nafion composite ion exchange membrane for vanadium redox-flow battery, *J. Membr. Sci.*, 2015, **484**, 1-9.
  159. J. Drillkens, D. Schulte and D. U. Sauer, Long-term stability of nafion hybrid membranes for use in vanadium redox-flow batteries, *ECS Trans.*, 2010, **28**, 167-177.
  160. M. Vijayakumar, B. Schwenzer, S. Kim, Z. Yang, S. Thevuthasan, J. Liu, G. L. Graff and J. Hu, Investigation of local environments in Nafion–SiO<sub>2</sub> composite membranes used in vanadium redox flow batteries, *Solid State Nucl. Magn. Reson.*, 2012, **42**, 71-80.
  161. J. Kim, J. D. Jeon and S. Y. Kwak, Nafion-based composite membrane with a permselective layered silicate layer for vanadium redox flow battery, *Electrochem. Commun.*, 2014, **38**, 68-70.
  162. K. J. Lee and Y. H. Chu, Preparation of the graphene oxide (GO)/Nafion composite membrane for the vanadium redox flow battery (VRB) system, *Vacuum*, 2014, **107**, 269-276.
  163. D. Zhang, Q. Wang, S. Peng, X. Yan, X. Wu and G. He, An interface-strengthened cross-linked graphene oxide/Nafion212 composite membrane for vanadium flow batteries, *J. Membr. Sci.*, 2019, **587**, 117189.
  164. M. S. Kondratenko, E. A. Karpushkin, N. A. Gvozdik, M. O. Gallyamov, K. J. Stevenson and V. G. Sergeev, Influence of aminosilane precursor concentration on physicochemical properties of composite Nafion membranes for vanadium redox flow battery applications, *J. Power Sources*, 2017, **340**, 32-39.
  165. S. M. Park and H. Kim, Hybrid membranes with low permeability for vanadium redox flow batteries using in situ sol-gel process, *Korean J. Chem. Eng.*, 2015, **32**, 2434-2442.
  166. X. Teng, J. Lei, X. Gu, J. Dai, Y. Zhu and F. Li, Nafion-sulfonated organosilica composite membrane for all vanadium redoxflow battery, *Ionics*, 2012, **18**, 513-521.
  167. C. Sun, A. Zlotorowicz, G. Nawn, E. Negro, F. Bertasi, G. Pagot, K. Vezzù, G. Pace, M. Guarnieri and V. Di Noto, [Nafion/(WO<sub>3</sub>)<sub>x</sub>] hybrid membranes for vanadium redox

- flow batteries, *Solid State Ion.*, 2018, **319**, 110-116.
168. X. B. Yang, L. Zhao, K. Goh, X. L. Sui, L. H. Meng and Z. B. Wang, A highly proton-/vanadium-selective perfluorosulfonic acid membrane for vanadium redox flow batteries, *New J. Chem.*, 2019, **43**, 11374-11381.
  169. S. I. Hossain, M. A. Aziz and S. Shanmugam, Ultra-high ion-selective and durable Nafion-NdZr Composite Layer Membrane for All-vanadium Redox Flow Batteries, *ACS Sustain. Chem. Eng.*, 2020.
  170. X. B. Yang, L. Zhao, K. Goh, X. L. Sui, L. H. Meng and Z. B. Wang, A phosphotungstic acid coupled silica-Nafion composite membrane with significantly enhanced ion selectivity for vanadium redox flow battery, *J. Energy Chem.*, 2020, **41**, 177-184.
  171. S. Liu, L. Wang, Y. Ding, B. Liu, X. Han and Y. Song, Novel sulfonated poly (ether ether ketone)/polyetherimide acid-base blend membranes for vanadium redox flow battery applications, *Electrochim. Acta*, 2014, **130**, 90-96.
  172. J. Xi, W. Dai and L. Yu, Polydopamine coated SPEEK membrane for a vanadium redox flow battery, *RSC Adv.*, 2015, **5**, 33400-33406.
  173. Z. Fu, J. Liu and Q. Liu, SPEEK/PVDF/PES composite as alternative proton exchange membrane for vanadium redox flow batteries, *J. Electron. Mater.*, 2016, **45**, 666-671.
  174. L. Zhao, F. Li, Y. Guo, Y. Dong, J. Liu, Y. Wang, J. Kang, G. Zhou and Q. Liu, SPEEK/PVDF binary membrane as an alternative proton-exchange membrane in vanadium redox flow battery application, *High Perform. Polym.*, 2017, **29**, 127-132.
  175. B. Yin, L. Yu, B. Jiang, L. Wang and J. Xi, Nano oxides incorporated sulfonated poly(ether ether ketone) membranes with improved selectivity and stability for vanadium redox flow battery, *J. Solid State Electrochem.*, 2016, **20**, 1271-1283.
  176. S. Park and H. Kim, Preparation of a sulfonated poly (ether ether ketone)-based composite membrane with phenyl isocyanate treated sulfonated graphene oxide for a vanadium redox flow battery, *J. Electrochem. Soc.*, 2016, **163**, A2293-A2298.
  177. J. Kim, J. D. Jeon and S. Y. Kwak, Sulfonated poly(ether ether ketone) composite membranes containing microporous layered silicate AMH-3 for improved membrane performance in vanadium redox flow batteries, *Electrochim. Acta*, 2017, **243**, 220-227.
  178. L. Kong, L. Zheng, R. Niu, H. Wang and H. Shi, A sulfonated poly (ether ether ketone)/amine-functionalized graphene oxide hybrid membrane for vanadium redox flow batteries, *RSC Adv.*, 2016, **6**, 100262-100270.
  179. Y. Zhang, H. Wang, P. Qian, Y. Zhou, J. Shi and H. Shi, Sulfonated poly (ether ether ketone)/amine-functionalized graphene oxide hybrid membrane with various chain lengths for vanadium redox flow battery: A comparative study, *J. Membr. Sci.*, 2020, 118232.
  180. A. Li, G. Wang, Y. Quan, X. Wei, F. Li, M. Zhang, R. I. Ur, J. Zhang, J. Chen and R. Wang, Sulfonated poly (ether ether ketone)/polyimide acid-base hybrid membranes for vanadium redox flow battery applications, *Ionics*, 2019, 1-9.
  181. G. Wang, F. Wang, A. Li, M. Zhang, J. Zhang, J. Chen and R. Wang, Sulfonated poly (ether ether ketone)/s-TiO<sub>2</sub> composite membrane for a vanadium redox flow battery, *J. Appl. Polym. Sci.*, 2020, **137**, 48830.
  182. J. Li, Q. Zhang, S. Peng, D. Zhang, X. Yan, X. Wu, X. Gong, Q. Wang and G. He, Electrospinning fiberization of carbon nanotube hybrid sulfonated poly (ether ether

- ketone) ion conductive membranes for a vanadium redox flow battery, *J. Membr. Sci.*, 2019, **583**, 93-102.
183. Y. Zhang, H. Wang, B. Liu, J. Shi, J. Zhang and H. Shi, An ultra-high ion selective hybrid proton exchange membrane incorporated with zwitterion-decorated graphene oxide for vanadium redox flow batteries, *J. Mater. Chem. A*, 2019, **7**, 12669-12680.
  184. C. Sun, E. Negro, K. Vezzù, G. Pagot, G. Cavinato, A. Nale, Y. H. Bang and V. Di Noto, Hybrid inorganic-organic proton-conducting membranes based on SPEEK doped with WO<sub>3</sub> nanoparticles for application in vanadium redox flow batteries, *Electrochim. Acta*, 2019, **309**, 311-325.
  185. Y. Quan, G. Wang, A. Li, X. Wei, F. Li, J. Zhang, J. Chen and R. Wang, Novel sulfonated poly (ether ether ketone)/triphenylamine hybrid membrane for vanadium redox flow battery applications, *RSC Adv.*, 2019, **9**, 3838-3846.
  186. L. Zeng, J. Ye, J. Zhang, J. Liu and C. Jia, A promising SPEEK/MCM composite membrane for highly efficient vanadium redox flow battery, *Surf. Coat. Technol.*, 2019, **358**, 167-172.
  187. J. Ye, Y. Cheng, L. Sun, M. Ding, C. Wu, D. Yuan, X. Zhao, C. Xiang and C. Jia, A green SPEEK/lignin composite membrane with high ion selectivity for vanadium redox flow battery, *J. Membr. Sci.*, 2019, **572**, 110-118.
  188. Y. Zhang, H. Wang, W. Yu, J. Shi and H. Shi, Sulfonated poly (ether ether ketone)-based hybrid membranes containing polydopamine-decorated multiwalled carbon nanotubes with acid-base pairs for all vanadium redox flow battery, *J. Membr. Sci.*, 2018, **564**, 916-925.
  189. H. Y. Jung, M. S. Cho, T. Sadhasivam, J. Y. Kim, S. H. Roh and Y. Kwon, High ionic selectivity of low permeable organic composite membrane with amphiphilic polymer for vanadium redox flow batteries, *Solid State Ion.*, 2018, **324**, 69-76.
  190. L. Zheng, H. Wang, R. Niu, Y. Zhang and H. Shi, Sulfonated poly (ether ether ketone)/sulfonated graphene oxide hybrid membrane for vanadium redox flow battery, *Electrochim. Acta*, 2018, **282**, 437-447.
  191. D. Chen, X. Chen, L. Ding and X. Li, Advanced acid-base blend ion exchange membranes with high performance for vanadium flow battery application, *J. Membr. Sci.*, 2018, **553**, 25-31.
  192. L. Yu, F. Lin, W. Xiao, D. Luo and J. Xi, CNT@ polydopamine embedded mixed matrix membranes for high-rate and long-life vanadium flow batteries, *J. Membr. Sci.*, 2018, **549**, 411-419.
  193. F. Wang, G. Wang, J. Zhang, B. Li, J. Zhang, J. Deng, J. Chen and R. Wang, Novel sulfonated poly(ether ether ketone)/oxidized g-C<sub>3</sub>N<sub>4</sub> composite membrane for vanadium redox flow battery applications, *J. Electroanal. Chem.*, 2017, **797**, 107-112.
  194. L. Yu and J. Xi, Durable and efficient PTFE sandwiched SPEEK membrane for vanadium flow batteries, *ACS Appl. Mater. Interfaces*, 2016, **8**, 23425.
  195. R. Niu, L. Kong, L. Zheng, H. Wang and H. Shi, Novel graphitic carbon nitride nanosheets /sulfonated poly(ether ether ketone) acid-base hybrid membrane for vanadium redox flow battery, *J. Membr. Sci.*, 2016, **525**, 220-228.
  196. Y. Ji, Z. Y. Tay and S. F. Y. Li, Highly selective sulfonated poly (ether ether ketone)/titanium oxide composite membranes for vanadium redox flow batteries, *J.*



- Membr. Sci.*, 2017, **539**, 197-205.
197. H. H. Dong, J. H. Chun, H. L. Chang, H. C. Jung and S. H. Kim, Composite membranes based on sulfonated poly(ether ether ketone) and SiO<sub>2</sub> for a vanadium redox flow battery, *Korean J. Chem. Eng.*, 2015, **32**, 1-10.
  198. C. Jia, Y. Cheng, L. Xiao, G. Wei, J. Liu and C. Yan, Sulfonated poly(ether ether ketone)/functionalized carbon nanotube composite membrane for vanadium redox flow battery applications, *Electrochim. Acta*, 2015, **153**, 44-48.
  199. W. Dai, Y. Shen, Z. Li, L. Yu and X. Qiu, SPEEK/Graphene oxide nanocomposite membranes with superior cyclability for highly efficient vanadium redox flow battery, *J. Mater. Chem. A*, 2014, **2**, 12423-12432.
  200. J. Xi, Z. Li, L. Yu, B. Yin, W. Lei, L. Le, X. Qiu and L. Chen, Effect of degree of sulfonation and casting solvent on sulfonated poly(ether ether ketone) membrane for vanadium redox flow battery, *J. Power Sources*, 2015, **285**, 195-204.
  201. D. Chen and X. Li, Sulfonated poly(ether ether ketone) membranes containing pendent carboxylic acid groups and their application in vanadium flow battery, *J. Power Sources*, 2014, **247**, 629-635.
  202. Z. Yuan, X. Li, J. Hu, W. Xu, J. Cao and H. Zhang, Degradation mechanism of sulfonated poly(ether ether ketone) (SPEEK) ion exchange membranes under vanadium flow battery medium, *Phys. Chem. Chem. Phys.*, 2014, **16**, 19841-19847.
  203. S. Macksasitorn, S. Changkhamchom, A. Sirivat and K. Siemanond, Sulfonated poly(ether ether ketone) and sulfonated poly(1, 4-phenylene ether ether sulfone) membranes for vanadium redox flow batteries, *High Perform. Polym.*, 2012, **24**, 603-608.
  204. Z. Yuan, X. Li, Y. Duan, Y. Zhao and H. Zhang, Highly stable membranes based on sulfonated fluorinated poly(ether ether ketone)s with bifunctional groups for vanadium flow battery application, *Polym. Chem.*, 2015, **6**, 5385-5392.
  205. S. Winardi, S. C. Raghu, M. O. Oo, Q. Yan, N. Wai, T. M. Lim and M. Skyllas-Kazacos, Sulfonated poly(ether ether ketone)-based proton exchange membranes for vanadium redox battery applications, *J. Membr. Sci.*, 2014, **450**, 313-322.
  206. J. Li, Y. Zhang, S. Zhang, X. Huang and L. Wang, Novel sulfonated polyimide/ZrO<sub>2</sub> composite membrane as a separator of vanadium redox flow battery, *Polym. Adv. Technol.*, 2015, **25**, 1610-1615.
  207. Y. Zhang, J. Li, L. Wang and S. Zhang, Sulfonated polyimide/AlOOH composite membranes with decreased vanadium permeability and increased stability for vanadium redox flow battery, *J. Solid State Electrochem.*, 2014, **18**, 3479-3490.
  208. Y. Zhang, J. Li, H. Zhang, S. Zhang and X. Huang, Sulfonated polyimide membranes with different non-sulfonated diamines for vanadium redox battery applications, *Electrochim. Acta*, 2014, **150**, 114-122.
  209. S. Liu, L. Wang, B. Zhang, B. Liu, J. Wang and Y. Song, Novel sulfonated polyimide/polyvinyl alcohol blend membranes for vanadium redox flow battery applications, *J. Mater. Chem. A*, 2015, **3**, 2072-2081.
  210. L. Cao, Q. Sun, Y. Gao, L. Liu and H. Shi, Novel acid-base hybrid membrane based on amine-functionalized reduced graphene oxide and sulfonated polyimide for vanadium redox flow battery, *Electrochim. Acta*, 2015, **158**, 24-34.

211. X. Huang, P. Yang, Y. Zhou, Y. Zhang and H. Zhang, In-situ and ex-situ degradation of sulfonated polyimide membrane for vanadium redox flow battery application, *J. Membr. Sci.*, 2016, **526**, 281-292.
212. Y. Zhang, S. Zhang, X. Huang, Y. Zhou, P. Yang and H. Zhang, Synthesis and properties of branched sulfonated polyimides for membranes in vanadium redox flow battery application, *Electrochim. Acta*, 2016, **210**, 308-320.
213. J. Li, S. Liu, Z. He and Z. Zhou, Semi-fluorinated sulfonated polyimide membranes with enhanced proton selectivity and stability for vanadium redox flow batteries, *Electrochim. Acta*, 2016, **216**, 320-331.
214. J. Li, S. Liu, Z. He and Z. Zhou, A novel branched side-chain-type sulfonated polyimide membrane with flexible sulfoalkyl pendants and trifluoromethyl groups for vanadium redox flow batteries, *J. Power Sources*, 2017, **347**, 114-126.
215. J. Li, X. Yuan, S. Liu, Z. He, Z. Zhou and A. Li, A low-cost and high-performance sulfonated polyimide proton conductive membrane for vanadium redox flow/static batteries, *ACS Appl. Mater. Interfaces*, 2017, **9**, 32643-32651.
216. Y. Zhang, Y. Pu, P. Yang, H. Yang, S. Xuan, J. Long, Y. Wang and H. Zhang, Branched sulfonated polyimide/functionalized silicon carbide composite membranes with improved chemical stabilities and proton selectivities for vanadium redox flow battery application, *Electrochim. Acta*, 2018, **53**, 14506-14524.
217. Y. Pu, S. Zhu, P. Wang, Y. Zhou, P. Yang, S. Xuan, Y. Zhang and H. Zhang, Novel branched sulfonated polyimide/molybdenum disulfide nanosheets composite membrane for vanadium redox flow battery application, *Appl. Surf. Sci.*, 2018, **448**, 186-202.
218. L. Yu, L. Wang, L. Yu, D. Mu, L. Wang and J. Xi, Aliphatic/aromatic sulfonated polyimide membranes with cross-linked structures for vanadium flow batteries, *J. Membr. Sci.*, 2019, **572**, 119-127.
219. L. Wang, L. Yu, D. Mu, L. Yu, L. Wang and J. Xi, Acid-base membranes of imidazole-based sulfonated polyimides for vanadium flow batteries, *J. Membr. Sci.*, 2018, **552**, 167-176.
220. X. Huang, S. Zhang, Y. Zhang, H. Zhang and X. Yang, Sulfonated polyimide/chitosan composite membranes for a vanadium redox flow battery: influence of the sulfonation degree of the sulfonated polyimide, *Polym. J.*, 2016, **48**.
221. L. Cao, L. Kong, L. Kong, X. Zhang and H. Shi, Novel sulfonated polyimide/zwitterionic polymer-functionalized graphene oxide hybrid membranes for vanadium redox flow battery, *J. Power Sources*, 2015, **299**, 255-264.
222. M. Yue, Y. Zhang and L. Wang, Sulfonated polyimide/chitosan composite membrane for vanadium redox flow battery: Influence of the infiltration time with chitosan solution, *Solid State Ion.*, 2012, **217**, 6-12.
223. D. Chen, S. Wang, M. Xiao, D. Han and Y. Meng, Sulfonated poly (fluorenyl ether ketone) membrane with embedded silica rich layer and enhanced proton selectivity for vanadium redox flow battery, *J. Power Sources*, 2010, **195**, 7701-7708.
224. D. Chen, M. A. Hickner, S. Wang, J. Pan, X. Min and Y. Meng, Directly fluorinated polyaromatic composite membranes for vanadium redox flow batteries, *J. Membr. Sci.*, 2012, **415-416**, 139-144.

225. J. Pan, S. Wang, M. Xiao, M. Hickner and Y. Meng, Layered zirconium phosphate sulfophenylphosphonates reinforced sulfonated poly (fluorenyl ether ketone) hybrid membranes with high proton conductivity and low vanadium ion permeability, *J. Membr. Sci.*, 2013, **443**, 19-27.
226. Y. Wang, S. Wang, M. Xiao, D. Han, M. Hickner and Y. Meng, Layer-by-layer self-assembly of PDDA/PSS-SPFEK composite membrane with low vanadium permeability for vanadium redox flow battery, *RSC Adv.*, 2013, **3**, 15467.
227. D. Chen, S. Wang, M. Xiao and Y. Meng, Preparation and properties of sulfonated poly(fluorenyl ether ketone) membrane for vanadium redox flow battery application, *J. Power Sources*, 2010, **195**, 2089-2095.
228. J. Kim, Y. Lee, J. D. Jeon and S. Y. Kwak, Ion-exchange composite membranes pore-filled with sulfonated poly (ether ether ketone) and Engelhard titanosilicate-10 for improved performance of vanadium redox flow batteries, *J. Power Sources*, 2018, **383**, 1-9.
229. J. Dai, X. Teng, Y. Song, X. Jiang and G. Yin, A super thin polytetrafluoroethylene/sulfonated poly(ether ether ketone) membrane with 91% energy efficiency and high stability for vanadium redox flow battery, *J. Appl. Polym. Sci.*, 2016, **133**.
230. J. Qiu, J. Ni, M. Zhai, J. Peng, H. Zhou, J. Li and G. Wei, Radiation grafting of styrene and maleic anhydride onto PTFE membranes and sequent sulfonation for applications of vanadium redox battery, *Radiat. Phys. Chem.*, 2007, **76**, 1703-1707.
231. M. M. Seepana, J. Pandey and A. Shukla, Design and synthesis of highly stable poly (tetrafluoroethylene)-zirconium phosphate (PTFE-ZrP) ion-exchange membrane for vanadium redox flow battery (VRFB), *Ionics*, 2017, **23**, 1471-1480.
232. Z. Yuan, Q. Dai, Q. Lin, Y. Zhao, H. Zhang and X. Li, Highly stable aromatic poly (ether sulfone) composite ion exchange membrane for vanadium flow battery, *J. Membr. Sci.*, 2017, **541**.
233. X. Ling, C. K. Jia, J. G. Liu and C. W. Yan, Preparation and characterization of sulfonated poly(ether sulfone)/sulfonated poly(ether ether ketone) blend membrane for vanadium redox flow battery, *J. Membr. Sci.*, 2012, **415-416**, 306-312.
234. Y. Zhang, X. Zhou, R. Xue, Q. Yu, F. Jiang and Y. Zhong, Proton exchange membranes with ultra-low vanadium ions permeability improved by sulfated zirconia for all vanadium redox flow battery, *Int. J. Hydrogen Energy*, 2019, **44**, 5997-6006.
235. J. Qiu, L. Zhao, M. Zhai, J. Ni, H. Zhou, J. Peng, J. Li and G. Wei, Pre-irradiation grafting of styrene and maleic anhydride onto PVDF membrane and subsequent sulfonation for application in vanadium redox batteries, *J. Power Sources*, 2008, **177**, 617-623.
236. L. Ling, M. Xiao, D. Han, S. Ren, S. Wang and Y. Meng, Porous composite membrane of PVDF/Sulfonic silica with high ion selectivity for vanadium redox flow battery, *J. Membr. Sci.*, 2019, **585**, 230-237.
237. N. Wang, S. Peng, H. Wang, Y. Li, S. Liu and Y. Liu, SPPEK/WO<sub>3</sub> hybrid membrane fabricated via hydrothermal method for vanadium redox flow battery, *Electrochem. Commun.*, 2012, **17**, 30-33.
238. N. Wang, J. Yu, Z. Zhou, D. Fang, S. Liu and Y. Liu, SPPEK/TPA composite membrane

- as a separator of vanadium redox flow battery, *J. Membr. Sci.*, 2013, **437**, 114-121.
239. J. Li, Y. Zhang, Z. Shuai and X. Huang, Sulfonated polyimide/s-MoS<sub>2</sub> composite membrane with high proton selectivity and good stability for vanadium redox flow battery, *J. Membr. Sci.*, 2015, **490**, 179-189.
240. Y. Li, H. Zhang, X. Li, H. Zhang and W. Wei, Porous poly (ether sulfone) membranes with tunable morphology: Fabrication and their application for vanadium flow battery, *J. Power Sources*, 2013, **233**, 202-208.
241. X. Zhou, R. Xue, Y. Zhong, Y. Zhang and F. Jiang, Asymmetric porous membranes with ultra-high ion selectivity for vanadium redox flow batteries, *J. Membr. Sci.*, 2020, **595**, 117614.
242. S. Yang, Y. Ahn and D. Kim, Poly(arylene ether ketone) proton exchange membranes grafted with long aliphatic pendant sulfonated groups for vanadium redox flow batteries, *J. Mater. Chem. A*, 2017, **5**.
243. A. M. Abdul, K. Oh and S. Shanmugam, A sulfonated poly(arylene ether ketone)/polyoxometalate-graphene oxide composite: a highly ion selective membrane for all vanadium redox flow batteries, *ChemComm*, 2016, **53**, 917-920.
244. S. I. Hossain, M. A. Aziz, D. Han, P. Selvam and S. Shanmugam, Fabrication of SPAEK–cerium zirconium oxide nanotube composite membrane with outstanding performance and durability for vanadium redox flow batteries, *J. Mater. Chem. A*, 2018, **6**, 20205-20213.
245. D. Chen, S. Kim, L. Li, G. Yang and M. A. Hickner, Stable fluorinated sulfonated poly(arylene ether) membranes for vanadium redox flow batteries, *RSC Adv.*, 2012, **2**, 8087-8094.
246. H. Y. Shin, S. C. Min, S. H. Hong, T. H. Kim, D. S. Yang, S. G. Oh, J. Y. Lee and Y. T. Hong, Poly(p-phenylene)-based membrane materials with excellent cell efficiencies and durability for use in vanadium redox flow batteries, *J. Mater. Chem. A*, 2017, **5**, 12285-12296.
247. H. Zhang, H. Zhang, X. Li, Z. Mai, W. Wei and Y. Li, Crosslinkable sulfonated poly (diallyl-bisphenol ether ether ketone) membranes for vanadium redox flow battery application, *J. Power Sources*, 2012, **217**, 309-315.
248. B. Liu, Y. Zhang, Y. Jiang, P. Qian and H. Shi, High performance acid-base composite membranes from sulfonated polysulfone containing graphitic carbon nitride nanosheets for vanadium redox flow battery, *J. Membr. Sci.*, 2019, **591**, 117332.
249. Y. Zhang, L. Zheng, B. Liu, H. Wang and H. Shi, Sulfonated polysulfone proton exchange membrane influenced by a varied sulfonation degree for vanadium redox flow battery, *J. Membr. Sci.*, 2019, **584**, 173-180.
250. S. Kim, J. Yan, B. Schwenzer, J. Zhang, L. Li, J. Liu, Z. Yang and M. A. Hickner, Cycling performance and efficiency of sulfonated poly(sulfone) membranes in vanadium redox flow batteries, *Electrochem. Commun.*, 2010, **12**, 1650-1653.
251. B. Yin, Z. Li, W. Dai, W. Lei, L. Yu and J. Xi, Highly branched sulfonated poly(fluorenyl ether ketone sulfone)s membrane for energy efficient vanadium redox flow battery, *J. Power Sources*, 2015, **285**, 109-118.
252. C. Jia, J. Liu and C. Yan, A multilayered membrane for vanadium redox flow battery, *J. Power Sources*, 2012, **203**, 190-194.

253. C. Jia, J. Liu and C. Yan, A significantly improved membrane for vanadium redox flow battery, *J. Power Sources*, 2010, **195**, 4380-4383.
254. Z. Tang, J. S. Lawton, C. N. Sun, J. Chen, M. I. Bright, A. M. Jones, A. B. Papandrew, C. H. Fujimoto and T. A. Zawodzinski, Characterization of sulfonated diels-alder poly (phenylene) membranes for electrolyte separators in vanadium redox flow batteries, *J. Electrochem. Soc.*, 2014, **161**, A1860-A1868.
255. Z. Mai, H. Zhang, X. Li, C. Bi and H. Dai, Sulfonated poly(tetramethyldiphenyl ether ether ketone) membranes for vanadium redox flow battery application, *J. Power Sources*, 2011, **196**, 482-487.
256. M. A. Aziz and S. Shanmugam, Sulfonated graphene oxide-decorated block copolymer as a proton-exchange membrane: improving the ion selectivity for all-vanadium redox flow batteries, *J. Mater. Chem. A*, 2018, **6**, 17740-17750.
257. A. Chromik, A. R. D. Santos, T. Turek, U. Kunz, T. Häring and J. Kerres, Stability of acid-excess acid–base blend membranes in all-vanadium redox-flow batteries, *J. Membr. Sci.*, 2015, **476**, 148-155.
258. S. Zhang, J. Li, X. Huang, Y. Zhang and Y. Zhang, Sulfonated poly(imide-siloxane) membrane as a low vanadium ion permeable separator for a vanadium redox flow battery, *Polym. J.*, 2015, **47**.
259. C. Ding, H. Zhang, X. Li, H. Zhang, C. Yao and D. Shi, Morphology and Electrochemical Properties of Perfluorosulfonic Acid Ionomes for Vanadium Flow Battery Applications: Effect of Side-Chain Length, *ChemSusChem*, 2013, **6**, 1262-1269.
260. C. Fujimoto, S. Kim, R. Stains, X. Wei, L. Li and Z. G. Yang, Vanadium redox flow battery efficiency and durability studies of sulfonated Diels Alder poly(phenylene)s, *Electrochem. Commun.*, 2012, **20**, 48-51.
261. T. Mohammadi and M. Skyllas-Kazacos, Use of polyelectrolyte for incorporation of ion-exchange groups in composite membranes for vanadium redox flow battery applications, *J. Power Sources*, 1995, **56**, 91-96.
262. M. Branchi, M. Gigli, B. Mecheri, F. Zurlo, S. Licoccia and A. D’Epifanio, Highly ion selective hydrocarbon-based membranes containing sulfonated hypercrosslinked polystyrene nanoparticles for vanadium redox flow batteries, *J. Membr. Sci.*, 2018, **563**, 552-560.
263. X. Yan, J. Sun, L. Gao, W. Zheng, Y. Dai, X. Ruan and G. He, A novel long-side-chain sulfonated poly (2, 6-dimethyl-1, 4-phenylene oxide) membrane for vanadium redox flow battery, *Int. J. Hydrogen Energy*, 2018, **43**, 301-310.
264. Z. Yuan, X. Li, Y. Zhao and H. Zhang, Mechanism of polysulfone-based anion exchange membranes degradation in vanadium flow battery, *ACS Appl. Mater. Interfaces*, 2015, **7**, 19446-19454.
265. F. Zhang, H. Zhang and C. Qu, A dication cross-linked composite anion-exchange membrane for all-vanadium flow battery applications, *ChemSusChem*, 2013, **6**, 2290-2298.
266. G. J. Hwang and H. Ohya, Crosslinking of anion exchange membrane by accelerated electron radiation as a separator for the all-vanadium redox flow battery, *J. Membr. Sci.*, 1997, **132**, 55-61.
267. F. Zhang, H. Zhang and C. Qu, Influence of solvent on polymer prequaternization

- toward anion-conductive membrane fabrication for all-vanadium flow battery, *J. Phys. Chem. B*, 2012, **116**, 9016-9022.
268. D. Zhang, X. Yan, G. He, L. Zhang, X. Liu, F. Zhang, M. Hu, Y. Dai and S. Peng, An integrally thin skinned asymmetric architecture design for advanced anion exchange membranes for vanadium flow batteries, *J. Mater. Chem. A*, 2015, **3**, 16948-16952.
269. J. Si, Y. Lv, S. Lu and Y. Xiang, Microscopic phase-segregated quaternary ammonia polysulfone membrane for vanadium redox flow batteries, *J. Power Sources*, 2019, **428**, 88-92.
270. Y. Xing, L. Liu, C. Wang and N. Li, Side-chain-type anion exchange membranes for vanadium flow battery: properties and degradation mechanism, *J. Mater. Chem. A*, 2018, **6**, 22778-22789.
271. M. S. Cha, H. Y. Jeong, H. Y. Shin, S. H. Hong, T. H. Kim, S. G. Oh, J. Y. Lee and Y. T. Hong, Crosslinked anion exchange membranes with primary diamine-based crosslinkers for vanadium redox flow battery application, *J. Power Sources*, 2017, **363**, 78-86.
272. Y. Zhao, M. Li, Z. Yuan, X. Li, H. Zhang and I. F. J. Vankelecom, Advanced Charged Sponge-Like Membrane with Ultrahigh Stability and Selectivity for Vanadium Flow Batteries, *Adv. Funct. Mater.*, 2016, **26**, 210-218.
273. S. Zhang, B. Zhang, D. Xing and X. Jian, Poly (phthalazinone ether ketone ketone) anion exchange membranes with pyridinium as ion exchange groups for vanadium redox flow battery applications, *J. Mater. Chem. A*, 2013, **1**, 12246-12254.
274. B. Zhang, S. Zhang, D. Xing, R. Han, C. Yin and X. Jian, Quaternized poly (phthalazinone ether ketone ketone) anion exchange membrane with low permeability of vanadium ions for vanadium redox flow battery application, *J. Power Sources*, 2012, **217**, 296-302.
275. S. Zhang, B. Zhang, G. Zhao and X. Jian, Anion exchange membranes from brominated poly (aryl ether ketone) containing 3, 5-dimethyl phthalazinone moieties for vanadium redox flow batteries, *J. Mater. Chem. A*, 2014, **2**, 3083-3091.
276. B. Zhang, S. Zhang, Z. Weng, G. Wang, E. Zhang, P. Yu, X. Chen and X. Wang, Quaternized adamantane-containing poly (aryl ether ketone) anion exchange membranes for vanadium redox flow battery applications, *J. Power Sources*, 2016, **325**, 801-807.
277. B. Zhang, Q. Wang, S. Guan, Z. Weng, E. Zhang, G. Wang, Z. Zhang, J. Hu and S. Zhang, High performance membranes based on new 2-adamantane containing poly (aryl ether ketone) for vanadium redox flow battery applications, *J. Power Sources*, 2018, **399**, 18-25.
278. Y. Ahn and D. Kim, Anion exchange membrane prepared from imidazolium grafted poly (arylene ether ketone) with enhanced durability for vanadium redox flow battery, *J. Ind. Eng. Chem.*, 2019, **71**, 361-368.
279. Q. Zhang, Q. F. Dong, M. S. Zheng and Z. W. Tian, The preparation of a novel anion-exchange membrane and its application in all-vanadium redox batteries, *J. Membr. Sci.*, 2012, **421**, 232-237.
280. G. Shukla and V. K. Shahi, Amine functionalized graphene oxide containing C16 chain grafted with poly (ether sulfone) by DABCO coupling: Anion exchange membrane for

- vanadium redox flow battery, *J. Membr. Sci.*, 2019, **575**, 109-117.
281. D. Chen, M. A. Hickner, E. Agar and E. C. Kumbur, Selective anion exchange membranes for high coulombic efficiency vanadium redox flow batteries, *Electrochem. Commun.*, 2013, **26**, 37-40.
  282. R. Chen, D. Henkensmeier, S. Kim, S. J. Yoon, T. Zinkevich and S. Indris, Improved all-vanadium redox flow batteries using catholyte additive and a cross-linked methylated polybenzimidazole membrane, *ACS Appl. Energy Mater.*, 2018, **1**, 6047-6055.
  283. Y. Lee, S. Kim, A. Maljusch, O. Conradi, H.-J. Kim, J. H. Jang, J. Han, J. Kim and D. Henkensmeier, Polybenzimidazole membranes functionalised with 1-methyl-2-mesitylbenzimidazolium ions via a hexyl linker for use in vanadium flow batteries, *Polymer*, 2019, **174**, 210-217.
  284. C. N. Sun, Z. Tang, C. Belcher, T. A. Zawodzinski and C. Fujimoto, Evaluation of Diels–Alder poly (phenylene) anion exchange membranes in all-vanadium redox flow batteries, *Electrochem. Commun.*, 2014, **43**, 63-66.
  285. S. J. Seo, B. C. Kim, K. W. Sung, J. Shim, J. D. Jeon, K. H. Shin, S. H. Shin, S. H. Yun, J. Y. Lee and S. H. Moo, Electrochemical properties of pore-filled anion exchange membranes and their ionic transport phenomena for vanadium redox flow battery applications., *J. Membr. Sci.*, 2013, **428**, 17-23.
  286. D. Lu, L. Wen, F. Nie and L. Xue, Synthesis and investigation of imidazolium functionalized poly (arylene ether sulfone) s as anion exchange membranes for all-vanadium redox flow batteries, *RSC Adv.*, 2016, **6**, 6029-6037.
  287. S. Yun, J. Parrondo and V. Ramani, Derivatized cardo-polyetherketone anion exchange membranes for all-vanadium redox flow batteries, *J. Mater. Chem. A*, 2014, **2**, 6605-6615.
  288. D. Xing, S. Zhang, C. Yin, C. Yan and X. Jian, Preparation and characterization of chloromethylated/quaternized poly (phthalazinone ether sulfone) anion exchange membrane, *Mater. Sci. Eng. B*, 2009, **157**, 1-5.
  289. C. W. Hwang, H. M. Park, C. M. Oh, T. S. Hwang, J. Shim and C. S. Jin, Synthesis and characterization of vinylimidazole-co-trifluoroethylmethacrylate-co-divinylbenzene anion-exchange membrane for all-vanadium redox flow battery, *J. Membr. Sci.*, 2014, **468**, 98-106.
  290. J. Fang, H. Xu, X. Wei, M. Guo, X. Lu, C. Lan, Y. Zhang, Y. Liu and T. Peng, Preparation and characterization of quaternized poly (2, 2, 2 - trifluoroethyl methacrylate - co - N - vinylimidazole) membrane for vanadium redox flow battery, *Polym. Adv. Technol.*, 2013, **24**, 168-173.
  291. D. Xing, S. Zhang, C. Yin, B. Zhang and X. Jian, Effect of amination agent on the properties of quaternized poly (phthalazinone ether sulfone) anion exchange membrane for vanadium redox flow battery application, *J. Membr. Sci.*, 2010, **354**, 68-73.
  292. D. Chen, M. A. Hickner, E. Agar and E. C. Kumbur, Anion exchange membranes for vanadium redox flow batteries, *ECS Trans.*, 2013, **53**, 83-89.
  293. D. Chen, M. A. Hickner, E. Agar and E. C. Kumbur, Optimized anion exchange membranes for vanadium redox flow batteries, *ACS Appl. Mater. Interfaces*, 2013, **5**, 7559-7566.

294. Z. Mai, H. Zhang, H. Zhang, W. Xu, W. Wei, H. Na and X. Li, Anion - Conductive Membranes with Ultralow Vanadium Permeability and Excellent Performance in Vanadium Flow Batteries, *ChemSusChem*, 2013, **6**, 328-335.
295. T. Mohammadi and M. Skyllas-Kazacos, Modification of anion-exchange membranes for vanadium redox flow battery applications, *J. Power Sources*, 1996, **63**, 179-186.
296. H. Choi, Y. Oh, C. Ryu and G. Hwang, Characteristics of the all-vanadium redox flow battery using anion exchange membrane, *J. Taiwan Inst. Chem. Eng.*, 2014, **45**, 2920-2925.
297. S. L. Mallinson, J. R. Varcoe and R. C. Slade, Examination of amine-functionalised anion-exchange membranes for possible use in the all-vanadium redox flow battery, *Electrochim. Acta*, 2014, **140**, 145-151.
298. T. Wang, J. Y. Jeon, Han Junyoung, J. H. Kim, C. Bae and S. Kim, Poly(terphenylene) anion exchange membranes with high conductivity and low vanadium permeability for vanadium redox flow batteries (VRFBs), *J. Power Sources*, 2020, **598**, 117665.
299. B. Shanahan, T. Böhm, B. Britton, S. Holdcroft, R. Zengerle, S. Vierrath, S. Thiele and M. Breitwieser, 30  $\mu\text{m}$  thin hexamethyl-p-terphenyl poly (benzimidazolium) anion exchange membrane for vanadium redox flow batteries, *Electrochem. Commun.*, 2019, **102**, 37-40.
300. M. Abdiani, E. Abouzari-Lotf, T. M. Ting, P. M. Nia, S. S. Sha'rani, A. Shockravi and A. Ahmad, Novel polyolefin based alkaline polymer electrolyte membrane for vanadium redox flow batteries, *J. Power Sources*, 2019, **424**, 245-253.
301. S. H. Roh, M. H. Lim, T. Sadhasivam and H. Y. Jung, Investigation on physico-chemical and electrochemical performance of poly (phenylene oxide)-based anion exchange membrane for vanadium redox flow battery systems, *Electrochim. Acta*, 2019, **325**, 134944.
302. L. Cao, A. Kronander, A. Tang, D.-W. Wang and M. Skyllas-Kazacos, Membrane permeability rates of vanadium ions and their effects on temperature variation in vanadium redox batteries, *Energies*, 2016, **9**, 1058.
303. E. Bülbül, V. Atanasov, M. Mehlhorn, M. Bürger, A. Chromik, T. Häring and J. Kerres, Highly phosphonated polypentafluorostyrene blended with polybenzimidazole: Application in vanadium redox flow battery, *J. Membr. Sci.*, 2019, **570**, 194-203.
304. J. Qiu, J. Zhang, J. Chen, J. Peng, L. Xu, M. Zhai, J. Li and G. Wei, Amphoteric ion exchange membrane synthesized by radiation-induced graft copolymerization of styrene and dimethylaminoethyl methacrylate into PVDF film for vanadium redox flow battery applications, *J. Membr. Sci.*, 2009, **334**, 9-15.
305. J. Ma, Y. Wang, J. Peng, J. Qiu, L. Xu, J. Li and M. Zhai, Designing a new process to prepare amphoteric ion exchange membrane with well-distributed grafted chains for vanadium redox flow battery, *J. Membr. Sci.*, 2012, **419-420**, 1-8.
306. G. Hu, Y. Wang, J. Ma, J. Qiu, J. Peng, J. Li and M. Zhai, A novel amphoteric ion exchange membrane synthesized by radiation-induced grafting  $\alpha$ -methylstyrene and N,N-dimethylaminoethyl methacrylate for vanadium redox flow battery application, *J. Membr. Sci.*, 2012, **407-408**, 184-192.
307. J. Yuan, C. Yu, J. Peng, Y. Wang, J. Ma, J. Qiu, J. Li and M. Zhai, Facile synthesis of amphoteric ion exchange membrane by radiation grafting of sodium styrene sulfonate



- and N, N - dimethylaminoethyl methacrylate for vanadium redox flow battery, *J. Polym. Sci., Part A: Polym. Chem.*, 2013, **51**, 5194-5202.
308. J. Qiu, M. Zhai, J. Chen, Y. Wang, J. Peng, L. Xu, J. Li and G. Wei, Performance of vanadium redox flow battery with a novel amphoteric ion exchange membrane synthesized by two-step grafting method, *J. Membr. Sci.*, 2009, **342**, 215-220.
309. O. Nibel, T. Rojek, T. J. Schmidt and L. Gubler, Amphoteric Ion-Exchange Membranes with Significantly Improved Vanadium Barrier Properties for All-Vanadium Redox Flow Batteries, *ChemSusChem*, 2017, **10**, 2767-2777.
310. R. Gan, Y. Ma, S. Li, F. Zhang and G. He, Facile fabrication of amphoteric semi-interpenetrating network membranes for vanadium flow battery applications, *J. Energy Chem.*, 2018, **27**, 1189-1197.
311. H. Zhang, X. Yan, L. Gao, L. Hu, X. Ruan, W. Zheng and G. He, Novel triple tertiary amine polymer-based hydrogen bond network inducing highly efficient proton-conducting channels of amphoteric membranes for high-performance vanadium redox flow battery, *ACS Appl. Mater. Interfaces*, 2019, **11**, 5003-5014.
312. S. Liu, L. Wang, D. Li, B. Liu, J. Wang and Y. Song, Novel amphoteric ion exchange membranes by blending sulfonated poly (ether ether ketone)/quaternized poly (ether imide) for vanadium redox flow battery applications, *J. Mater. Chem. A*, 2015, **3**, 17590-17597.
313. M. S. Lee, H. G. Kang, J. D. Jeon, Y. W. Choi and Y. G. Yoon, A novel amphoteric ion-exchange membrane prepared by the pore-filling technique for vanadium redox flow batteries, *RSC Adv.*, 2016, **6**, 63023-63029.
314. Y. Chen, S. Zhang, J. Jin, C. Liu, Q. Liu and X. Jian, Poly (phthalazinone ether ketone) amphoteric ion exchange membranes with low water transport and vanadium permeability for vanadium redox flow battery application, *ACS Appl. Energy Mater.*, 2019, **2**, 8207-8218.
315. Y. Chen, S. Zhang, Q. Liu and X. Jian, Sulfonated component-incorporated quaternized poly (phthalazinone ether ketone) membranes with improved ion selectivity, stability and water transport resistance in a vanadium redox flow battery, *RSC Adv.*, 2019, **9**, 26097-26108.
316. X. Yan, C. Zhang, Z. Dong, B. Jiang, Y. Dai, X. Wu and G. He, Amphiprotic side-chain functionalization constructing highly proton/vanadium-selective transport channels for high-performance membranes in vanadium redox flow batteries, *ACS Appl. Mater. Interfaces*, 2018, **10**, 32247-32255.
317. Y. Wang, S. Wang, M. Xiao, S. Song, D. Han, M. A. Hickner and Y. Meng, Amphoteric ion exchange membrane synthesized by direct polymerization for vanadium redox flow battery application, *Int. J. Hydrogen Energy*, 2014, **39**, 16123-16131.
318. Y. Li, X. Lin, L. Wu, C. Jiang, M. M. Hossain and T. Xu, Quaternized membranes bearing zwitterionic groups for vanadium redox flow battery through a green route, *J. Membr. Sci.*, 2015, **483**, 60-69.
319. W. Lu, Z. Yuan, M. Li, X. Li, H. Zhang and I. Vankelecom, Solvent-induced rearrangement of ion-transport channels: a way to create advanced porous membranes for vanadium flow batteries, *Adv. Funct. Mater.*, 2017, **27**.
320. Z. Yuan, Q. Dai, Y. Zhao, W. Lu, X. Li and H. Zhang, Polypyrrole modified porous

- poly(ether sulfone) membranes with high performance for vanadium flow batteries, *J. Mater. Chem. A*, 2016, **4**, 12955-12962.
321. J. Cao, Z. Yuan, X. Li, W. Xu and H. Zhang, Hydrophilic poly (vinylidene fluoride) porous membrane with well connected ion transport networks for vanadium flow battery, *J. Power Sources*, 2015, **298**, 228-235.
  322. W. Lu, Z. Yuan, Y. Zhao, X. Li, H. Zhang and I. F. J. Vankelecom, High-performance porous uncharged membranes for vanadium flow battery applications created by tuning cohesive and swelling forces, *Energy Environ. Sci.*, 2016, **9**, 2319-2325.
  323. W. Xu, X. Li, J. Cao, H. Zhang and H. Zhang, Membranes with well-defined ions transport channels fabricated via solvent-responsive layer-by-layer assembly method for vanadium flow battery, *Sci. Rep.*, 2014, **4**, 4016.
  324. H. Zhang, C. Ding, J. Cao, W. Xu, X. Li and H. Zhang, A novel solvent-template method to manufacture nano-scale porous membranes for vanadium flow battery applications, *J. Mater. Chem. A*, 2014, **2**.
  325. H. Zhang, H. Zhang, X. Li, Z. Mai and W. Wei, Silica modified nanofiltration membranes with improved selectivity for redox flow battery application, *Energy Environ. Sci.*, 2012, **5**, 6299-6303.
  326. L. Qiao, H. Zhang, W. Lu, Q. Dai and X. Li, Advanced Porous Membranes with Tunable Morphology Regulated by Ionic Strength of Nonsolvent for Flow Battery, *ACS Appl. Mater. Interfaces*, 2019, **11**, 24107-24113.
  327. Y. Li, H. Zhang, H. Zhang, J. Cao, W. Xu and X. Li, Hydrophilic porous poly(sulfone) membranes modified by UV-initiated polymerization for vanadium flow battery application, *J. Membr. Sci.*, 2014, **454**, 478-487.
  328. Z. Yuan, Y. Duan, H. Zhang, X. Li, H. Zhang and I. Vankelecom, Advanced porous membranes with ultra-high selectivity and stability for vanadium flow batteries, *Energy Environ. Sci.*, 2016, **9**, 441-447.
  329. S. Maurya, S. H. Shin, J. Y. Lee, Y. Kim and S. H. Moon, Amphoteric nanoporous polybenzimidazole membrane with extremely low crossover for a vanadium redox flow battery, *RSC Adv.*, 2016, **6**, 5198-5204.
  330. D. Chen, H. Qi, T. Sun, C. Yan, Y. He, C. Kang, Z. Yuan and X. Li, Polybenzimidazole membrane with dual proton transport channels for vanadium flow battery applications, *J. Membr. Sci.*, 2019, **586**, 202-210.
  331. K. Geng, Y. Li, Y. Xing, L. Wang and N. Li, A novel polybenzimidazole membrane containing bulky naphthalene group for vanadium flow battery, *J. Membr. Sci.*, 2019, **586**, 231-239.
  332. L. Ding, X. Song, L. Wang, Z. Zhao and G. He, Preparation of dense polybenzimidazole proton exchange membranes with different basicity and flexibility for vanadium redox flow battery applications, *Electrochim. Acta*, 2018, **292**, 10-19.
  333. V. E. Sizov, M. S. Kondratenko and M. O. Gallyamov, Ion transport properties of porous polybenzimidazole membranes for vanadium redox flow batteries obtained via supercritical drying of swollen polymer films, *J. Appl. Polym. Sci.*, 2018, **135**, 46262.
  334. S. Peng, X. Wu, X. Yan, L. Gao, Y. Zhu, D. Zhang, J. Li, Q. Wang and G. He, Polybenzimidazole membranes with nanophase-separated structure induced by non-ionic hydrophilic side chains for vanadium flow batteries, *J. Mater. Chem. A*, 2018, **6**,

- 3895-3905.
335. W. Lu, Z. Yuan, Y. Zhao, L. Qiao, H. Zhang and X. Li, Advanced porous PBI membranes with tunable performance induced by the polymer-solvent interaction for flow battery application, *Energy Stor. Mater.*, 2018, **10**, 40-47.
  336. J. K. Jang, T. H. Kim, S. Yoon, J. Y. Lee, J. C. Lee and Y. T. Hong, Highly proton conductive, dense polybenzimidazole membranes with low permeability to vanadium and enhanced H<sub>2</sub>SO<sub>4</sub> absorption capability for use in vanadium redox flow batteries, *J. Mater. Chem. A*, 2016, **4**, 14342-14355.
  337. X. Teng, Y. Guo, D. Liu, G. Li, C. Yu and J. Dai, A polydopamine-coated polyamide thin film composite membrane with enhanced selectivity and stability for vanadium redox flow battery, *J. Membr. Sci.*, 2020, **601**, 117906.
  338. Q. Dai, Z. Liu, L. Huang, C. Wang, Y. Zhao, Q. Fu, A. Zheng, H. Zhang and X. Li, Thin-film composite membrane breaking the trade-off between conductivity and selectivity for a flow battery, *Nat. Commun.*, 2020, **11**, 1-9.
  339. L. Qiao, H. Zhang, W. Lu, C. Xiao, Q. Fu, X. Li and I. F. Vankelecom, Advanced porous membranes with slit-like selective layer for flow battery, *Nano Energy*, 2018, **54**, 73-81.
  340. D. Chen, D. Li and X. Li, Hierarchical porous poly (ether sulfone) membranes with excellent capacity retention for vanadium flow battery application, *J. Power Sources*, 2017, **353**, 11-18.
  341. Y. Zhao, Z. Yuan, W. Lu, X. Li and H. Zhang, The porous membrane with tunable performance for vanadium flow battery: the effect of charge, *J. Power Sources*, 2017, **342**, 327-334.
  342. D. Chen, D. Li and X. Li, Highly symmetric spongy porous poly(ether sulfone) membranes with selective open-cells for vanadium flow battery application, *RSC Adv.*, 2016, **6**, 87104-87109.
  343. H. Zhang, H. Zhang and X. Li, Nanofiltration membranes for vanadium flow battery application, *ECS Trans.*, 2013, **53**, 65-68.
  344. H. Zhang, H. Zhang, X. Li, Z. Mai and J. Zhang, Nanofiltration (NF) membranes: the next generation separators for all vanadium redox flow batteries (VRBs)?, *Energy Environ. Sci.*, 2011, **4**.
  345. I. S. Chae, T. Luo, G. H. Moon, W. Ogieglo, Y. S. Kang and M. Wessling, Ultra-high proton/vanadium delectivity for hydrophobic polymer membranes with intrinsic nanopores for redox flow battery, *Adv. Energy Mater.*, 2016, **6**.
  346. B. Fang, Y. Wei, T. Arai, S. Iwasa and M. Kumagai, Development of a novel redox flow battery for electricity storage system, *J. Appl. Electrochem.*, 2003, **33**, 197-203.
  347. H. Mögelin, A. Barascu, S. Krenkel, D. Enke, T. Turek and U. Kunz, Effect of the pore size and surface modification of porous glass membranes on vanadium redox-flow battery performance, *J. Appl. Electrochem.*, 2018, **48**, 651-662.
  348. I. Michos, Z. Cao, Z. Xu, W. Jing and J. Dong, Investigations on a Mesoporous Glass Membrane as Ion Separator for a Redox Flow Battery, *Batteries*, 2019, **5**, 6.
  349. H. Mögelin, G. Yao, H. Zhong, A. dos Santos, A. Barascu, R. Meyer, S. Krenkel, S. Wassersleben, T. Hickmann and D. Enke, Porous glass membranes for vanadium redox-flow battery application-Effect of pore size on the performance, *J. Power Sources*, 2018,

- 377, 18-25.
350. C. Wu, H. Bai, Y. Lv, Z. Lv, Y. Xiang and S. Lu, Enhanced membrane ion selectivity by incorporating graphene oxide nanosheet for vanadium redox flow battery application, *Electrochim. Acta*, 2017, **248**, 454-461.
  351. Q. Chen, Y. Y. Du, K. M. Li, H. F. Xiao, W. Wang and W. M. Zhang, Graphene enhances the proton selectivity of porous membrane in vanadium flow batteries, *Mater. Des.*, 2017, **113**, 149-156.
  352. C. Wu, S. Lu, H. Wang, X. Xu, S. Peng, Q. Tan and Y. Xiang, A novel polysulfone–polyvinylpyrrolidone membrane with superior proton-to-vanadium ion selectivity for vanadium redox flow batteries, *J. Mater. Chem. A*, 2016, **4**, 1174-1179.
  353. J. Cao, H. Zhang, W. Xu and X. Li, Poly(vinylidene fluoride) porous membranes precipitated in water/ethanol dual-coagulation bath: The relationship between morphology and performance in vanadium flow battery, *J. Power Sources*, 2014, **249**, 84-91.
  354. R. Xue, F. Jiang, F. Wang and X. Zhou, Towards cost-effective proton-exchange membranes for redox flow batteries: A facile and innovative method, *J. Power Sources*, 2020, **449**, 227475.
  355. R. Yang, Z. Xu, S. Yang, I. Michos, L. F. Li, A. P. Angelopoulos and J. Dong, Nonionic zeolite membrane as potential ion separator in redox-flow battery, *J. Membr. Sci.*, 2014, **450**, 12-17.
  356. D. Enke, F. Janowski and W. Schwieger, Porous glasses in the 21st century—a short review, *Microporous Mesoporous Mater.*, 2003, **60**, 19-30.
  357. X. L. Zhou, T. S. Zhao, L. An, Y. K. Zeng and L. Wei, Critical transport issues for improving the performance of aqueous redox flow batteries, *J. Power Sources*, 2017, **339**, 1-12.
  358. S. J. Paddison and R. Paul, The nature of proton transport in fully hydrated Nafion®, *Phys. Chem. Chem. Phys.*, 2002, **4**, 1158-1163.
  359. E. Wiedemann, A. Heintz and R. N. Lichtenthaler, Sorption isotherms of vanadium with H<sub>3</sub>O<sup>+</sup> ions in cation exchange membranes, *J. Membr. Sci.*, 1998, **141**, 207-213.
  360. T. Xu, Ion exchange membranes: state of their development and perspective, *J. Membr. Sci.*, 2005, **263**, 1-29.
  361. J. H. Choi, S. H. Kim and S. H. Moon, Heterogeneity of ion-exchange membranes: the effects of membrane heterogeneity on transport properties, *J. Colloid Interface Sci.*, 2001, **241**, 120-126.
  362. K. W. Knehr and E. C. Kumbur, Role of convection and related effects on species crossover and capacity loss in vanadium redox flow batteries, *Electrochem. Commun.*, 2012, **23**, 76-79.
  363. K. W. Knehr, E. Agar, C. R. Dennison, A. R. Kalidindi and E. C. Kumbur, A transient vanadium flow battery model incorporating vanadium crossover and water transport through the membrane, *J. Electrochem. Soc.*, 2012, **159**, A1446-A1459.
  364. S. Won, K. Oh and H. Ju, Numerical analysis of vanadium crossover effects in all-vanadium redox flow batteries, *Electrochim. Acta*, 2015, **177**, 310-320.
  365. E. Agar, K. W. Knehr, D. Chen, M. A. Hickner and E. C. Kumbur, Species transport mechanisms governing capacity loss in vanadium flow batteries: Comparing Nafion®

- and sulfonated Radel membranes, *Electrochim. Acta*, 2013, **98**, 66-74.
366. X. L. Zhou, T. S. Zhao, L. An, Y. K. Zeng and L. Wei, Modeling of ion transport through a porous separator in vanadium redox flow batteries, *J. Power Sources*, 2016, **327**, 67-76.
367. K. Oh, S. Won and H. Ju, A comparative study of species migration and diffusion mechanisms in all-vanadium redox flow batteries, *Electrochim. Acta*, 2015, **181**, 238-247.
368. T. Mohammadi, S. C. Chieng and M. Skyllas-Kazacos, Water transport study across commercial ion exchange membranes in the vanadium redox flow battery, *J. Membr. Sci.*, 1997, **133**, 151-159.
369. K. Oh, M. Moazzam, G. Gwak and H. Ju, Water crossover phenomena in all-vanadium redox flow batteries, *Electrochim. Acta*, 2019, **297**, 101-111.
370. T. Sukkar and M. Skyllas-Kazacos, Water transfer behaviour across cation exchange membranes in the vanadium redox battery, *J. Membr. Sci.*, 2003, **222**, 235-247.
371. C. Sun, J. Chen, H. Zhang, X. Han and Q. Luo, Investigations on transfer of water and vanadium ions across Nafion membrane in an operating vanadium redox flow battery, *J. Power Sources*, 2010, **195**, 890-897.
372. S. C. Chieng, M. Kazacos and M. Skyllas-Kazacos, Preparation and evaluation of composite membrane for vanadium redox battery applications, *J. Power Sources*, 1992, **39**, 11-19.
373. D. Jeong and S. Jung, Numerical analysis of cycling performance of vanadium redox flow battery, *Int. J. Energy Res.*, 2020, **44**, 5209-5222.
374. D. K. Kim, S. J. Yoon and S. Kim, Transport phenomena associated with capacity loss of all-vanadium redox flow battery, *Int. J. Heat Mass Transfer*, 2020, **148**, 119040.
375. Q. Xu, T. S. Zhao and C. Zhang, Effects of SOC-dependent electrolyte viscosity on performance of vanadium redox flow batteries, *Appl. Energy*, 2014, **130**, 139-147.
376. M. J. Watt-Smith, P. Ridley, R. G. A. Wills, A. A. Shah and F. C. Walsh, The importance of key operational variables and electrolyte monitoring to the performance of an all vanadium redox flow battery, *J. Chem. Technol. Biotechnol.*, 2013, **88**, 126-138.
377. T. Sukkar and M. Skyllas-Kazacos, Modification of membranes using polyelectrolytes to improve water transfer properties in the vanadium redox battery, *J. Membr. Sci.*, 2003, **222**, 249-264.
378. S. Peng, X. Yan, X. Wu, D. Zhang, Y. Luo, L. Su and G. He, Thin skinned asymmetric polybenzimidazole membranes with readily tunable morphologies for high-performance vanadium flow batteries, *RSC Adv.*, 2017, **7**, 1852-1862.
379. C. Noh, M. Jung, D. Henkensmeier, S. W. Nam and Y. Kwon, Vanadium redox flow batteries using meta-polybenzimidazole-based membranes of different thicknesses, *ACS Appl. Mater. Interfaces*, 2017, **9**, 36799-36809.
380. H. Y. Jung, S. Jeong and Y. Kwon, The effects of different thick sulfonated poly (ether ether ketone) membranes on performance of vanadium redox flow battery, *J. Electrochem. Soc.*, 2016, **163**, A5090-A5096.
381. Nafionstore.eu, [http://www.nafionstore.com/store/pg/8-Contact\\_US.aspx](http://www.nafionstore.com/store/pg/8-Contact_US.aspx), (accessed 10 May, 2020).
382. *The Chemours Company. Technical information on Nafion membranes*, 2016.

383. L. Joerissen, J. Garche, C. Fabjan and G. Tomazic, Possible use of vanadium redox-flow batteries for energy storage in small grids and stand-alone photovoltaic systems, *J. Power Sources*, 2004, **127**, 98-104.
384. V. Viswanathan, A. Crawford, D. Stephenson, S. Kim, W. Wang, B. Li, G. Coffey, E. Thomsen, G. Graff and P. Balducci, Cost and performance model for redox flow batteries, *J. Power Sources*, 2014, **247**, 1040-1051.
385. A. Crawford, V. Viswanathan, D. Stephenson, W. Wang, E. Thomsen, D. Reed, B. Li, P. Balducci, M. Kintner-Meyer and V. Sprenkle, Comparative analysis for various redox flow batteries chemistries using a cost performance model, *J. Power Sources*, 2015, **293**, 388-399.
386. Fuelcellstore, <http://fuelcellstore.com>, (accessed 10 Feb, 2021).
387. R. L. Largent, M. Skylas-Kazacos and J. Chieng, Improved PV system performance using vanadium batteries, *In Conference Record of the Twenty Third IEEE Photovoltaic Specialists Conference-1993 (Cat. No. 93CH3283-9)*, 1993, **IEEE**, 1119-1124.
388. M. Skyllas - Kazacos, G. Kazacos, G. Poon and H. Verseema, Recent advances with UNSW vanadium - based redox flow batteries, *Int. J. Energy Res.*, 2010, **34**, 182-189.
389. G. Kear, A. A. Shah and F. C. Walsh, Development of the all-vanadium redox flow battery for energy storage: a review of technological, financial and policy aspects, *Int. J. Energy Res.*, 2012, **36**, 1105-1120.
390. C. Doetsch and J. Burfeind, Vanadium Redox Flow Batteries, *Storing Energy. Elsevier*, 2016, 227-246.

## Figure captions

**Fig. 1.** Schematic of (a) a typical redox flow battery system, (b) a single cell; and (c) a polymer electrolyte membrane.

**Fig. 2.** (a) Schematic of a H-cell for vanadium-ions permeability measurement. (b) Schematic of a tensile test machine.<sup>98</sup> Reproduced with permission. Copyright 2017, Elsevier.

**Fig. 3.** A typical polarization curve of VRFBs. Reproduced with permission.<sup>129</sup> Copyright 2013, Elsevier.

**Fig. 4.** Schematic of a (a) cation-exchange membrane; (b) anion-exchange membrane; (c) amphoteric-ion exchange membrane; and (d) porous membrane.

**Fig. 5.** (a) Vanadium-ions permeability comparison between BI $\rho$ PBI, B20N5, B20N10, and Nafion 115; Reproduced under the terms of the CC-BY license.<sup>151</sup> Copyright 2018, The Authors. (b) Design of a VANADion membrane.<sup>108</sup> Reproduced with permission. Copyright 2016, Elsevier.

**Fig. 6.** (a) Columbic efficiency comparison of recast-Nafion membrane and PVDF/Nafion composite membranes at 40-80 mA cm<sup>-2</sup>;<sup>125</sup> Reproduced with permission. Copyright 2011, Elsevier. (b) Schematic of the preparation of Nafion-[PDDA-PSS] $_n$  membranes;<sup>102</sup> Reproduced with permission. Copyright 2008, The Royal Society of Chemistry. (c) Schematics of vanadium-ions transport through the pristine Nafion and GO/Nafion composite membranes.<sup>98</sup> Reproduced with permission. Copyright 2017, Elsevier.

**Fig. 7.** (a) Efficiencies comparison among SPEEK/PPD-GO-1, SPEEK, and Nafion 117 membranes from 30 to 60 mA cm<sup>-2</sup>.<sup>178</sup> Reproduced with permission. Copyright 2016, The Royal Society of Chemistry. (b) Cycle performance of SPEEK/GO-NH<sub>2</sub>-2, SPEEK, and Nafion 115.<sup>148</sup> Reproduced with permission. Copyright 2017, Elsevier.

**Fig. 8.** (a) Cycle performance of a PES-based membrane at 140 mA cm<sup>-2</sup>.<sup>232</sup> Reproduced with permission. Copyright 2017, Elsevier. (b) Cycle performance of PVDF-g-PSSA-22 membrane at 60 mA cm<sup>-2</sup>.<sup>103</sup> Reproduced with permission. Copyright 2005, American Chemical Society.

**Fig. 9.** (a) Coulombic, voltage, and energy efficiencies of SPPEK-P-90 at 60 mA cm<sup>-2</sup> for 100 cycles.<sup>141</sup> Reproduced with permission. Copyright 2017, Elsevier. (b) Capacity retention ability of sPBSP-8 membrane after 1000 cycles (inset: catholyte and anolyte volume comparison after 1000 cycles).<sup>246</sup> Reproduced with permission. Copyright 2017, The Royal Society of Chemistry.

**Fig. 10.** (a) Efficiencies of the sIPN anion-exchange membrane (DCD= 4%).<sup>265</sup> Reproduced with permission. Copyright 2013, John Wiley & Sons. (b) Preparation procedures and working mechanisms of a PSF-based membrane.<sup>86</sup> Reproduced with permission. Copyright 2017, Elsevier.

**Fig. 11.** (a) Discharge capacity of the BrPPO/Py-56 and Nafion 212 at 200 mA cm<sup>-2</sup>.<sup>83</sup> Reproduced with permission. Copyright 2016, Elsevier. (b) Cycle stability of the PES-PVP anion-exchange membrane.<sup>279</sup> Reproduced with permission. Copyright 2012, Elsevier.

**Fig. 12.** (a) Open circuit voltage of the amphoteric-ion exchange membrane (A, DOG=42.7%) and Nafion 117 (B) membrane.<sup>307</sup> Reproduced with permission. Copyright 2013, John Wiley & Sons. (b) Schematic of the radiation grafting technique and solution phase-inversion method for membrane preparation.<sup>305</sup> Reproduced with permission. Copyright 2012, Elsevier.

**Fig. 13.** Cycling performance comparison between Nafion 115 and SPEEK/QAPEI-15 blend membranes.<sup>312</sup> Reproduced with permission. Copyright 2015, The Royal Society of Chemistry.

**Fig. 14.** (a) Cycle stability of a PBI-68 membrane for over 13000 cycles at current densities ranging from 80 to 120 mA cm<sup>-2</sup>.<sup>328</sup> Reproduced with permission. Copyright 2016, Royal Society of Chemistry. (b) Efficiencies of the NaCl-5M porous membrane for 10000 cycles at a current density of 160 mA cm<sup>-2</sup>.<sup>326</sup> Reproduced with permission. Copyright 2019, American Chemical Society.

**Fig. 15.** (a) Cycle performance of the PES-SPEEK membrane at 80 mA cm<sup>-2</sup>.<sup>319</sup> Reproduced with permission. Copyright 2016, John Wiley & Sons. (b) Schematic of the solvent-responsive layer-by-layer preparation procedure.<sup>323</sup> Reproduced with permission. Copyright 2014, Springer Nature.

**Fig. 16.** (a) The efficiencies of a nanofiltration membrane (M3) at 40-80 mA cm<sup>-2</sup>.<sup>325</sup> Reproduced with permission. Copyright 2012, The Royal Society of Chemistry. (b) Comparison of energy efficiencies between PIM-1/PAN and Nafion 112 membrane at 1-40 mA cm<sup>-2</sup>.<sup>345</sup> Reproduced with permission. Copyright 2016, John Wiley & Sons.

**Fig. 17.** (a) Diffusion and migration fluxes of vanadium species across three membrane of different thicknesses during (i) charging and (ii) discharging.<sup>364</sup> Reproduced with permission. Copyright 2015, Elsevier. (b) Schematic of species transport across the membrane under diffusion and migration mechanisms.<sup>367</sup> Reproduced with permission. Copyright 2015, Elsevier.

**Fig. 18.** (a) Schematic of various reactions and water sources and their transport mechanisms in VRFBs; contribution of different water crossover mechanisms on the water imbalance at the (b) negative and (c) positive half-cell.<sup>369</sup> Reproduced with permission. Copyright 2018, Elsevier.

**Fig. 19.** Cycle performance comparison of Nafion (green), PTFE<sub>30</sub>/Nafion/PTFE<sub>30</sub> (yellow), SPEEK (blue), and PTFE<sub>30</sub>/SPEEK/PTFE<sub>30</sub> (red) membranes.<sup>194</sup> Reproduced with permission. Copyright 2016, American Chemical Society.

**Fig. 20.** Comparison of (a) mechanical strength and (b) vanadium ions permeability of Nafion 212, SPEEK and SPEEK/SCCT membranes.<sup>198</sup> Reproduced with permission. Copyright 2014, Elsevier.



**Table captions**

**Table 1.** Performances of membranes according to the major materials used.

**Table 2.** Data of physicochemical properties, mechanical properties, VO<sup>2+</sup> permeability, and ion selectivity of Nafion 117, SPEEK, and SPEEK/PAN membranes.<sup>85</sup> Reproduced with permission. Copyright 2014, American Chemical Society.

**Table 3.** Summary and comparison of commercial membranes.

**Table 4.** Summary of some successful installations of large-scale VRFB systems at different locations.

## **Supplementary information**

**Table S1** Properties and performance of pure Nafion membranes.

**Table S2** Properties and performance of modified Nafion membranes (combining with other polymers).

**Table S3** Properties and performance of modified Nafion membranes (combining with organic/inorganic materials).

**Table S4** Properties and performance of SPEEK-based cation-exchange membranes.

**Table S5** Properties and performance of SPI-based cation-exchange membranes.

**Table S6** Properties and performance of SPFEK-based cation-exchange membranes.

**Table S7** Properties and performance of PTFE-based cation-exchange membranes.

**Table S8** Properties and performance of PES-based cation-exchange membranes.

**Table S9** Properties and performance of PVDF-based cation-exchange membranes.

**Table S10** Properties and performance of SPPEK-based cation-exchange membranes.

**Table S11** Properties and performance of PSF-based anion-exchange membranes.

**Table S12** Properties and performance of PAEK-based anion-exchange membranes.

**Table S13** Properties and performance of PVDF-based amphoteric-ion exchange membranes.

**Table S14** Properties and performance of PBI-based porous membranes.

**Table S15** Properties and performance of PES-based porous membranes.

**Table S16** Properties and performance of PAN-based porous membranes.

**Table S17** Properties and performance of porous glass-based porous membranes.

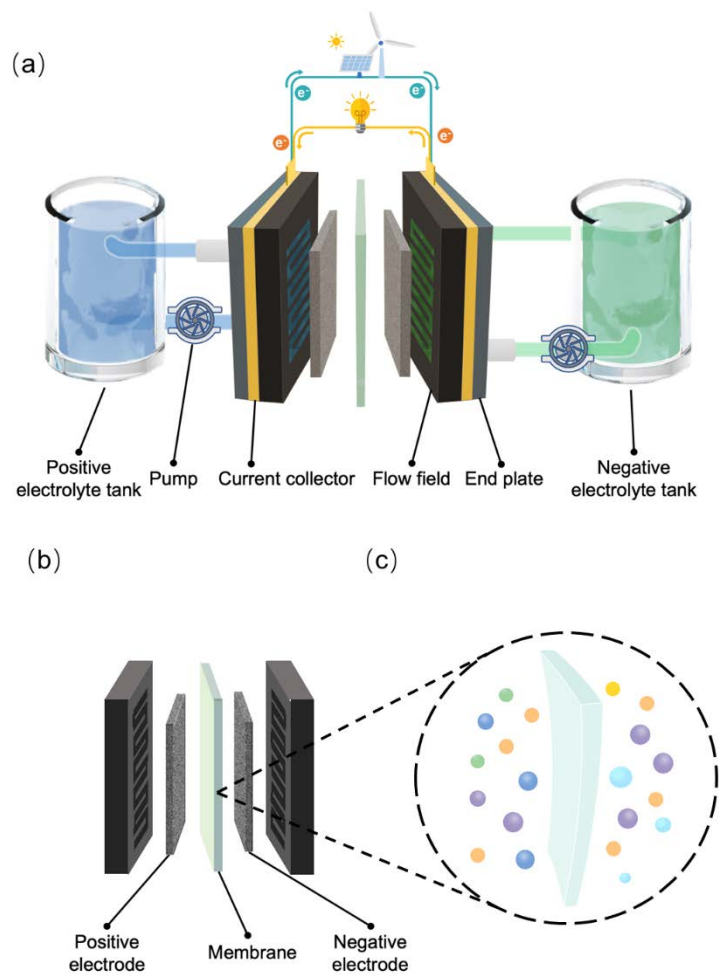


**Fig. 1.** Schematic of (a) a typical redox flow battery system, (b) a single cell; and (c) a polymer electrolyte membrane.

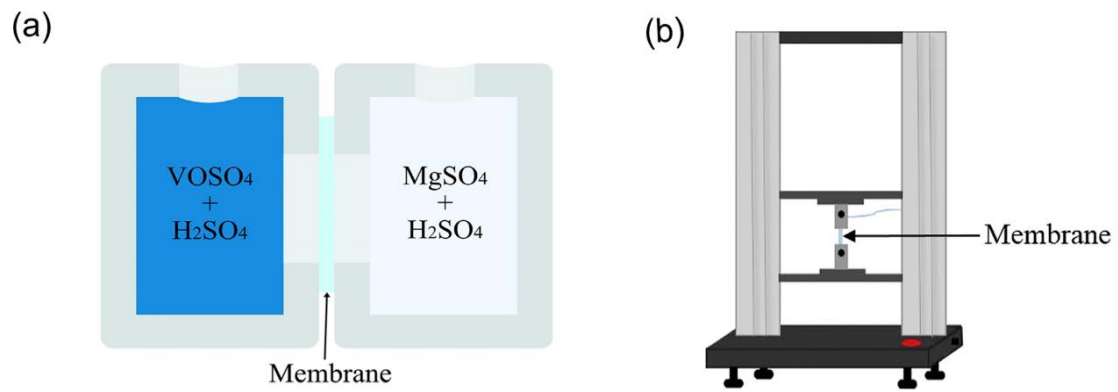


**Fig. 2.** (a) Schematic of a H-cell for vanadium-ions permeability measurement. (b) Schematic of a tensile test machine.<sup>98</sup> Reproduced with permission. Copyright 2017, Elsevier.

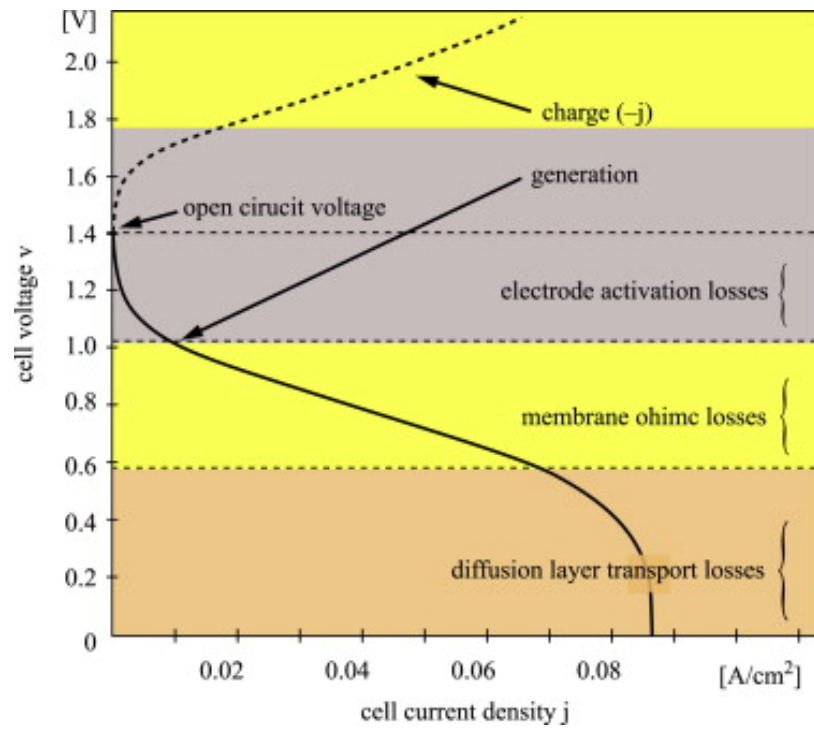


**Fig. 3.** A typical polarization curve of VRFBs. Reproduced with permission.<sup>129</sup> Copyright 2013, Elsevier.

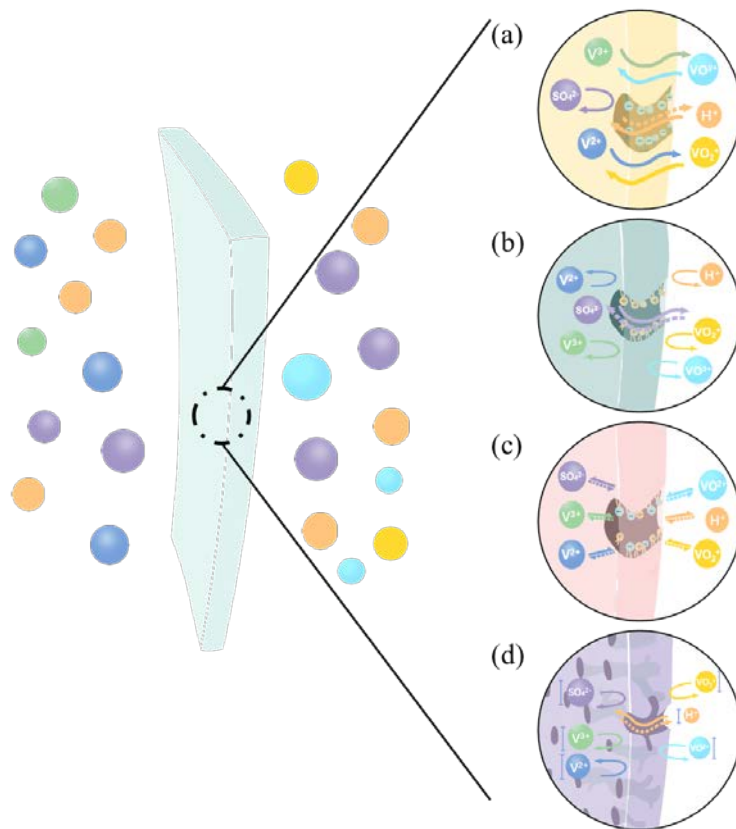


**Fig. 4.** Schematic of a (a) cation-exchange membrane; (b) anion-exchange membrane; (c) amphoteric-ion exchange membrane; and (d) porous membrane.

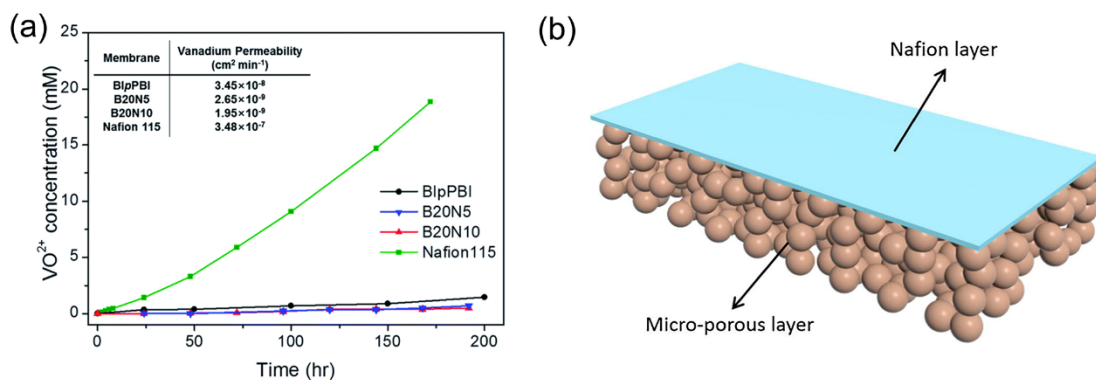


**Fig. 5.** (a) Vanadium-ions permeability comparison between BIpPBI, B20N5, B20N10, and Nafion 115; Reproduced under the terms of the CC-BY license.<sup>151</sup> Copyright 2018, The Authors. (b) Design of a VANADion membrane.<sup>108</sup> Reproduced with permission. Copyright 2016, Elsevier.

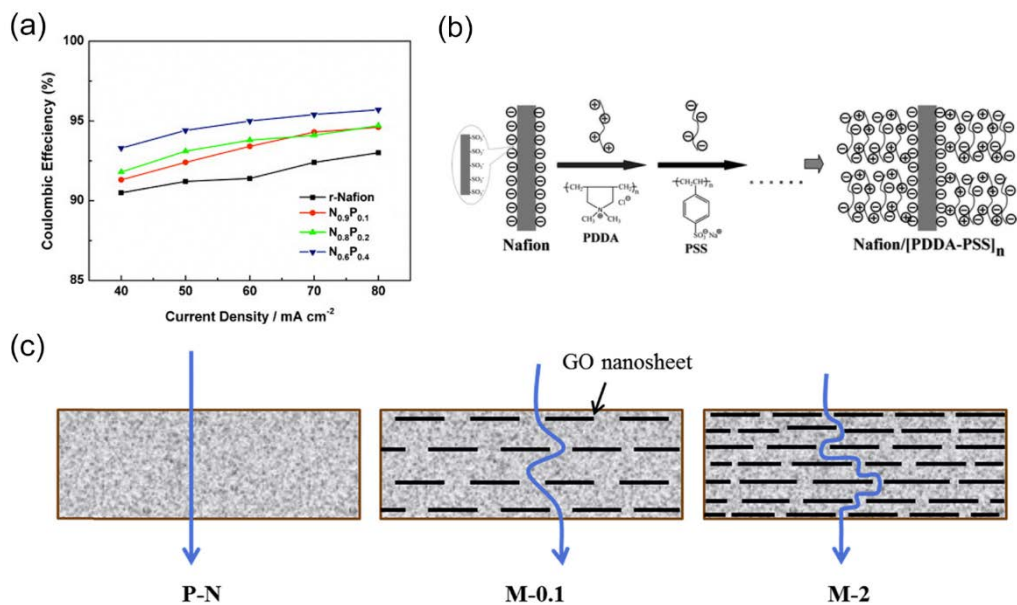


**Fig. 6.** (a) Coulombic efficiency comparison of recast-Nafion membrane and PVDF/Nafion composite membranes at 40-80 mA cm<sup>-2</sup>;<sup>125</sup> Reproduced with permission. Copyright 2011, Elsevier. (b) Schematic of the preparation of Nafion-[PDDA-PSS]<sub>n</sub> membranes;<sup>102</sup> Reproduced with permission. Copyright 2008, The Royal Society of Chemistry. (c) Schematics of vanadium-ions transport through the pristine Nafion and GO/Nafion composite membranes.<sup>98</sup> Reproduced with permission. Copyright 2017, Elsevier.



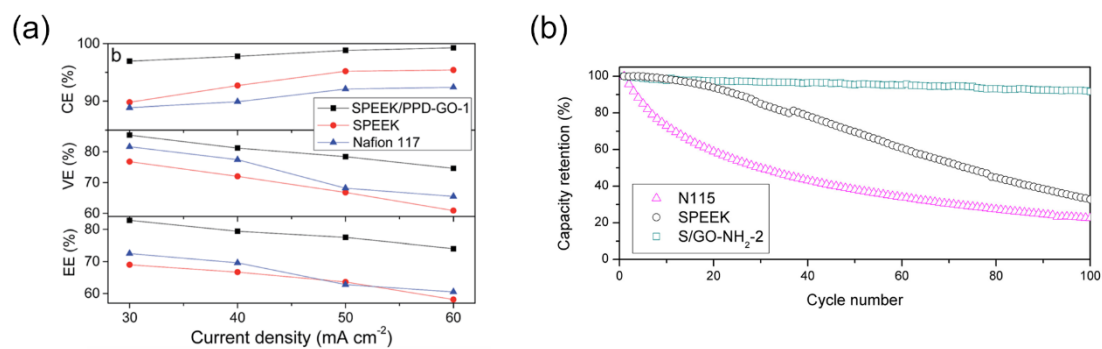


**Fig. 7.** (a) Efficiencies comparison among SPEEK/PPD-GO-1, SPEEK, and Nafion 117 membranes from 30 to 60 mA cm<sup>-2</sup>.<sup>178</sup> Reproduced with permission. Copyright 2016, The Royal Society of Chemistry. (b) Cycle performance of SPEEK/GO-NH<sub>2</sub>-2, SPEEK, and Nafion 115.<sup>148</sup> Reproduced with permission. Copyright 2017, Elsevier.

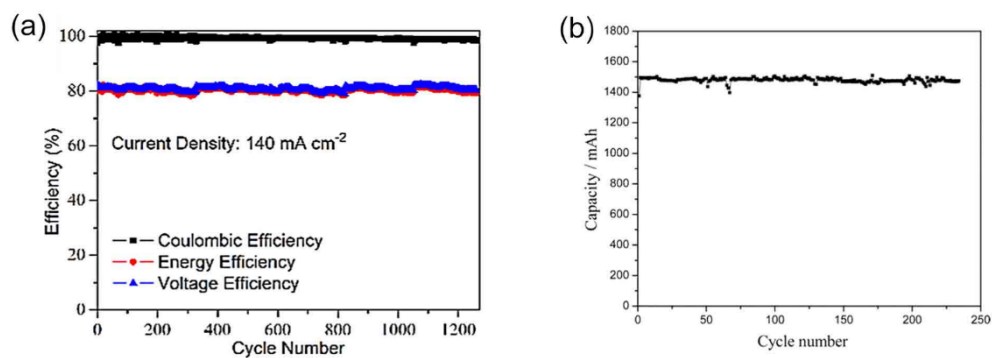


**Fig. 8.** (a) Cycle performance of a PES-based membrane at 140 mA cm<sup>-2</sup>.<sup>232</sup> Reproduced with permission. Copyright 2017, Elsevier. (b) Cycle performance of PVDF-g-PSSA-22 membrane at 60 mA cm<sup>-2</sup>.<sup>103</sup> Reproduced with permission. Copyright 2005, American Chemical Society.

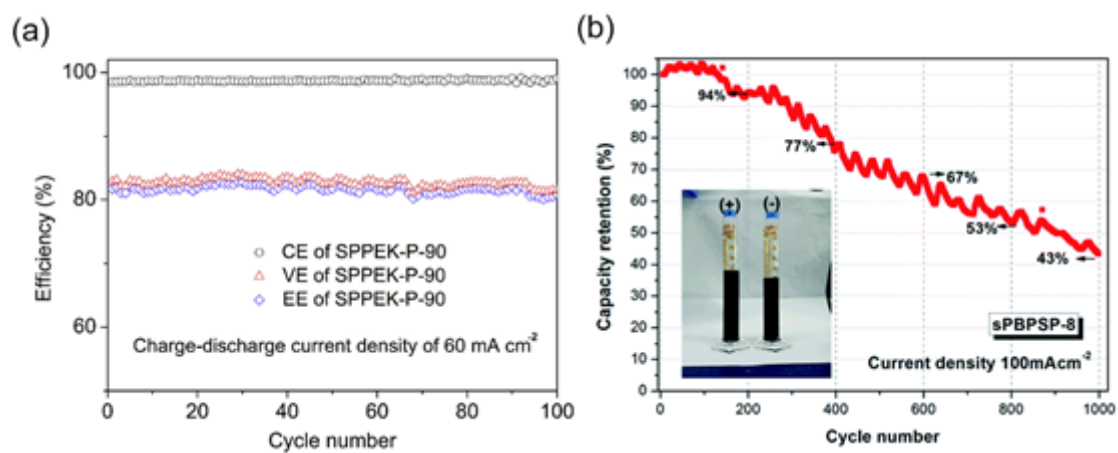


**Fig. 9.** (a) Coulombic, voltage, and energy efficiencies of SPPEK-P-90 at 60 mA cm<sup>-2</sup> for 100 cycles.<sup>141</sup> Reproduced with permission. Copyright 2017, Elsevier. (b) Capacity retention ability of sPBSP-8 membrane after 1000 cycles (inset: catholyte and anolyte volume comparison after 1000 cycles).<sup>246</sup> Reproduced with permission. Copyright 2017, The Royal Society of Chemistry.

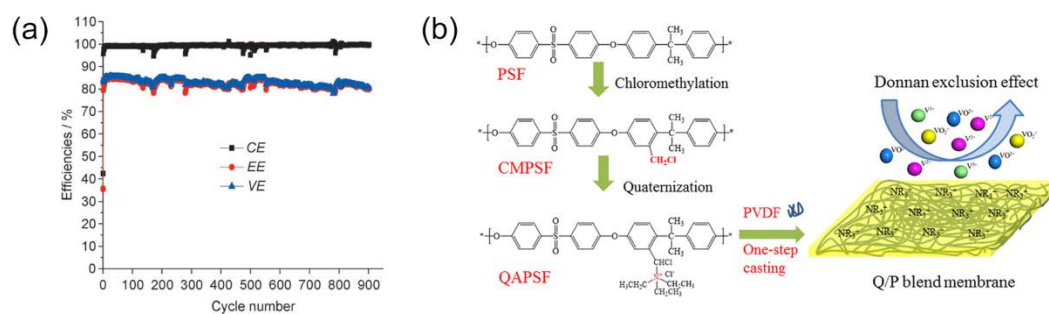


**Fig. 10.** (a) Efficiencies of the sIPN anion-exchange membrane (DCD= 4%).<sup>265</sup> Reproduced with permission. Copyright 2013, John Wiley & Sons. (b) Preparation procedures and working mechanisms of a PSF-based membrane.<sup>86</sup> Reproduced with permission. Copyright 2017, Elsevier.

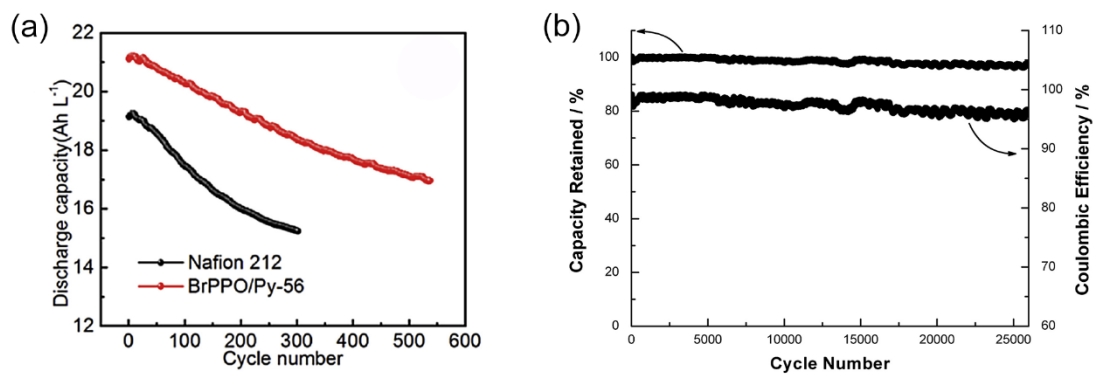


**Fig. 11.** (a) Discharge capacity of the BrPPO/Py-56 and Nafion 212 at  $200 \text{ mA cm}^{-2}$ .<sup>83</sup> Reproduced with permission. Copyright 2016, Elsevier. (b) Cycle stability of the PES-PVP anion-exchange membrane.<sup>279</sup> Reproduced with permission. Copyright 2012, Elsevier.

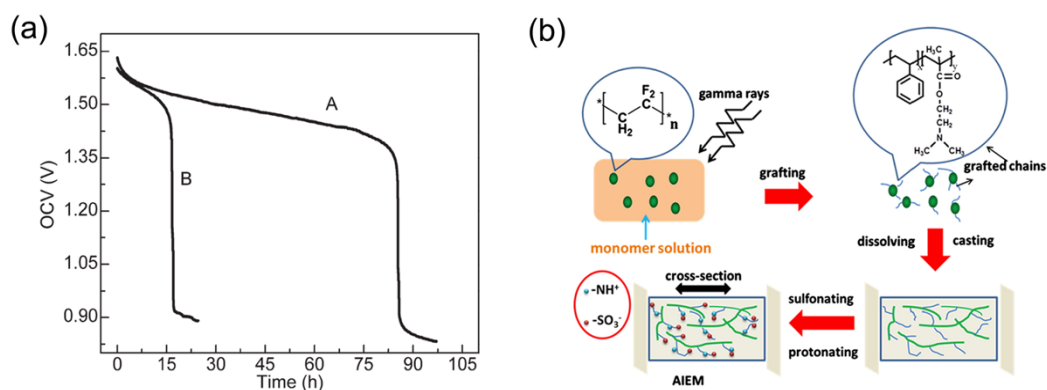


**Fig. 12.** (a) Open circuit voltage of the amphoteric-ion exchange membrane (A, DOG=42.7%) and Nafion 117 (B) membrane.<sup>307</sup> Reproduced with permission. Copyright 2013, John Wiley & Sons. (b) Schematic of the radiation grafting technique and solution phase-inversion method for membrane preparation.<sup>305</sup> Reproduced with permission. Copyright 2012, Elsevier.

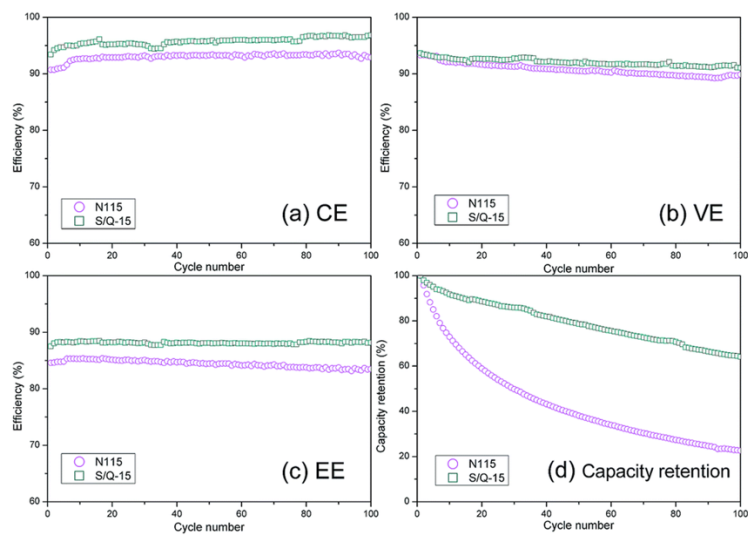


**Fig. 13.** Cycling performance comparison between Nafion 115 and SPEEK/QAPEI-15 blend membranes.<sup>312</sup> Reproduced with permission. Copyright 2015, The Royal Society of Chemistry.

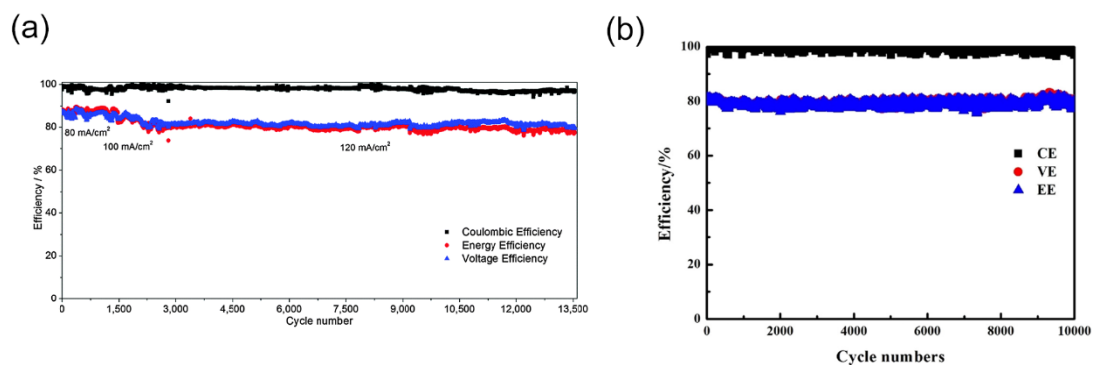


**Fig. 14.** (a) Cycle stability of a PBI-68 membrane for over 13000 cycles at current densities ranging from 80 to 120 mA cm<sup>-2</sup>.<sup>328</sup> Reproduced with permission. Copyright 2016, Royal Society of Chemistry. (b) Efficiencies of the NaCl-5M porous membrane for 10000 cycles at a current density of 160 mA cm<sup>-2</sup>.<sup>326</sup> Reproduced with permission. Copyright 2019, American Chemical Society.



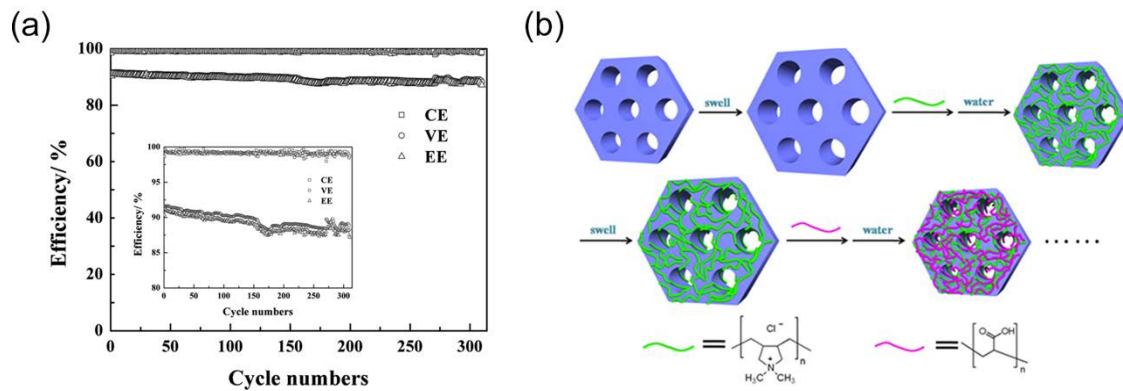


**Fig. 15.** (a) Cycle performance of the PES-SPEEK membrane at  $80 \text{ mA cm}^{-2}$ .<sup>319</sup> Reproduced with permission. Copyright 2016, John Wiley & Sons. (b) Schematic of the solvent-responsive layer-by-layer preparation procedure.<sup>323</sup> Reproduced with permission. Copyright 2014, Springer Nature.

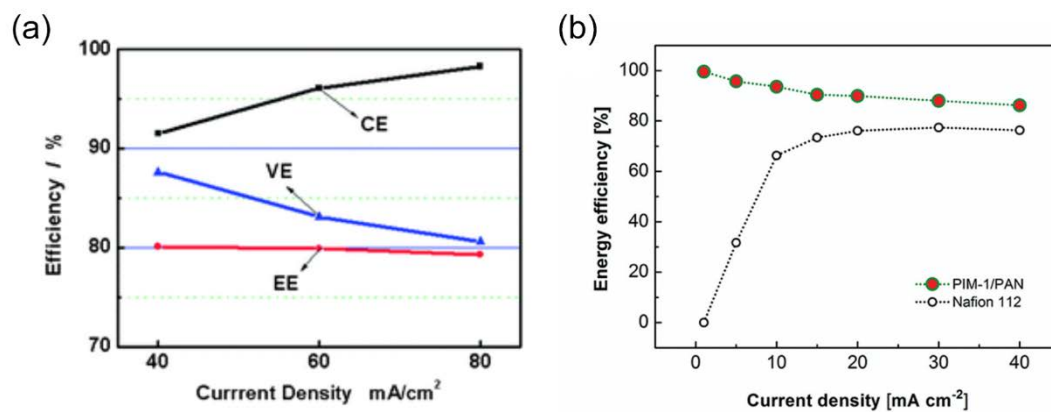


**Fig. 16.** (a) The efficiencies of a nanofiltration membrane (M3) at 40-80 mA cm<sup>-2</sup>.<sup>325</sup> Reproduced with permission. Copyright 2012, The Royal Society of Chemistry. (b) Comparison of energy efficiencies between PIM-1/PAN and Nafion 112 membrane at 1-40 mA cm<sup>-2</sup>.<sup>345</sup> Reproduced with permission. Copyright 2016, John Wiley & Sons.

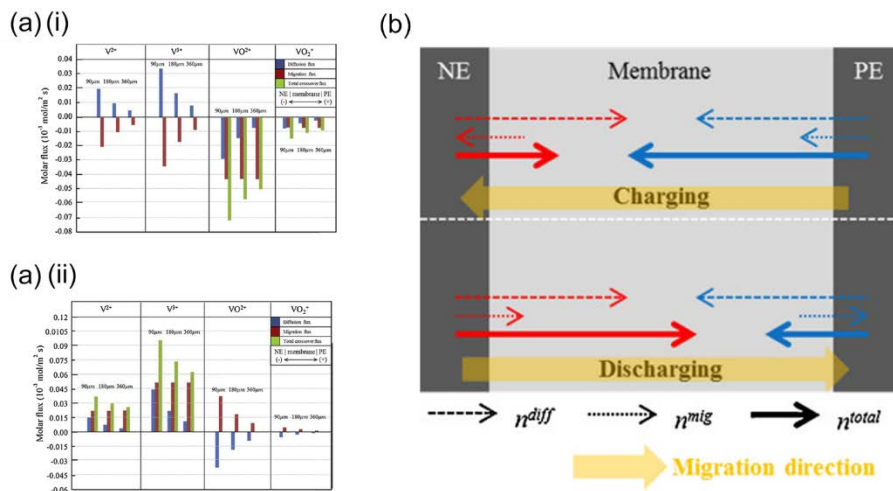


**Fig. 17.** (a) Diffusion and migration fluxes of vanadium species across three membrane of different thicknesses during (i) charging and (ii) discharging.<sup>364</sup> Reproduced with permission. Copyright 2015, Elsevier. (b) Schematic of species transport across the membrane under diffusion and migration mechanisms.<sup>367</sup> Reproduced with permission. Copyright 2015, Elsevier.

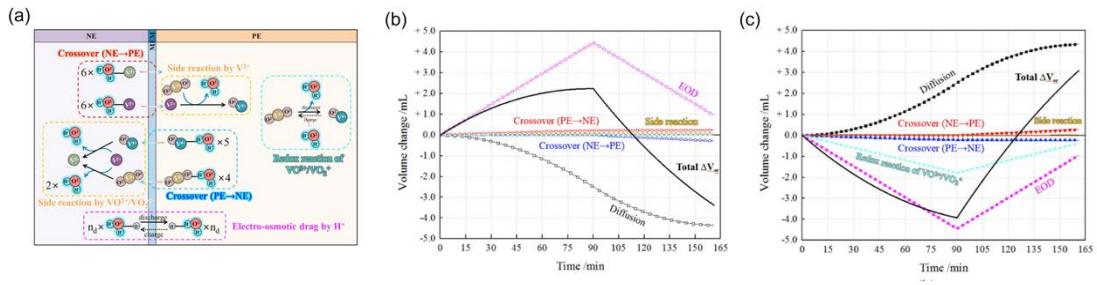


**Fig. 18.** (a) Schematic of various reactions and water sources and their transport mechanisms in VRFBs; contribution of different water crossover mechanisms on the water imbalance at the (b) negative and (c) positive half-cell.<sup>369</sup> Reproduced with permission. Copyright 2018, Elsevier.

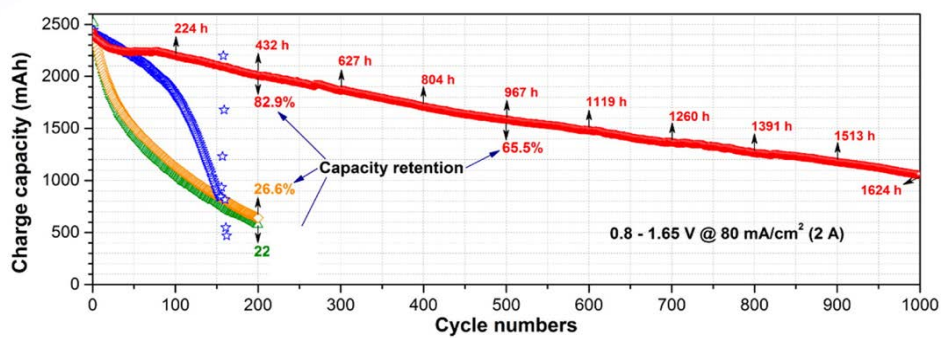


**Fig. 19.** Cycle performance comparison of Nafion (green), PTFE<sub>30</sub>/Nafion/PTFE<sub>30</sub> (yellow), SPEEK (blue), and PTFE<sub>30</sub>/SPEEK/PTFE<sub>30</sub> (red) membranes.<sup>194</sup> Reproduced with permission. Copyright 2016, American Chemical Society.

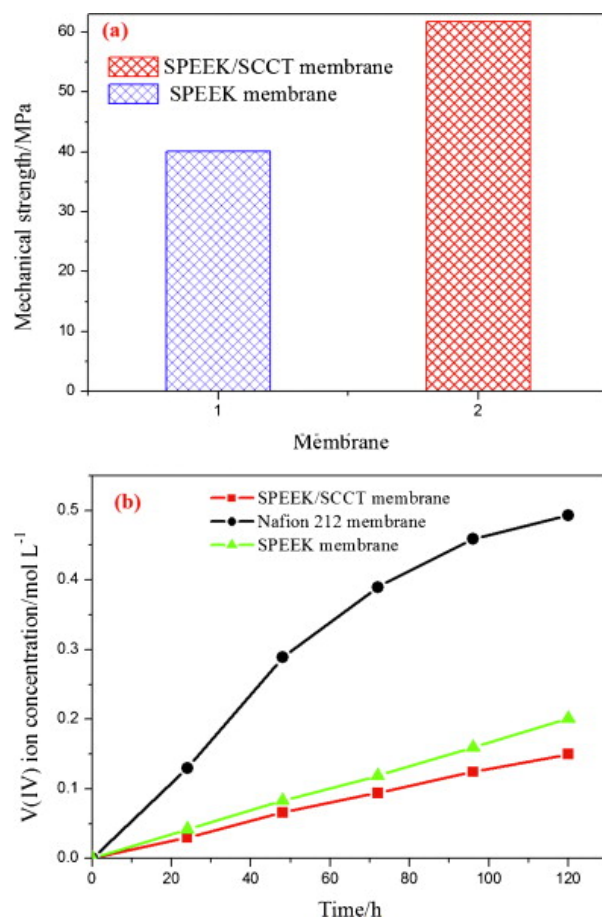


**Fig. 20.** Comparison of (a) mechanical strength and (b) vanadium ions permeability of Nafion 212, SPEEK and SPEEK/SCCT membranes.<sup>198</sup> Reproduced with permission. Copyright 2014, Elsevier.